Technische Universität München
TUM School of Engineering and Design

Co-cultivation of *Aspergillus niger* and *Trichoderma reesei* for the hydrolysis of wheat bran

Fabian Johannes Mittermeier

Vollständiger Abdruck der von der TUM School of Engineering and Design der Technischen Universität München zur Erlangung eines

Doktors der Ingenieurwissenschaften (Dr. Ing.)

genehmigten Dissertation.

Vorsitz: Prof. Dr.-Ing. Hartmut Spliethoff

Prüfende der Dissertation:

1. Prof. Dr.-Ing. Dirk Weuster-Botz
2. Prof. Dr.-Ing. Michael Zavrel

Die Dissertation wurde am 06.12.2024 bei der Technischen Universität München eingereicht und durch die TUM School of Engineering and Design am 02.06.2025 angenommen.

Ich freue mich, wenn es regnet, denn wenn ich mich nicht freue, regnet es auch.

Karl Valentin (1882-1948)

Acknowledgements

This work was carried out in course of my research at the Chair of Biochemical Engineering at the Technical University of Munich and would not have been possible without the help and support of many people.

First, I express my gratitude to Prof. Dr.-Ing. Dirk Weuster-Botz for the opportunity to take my doctorate at the Chair of Biochemical Engineering. Thank you for your excellent supervision, your trust in me and my work, your patience, and your important input when needed.

Also, I would like to thank Prof. Dr.-Ing. Michael Zavrel for his role as my co-examiner and Prof. Dr.-Ing. Hartmut Spliethoff for his/her agreement to act as chairman of the examiners' board.

Thank you to my project partners in the research project EcoWashCycle: Melania Pilz, Dr. Farah Qoura and Prof. Thomas Brück (Werner Siemens Chair for Synthetic Biotechnology, TUM), Dr. Anne Waidelich and Marius Schraml (REMSGOLD Chemie GmbH & Co. KG) and Peter Hirschmann and Dr. Josef Rampl (Bayerischer Müllerbund e.V.), for the cooperation in the project and interesting discussions. Additional thanks go to the Federal Ministry of Education and Research for funding.

I want to express my special gratitude to all former colleagues at the Chair of Biochemical Engineering, especially but not exclusively my officemates Melli and Prasi. Thank you for constructive discussions as well as nonsense talks, comforting coffee breaks as well as entertaining evenings, and everything in between. You were a great reason why I enjoyed my time at the chair so much, and many of you have become friends.

Thank you to all the students who helped so diligently in the lab. Tina, Nathalie, Sebastian, Fabienne, Veronika, Franziska, Theresa, you have been great support on the way to this thesis. A further special thanks goes to Emil Korzin for his great assistance with the 1000 L experiments in the TUM Pilot Plant for Industrial Biotechnology.

A huge "merci!" to all my friends, who always supported me, listened to me whine about failed experiments and distracted me from work thoughts whenever necessary.

Last, but definitely not least, I want to thank my family for their constant efforts and support throughout the years and for just being there. This would not have been possible without you.

Table of content

1. Introduction

Our world is in flux and changes rapidly. Modern technologies are developed in all areas of human life to simplify and improve our everyday life. Present-day's possibilities of traffic and communication enable global networks and trading, and progress in medical research allows the treatment of health issues that have been hitherto severe or fatal. However, there are also challenges for modern humanity. Global population is rapidly increasing, which leads to nutritional, health or resource issues and consequently to conflicts, and climate change further intensifies those problems (Martin, 2007). In order to meet those concerns, and to navigate the world towards a future-proof direction, the United Nations General Assembly adopted the 2030 Agenda for Sustainable Development in 2015. This agenda, called a "plan of action for people, planet and prosperity", unites goals and targets to improve life quality (fight against poverty and hunger, provision of clean water and healthcare), social equality (for example education), environmental protection (actions against climate change, saving biodiversity) and sustainable economies (amongst them clean energy and industries, sustainable civil engineering). One of those goals, Sustainable Development Goal 12 is titled "Responsible consumption and production". It formulates 11 targets, among them achieving sustainable management and use of natural resources, decreasing the food waste, or reducing the general waste production, for example through recycling strategies. (UN, 2015)

The establishment of circular economies poses a promising approach towards this goal (Schroeder et al., 2019). The expression "circular economy" can be defined in several different ways. However, the avoidance of waste generation is a highly common aspect therein, with strategies towards the reduction of resource demand, or reusing and recycling old products (Kirchherr et al., 2017). In the agricultural sector, these aims can be approached by efficient utilization and valorization of abundant waste material, for instance byproducts or residues after processing of the original products (Yaashikaa et al., 2022). While some methods convert these biomass streams into energy by gasification or combustion, others can result in various value-added products (Berntsson et al., 2012).

Here, biotechnology is a key technology, offering a broad variety of potential products from enzymatic or fermentative processes. Those can either replace conventional chemical production processes, or lead to novel products (Soetaert and Vandamme, 2006, Yaashikaa et al., 2022). Especially complex compounds such as fine chemicals or pharmaceuticals are already produced biotechnologically on the industrial scale.

However, the production of low-value products like bulk chemicals or biofuels is not economically feasible so far, with the costs for the feedstocks being a great part of the total process costs (Woodley, 2020). The application of vastly abundant agricultural byproducts in those processes thus offers great potential in the development of such processes. Additionally, the usage of non-food byproducts lead towards a more efficient and sustainable valorization of cropland use and evades competition with human nutrition (Muscat et al., 2020).

2. Objective

Many byproducts that occur in agricultural industries consist of lignocellulosic biomass. This biomass poses a promising feedstock for modern biorefineries. These facilities are designed for the conversion of biomass into a cornucopia of potential products of higher value, amongst them energy, fuels or chemicals (Berntsson et al., 2012). Especially the carbohydrates in lignocellulosic biomass are of great interest for those processes, as they can be hydrolyzed into their respective monomers and subsequently be converted into a broad variety of desired products using different microorganisms (Kamm and Kamm, 2007, Singhania et al., 2017, Amoah et al., 2019).

Some of the most important agricultural residues stem from the processing of cereals for the food and feed industry. In Germany alone, more than 40 million tons of cereals are harvested each year, half of which is wheat (Destatis, 2023). Worldwide, the annual wheat production even adds up to nearly 800 million tons nowadays (Ahrens, 2023). Most of the wheat is processed into flour for the food industry, and wheat bran is left over as the major byproduct. It comprises ~25% of the grain weight, meaning that each year around 150-200 million tons of wheat bran accrue (Neves et al., 2006). Large amounts thereof are currently used as animal feed, and only smaller shares go into human nutrition (Prueckler et al., 2014, Saini et al., 2023). However, the usage for feeding livestock poses a rather low degree of valorization. Alternatively, the vast amounts of wheat bran offer great potential as a feedstock for biorefinery processes to form products of higher value.

Wheat bran has a complex composition of the polysaccharides cellulose, hemicellulose and starch together with smaller fractions of protein, lipids and lignin (Prueckler et al., 2014). Therefore, a saccharification step is necessary to release monomeric sugars for microbial conversion processes. Chemical procedures use either concentrated or diluted acids for the acidic hydrolysis of lignocellulosic biomass. Concentrated acids allow hydrolysis processes at temperatures below 100 °C and atmospheric pressure but necessitate elaborate separation methods like chromatography or dialysis for product recovery. The hydrolysis of lignocellulosic biomass with diluted acids minimizes the input of hazardous chemicals but requires higher temperatures (often > 200 °C). These conditions can lead to the reaction of sugars to byproducts like furfural, 5-hydroxymethyl-furfural or formic acid, which are inhibitory for subsequent microbial conversion processes (Zhou et al., 2021).

The saccharification of lignocellulosic biomass by hydrolytic enzymes poses a promising alternative with milder reactions conditions (mostly atmospheric pressure, 30-50 °C),

lower input of energy and corrosive reagents and consequently a significantly reduced environmental impact (Saini et al., 2022). However, the hydrolysis of wheat bran requires a variety of hydrolytically active enzymes. Mainly hemicellulases/xylanases, cellulases and amylases are necessary for the degradation of hemicellulose, cellulose, and starch, respectively. Most microbial enzyme producers, among them many fungal species, specialize in the secretion of a limited set of hydrolases. Therefore, the preparation of all enzymes for efficient hydrolysis of wheat bran requires multiple separate production processes and hence can become laborious and costly (Ferreira et al., 2021). Fungal co-cultures have been reviewed as a promising approach for the on-site production of such hydrolytic enzyme mixtures in a single cultivation process (Zoglowek et al., 2016). The application of lignocellulosic biomass as substrate further reduces the costs of enzyme production and results in an adapted enzyme mixture for efficient hydrolysis.

Aspergillus niger (*A. niger*) is one of the most studied and applied organisms in research and industry (Cairns et al., 2018). Its origin as a soil fungus presupposes the secretion of hydrolytic enzymes for the degradation of biomass (Culleton et al., 2013), some of which are produced and applied industrially today. In this work, the xylanases and amylases from *A. niger* are of special interest, as they can degrade hemicellulose and starch, respectively. Therefore, several different *A. niger* strains from different clusters are examined for their capability to form the desired enzymatic activities, among them industrially used glucoamylase producers and their mutants (van Dijck et al., 2003, Andersen et al., 2011) as well as original citric acid producers, which have also been investigated for their hydrolytic enzyme secretion (Perlman et al., 1946, Schäfer et al., 2020).

A potential partner is found in the cellulase-producing fungus *Trichoderma reesei* (*T. reesei*). Since its first isolation during World War II, *T. reesei* has been subject of researchers due to its ability to secrete high quantities of cellulases (Mandels and Reese, 1957, Bischof et al., 2016). Several rounds of mutagenesis and selection eventually resulted in the strain *T. reesei* RUT-C30, which demonstrates the secretion of large concentrations of cellulases without catabolite repression and therefore became the most applied *T. reesei* strain for scientific and industrial purposes (Peterson and Nevalainen, 2012).

Due to their complementing hydrolytic activities, a consortium of a selected *A. niger* strain and *T. reesei* RUT-C30 poses a promising approach to produce an enzyme mixture for the saccharification of wheat bran. However, potential negative interactions between two microorganisms must be considered in the design of artificial microbial consortia (Che and Men, 2019). Especially filamentous fungi are known for competitive and antagonistic

reactions towards other species, originating from their natural competition for nutrients (Boddy and Hiscox, 2016). The presence of another fungus can lead to the secretion of enzymes for mycoparasitism or the production of secondary metabolites like antibiotics. Therefore, the co-cultivation of *A. niger* and *T. reesei* is studied in batch cultivations in lab scale stirred-tank bioreactors to investigate those potential synergistic as well as antagonistic interactions between the strains. Cultivation processes with different inoculation strategies are applied for this purpose, aiming for a stable co-culture, where both strains can grow and produce their enzymes.

The cultivation conditions influence the growth, morphology and productivity of filamentous organisms as well (Pollard et al., 2007). In particular, the mechanical power input by stirring and the oxygen supply can have a crucial effect on the secretion of enzymes and hence are examined in detail to identify ideal process parameters. Subsequently, criteria for a process transfer to stirred-tank bioreactors on larger scales are tested for a stepwise scale-up.

The isolation, purification and stabilization of enzyme solutions is labor-intensive, costly and can cause a loss of enzyme yield. It requires several process steps including separation, sterilization as well as formulation procedures like spray-drying or the supplementation of stabilizers, and significantly rises the costs of enzyme production (Johnson, 2016). Therefore, the on-site application of the crude enzyme solution is a potential approach to avoid excessive downstream processing (Kolasa et al., 2014). In this work, the hydrolytically active supernatant is solely separated from biomass by centrifugation and filtration before the application for the hydrolysis of wheat bran. Ideal reaction conditions for this hydrolysis process are investigated by characterization of the enzyme mixture regarding its pH and temperature optimum. Subsequently, hydrolysis processes in L scale stirred-tank reactors are conducted to compare the hydrolytic activity of the co-culture enzymes with the respective monoculture enzymes produced under the same cultivation conditions. The maximum space-time sugar yield as well as the total sugar yield are used to evaluate the saccharification efficiency.

A further reduction of process steps appears possible by the integration of enzyme production and hydrolysis into a one-pot process (Pirota et al., 2013, Maehara et al., 2018, Knesebeck et al., 2023). Total process costs could consequently be reduced considerably by omitting the intermediate separation steps. However, this is only feasible if released sugars are not metabolized by the fungal enzyme producers and can accumulate in the medium. Additionally, the surface of wheat bran is often contaminated with mold or bacteria which are also potential consumers of sugars (Laca et al., 2006, Radenkovs et al., 2013). Sterilization of dry wheat bran prior to the addition to the process

by treatment with air heated to 180 °C is highly energy-intensive and needs special equipment (Hinrichs et al., 2018). Alternatively, microorganisms can be inactivated inside the bioreactor by changing the reaction conditions to unfavorable conditions for growth before enzymatic hydrolysis is initiated. This could be conducted by increasing the process temperature (Pirota et al., 2013, Maehara et al., 2018), creating anaerobic conditions in the reactor, or a combination of both (Knesebeck et al., 2023).

The process integration of enzyme production with a co-culture of *A. niger* and *T. reesei* and hydrolysis of wheat bran into a one-pot process is studied in a stirred-tank bioreactor on the 25 L scale. Investigations especially focus on the transition between enzyme production and hydrolysis, where conditions favorable for enzymatic activity must be set while potential contaminants as well as the enzyme producers have to be inactivated. Afterwards, fresh wheat bran is added into the reactor for hydrolysis. The overall sugar yield is applied as benchmark for the comparison between integrated and separate processes. Eventually, the integrated enzyme production and hydrolysis process is transferred to the 1000 L scale to demonstrate its technical feasibility.

The realization of the objectives described above was approached in the following steps:

1) Study of a co-culture of *A. niger* and *T. reesei* to produce enzymes for the hydrolysis of wheat bran
    a. Identification of an *A. niger* strain for maximum xylanase and amylase secretion
    b. Investigation of inoculation strategies and process parameters for the co-cultivation in stirred-tank bioreactors using a defined medium
    c. Process transfer from 0.7 L to 3.0 L and 25 L scale
2) Enzymatic hydrolysis of wheat bran with enzymes from a co-culture of *A. niger* and *T. reesei*
    a. Identification of optimal reaction conditions for the hydrolysis of wheat bran
    b. Comparative study of the hydrolysis of wheat bran using monoculture and co-culture enzymes
3) Process integration of enzyme production and saccharification of wheat bran
    a. Process integration on the 25 L scale
    b. Transfer of the integrated process to the 1000 L scale

3. Theoretical background

3.1. Biological background

3.1.1. *Aspergillus niger*

The genus *Aspergillus*, located in the Ascomycota division, contains a number of ubiquitous fungi. It was first described by the priest and botanist Pietro Antonio Micheli in 1729 and named after the shape of its conidiophores, which reminded him of the liturgic instrument “Aspergillum” (Scazzocchio, 2009). One of the most relevant species of this genus is *Aspergillus niger*. Its eponymous black spores are colored by different pigments, among them aspergillin (Ray and Eakin, 1975). As a soil fungus, it is able to grow on various kinds of organic matter, including plant biomass, and can be found in a large variety of environments (Schuster et al., 2002, Šimonovičová et al., 2021). It tolerates a broad range of temperatures of 6-47 °C and pH conditions from pH 1.4 to pH 9.8 (Schuster et al., 2002). Its growth on lignocellulosic biomass is enabled by its ability to produce and secrete a broad spectrum of hydrolytic enzymes such as hemicellulases, cellulases, amylases, proteases, pectinases or lipases, which degrade the organic matter and release consumable compounds (Culleton et al., 2013).

In contrast to other ascomycetes, *A. niger* does not possess a sexual cycle and thus is only able to reproduce asexually (Pontecorvo et al., 1953). The fungus grows conidiophores when in contact with air and form asexual spores, so-called conidia, on top of these special hyphae (Baltussen et al., 2020). Those spores are then distributed through the air and germinate at their new location when the environmental conditions are favorable (McCartney and West, 2007). Until then, the conidia remain in a dormant state and can withstand severe conditions like extreme temperatures, pH variations, or dehydration (Baltussen et al., 2020). In several *Aspergillus* species, among them *A. niger*, pigments in the conidia additionally protect the spores from UV or ionizing radiation (Chang et al., 2020).

A. niger has been applied for the industrial production of citric acid for more than 100 years now (Currie, 1917). Other chemicals such as gluconic acid or malic acid followed, and the production of organic acids with *A. niger* has grown to billion dollar markets nowadays (Blom et al., 1952, Cairns et al., 2021). This was enabled by advances in process development and genetic engineering of the producing strains throughout the decades, and recent processes achieve product titers of up to 200 g L^{-1} (Lubertozzi and Keasling, 2009, Xu et al., 2019, Cairns et al., 2021). Aside from organic acids, the industrial production of enzymes has become more and more important.

Especially the production of glucoamylase must be highlighted, which is used for the saccharification of starch to glucose and poses a billion dollar business (Cairns et al., 2021). Other industrially relevant enzymes from *A. niger* are for instance proteases, pectinases or phytases (Haefner et al., 2005, Souza et al., 2015, Cairns et al., 2018, Meyer et al., 2020). The separation of the product from the biomass is simplified by the morphological character of *A. niger*, since the products are secreted and the large fungal particles can easily be removed by a filtration step (Lubertozzi and Keasling, 2009).

Due to this large potential for biotechnological processes, the genus *Aspergillus* and especially *A. niger* has been of great interest for research and industry and belong to the most-studied ascomycetes nowadays (Meyer et al., 2011). Further developments in biotechnological production with these fungi have been accelerated with the first whole genome sequence of an *A. niger* strain in 2000 (Baker, 2006). Since then, many more studies have been conducted to further decrypt the genetic code of several *A. niger* strains (Pel et al., 2007, Andersen et al., 2011, Vesth et al., 2018, Ellena et al., 2021).

Some *A. niger* isolates were proven to form mycotoxins, e.g. ochratoxin A, which can cause various medical conditions (Abarca et al., 1994, Freire et al., 2018). Spores of *Aspergillus* can also infect human lungs and cause pulmonary aspergillosis. However, *A. niger* is seldom the infectant for this disease (Person et al., 2010), and in these cases, the patients had pre-existing illnesses or immunosuppressive conditions (Schuster et al., 2002). As the exposure to spores can be restricted by safety measures, and no toxin formation was observed under controlled growth conditions (Schuster et al., 2002, Frisvad et al., 2018), the US Food and Drug Administration (FDA) provided *A. niger* the status “Generally Recognized As Safe” (GRAS), allowing its use for the food and feed industry (Schuster et al., 2002).

3.1.2. *Trichoderma reesei*

Like *A. niger*, *Trichoderma reesei* is a mesophilic, filamentous fungus from the division of Ascomycota. It was initially isolated during World War II on the Solomon Islands, where it was found to be the reason for the degradation of the soldiers’ cotton tents (Peterson and Nevalainen, 2012, Bischof et al., 2016). This first isolate of *T.* reesei, named QM6a, demonstrated high secretion of cellulases (Mandels and Reese, 1957). As cellulases came into the focus of researchers for the valorization of cellulosic biomass to bioethanol, for example, it was attempted to further enhance the cellulase formation of *T. reesei* QM6a via mutagenesis and selection of promising strains. First irradiation experiments resulted in a mutant called QM9414, which already demonstrated a two- to four-fold increased cellulase production, but still remained catabolite-repressed,

hindering the release of high concentrations of glucose (Mandels et al., 1971, Montenecourt and Eveleigh, 1977). A first derepressed strain, NG14 was obtained by two further rounds of UV and chemical mutagenesis (Montenecourt and Eveleigh, 1977), before another round of UV radiation and subsequent selection for high cellulosic activities finally resulted in the strain RUT-C30 (Montenecourt and Eveleigh, 1979). It secreted large amounts of highly active cellulases and showed no catabolite repression up to 5% glucose, and has been the basis organism for strain development and process improvement ever since (Peterson and Nevalainen, 2012, Frisvad et al., 2018).

Due to its importance in research and industry, the cellulolytic enzyme system of *T. reesei* has been analyzed in detail throughout the decades. Genome sequencing and annotation revealed an unexpectedly low number of genes coding for carbohydrate-active enzymes (Martinez et al., 2008). However, this limited set of enzymes still suffices for the degradation of lignocellulosic biomass. Several specific genetic and physiological features were reported for the strain RUT-C30, among them changed formation of endoplasmic reticula, a lack of Golgi bodies, and immanent cellular stress after induction of cellulase production (Peterson and Nevalainen, 2012). The cellulosic enzyme machinery has also been investigated in detail. Herein, three major hydrolase classes are involved: endoglucanases, cellobiohydrolases (or exoglucanases) and β-glucosidases (Druzhinina and Kubicek, 2017). Seven endoglucanases are described for *T. reesei*, namely CEL5A, CEL7B, CEL12A, CEL45A and three unnamed enzymes (Druzhinina and Kubicek, 2017). These hydrolases are able to cleave cellulose chains at randomized locations. The probably most important cellulolytic enzymes of *T. reesei*, the cellobiohydrolases CEL7A (formerly known as CBH 1) and CEL6A (formerly CBH 2), account for approx. 60% and 20% of the secreted proteins, respectively (Merino and Cherry, 2007). Cellobiohydrolases cleave cellobiose units off the ends of glucose chains. The repression of CEL7A in presence of glucose in early strains of *T. reesei* was lifted by the truncation of the glucose repressor gene *cre1* in RUT-C30 (Ilmén et al., 1996), allowing the production and secretion of CEL7A in glucose-containing media. The final step of cellulose degradation, the cleavage of cellobiose to glucose, is performed by β-glucosidases, of which seven are described in *T. reesei* (Druzhinina and Kubicek, 2017). However, the β-glucosidases of *T. reesei* RUT-C30 are produced in insufficient amounts compared to other strains (Ryu and Mandels, 1980, Herpoël-Gimbert et al., 2008) and are subject to product inhibition (Woodward and Arnold, 1981). These points lead to a β-glucosidase deficiency in the RUT-C30 enzyme cocktail and consequently to limited or incomplete hydrolysis of cellulose. Aside from hydrolases, other enzymes play a role in the cellulolytic system of *T. reesei*. One of them is swollenin (SWOI), which disrupts hydrogen bonds between the glucose chains in crystalline areas of cellulose and thus

simplifies its degradation (Saloheimo et al., 2002). A rather recently discovered group of enzymes in the cellulose-degrading enzyme mixture are so-called lytic polysaccharide monooxygenases (LPMO). These enzymes roughen the surface of crystalline cellulose fibrils via an oxidative mechanism to enable hydrolytic action (Harris et al., 2010, Levasseur et al., 2013, Eibinger et al., 2014, Marjamaa et al., 2022).

Cellulases from *T. reesei* offer a broad variety of potential applications in modern industries. One of the most important fields is the production of 2nd generation biofuels, where cellulases are used for saccharification of lignocellulosic biomass (Seiboth et al., 2011). Further applications include the textile industry, the production of laundry detergents or the food and feed industry (Ferreira et al., 2014, Bischof et al., 2016, Fischer et al., 2021). Furthermore, *T. reesei* is used as a host organism for the expression of heterologous proteins due to its enormous secretion potential (Peterson and Nevalainen, 2012, Fischer et al., 2021). The safety of *T. reesei* has been demonstrated over the years of application (Nevalainen et al., 1994). It is presumed not to produce any mycotoxins under controlled conditions (Frisvad et al., 2018) and was therefore certified with the GRAS status (Seiboth et al., 2011).

3.1.3. Growth and morphology of filamentous fungi

In contrast to single-cell organisms like the bacterium *Escherichia coli* or the yeast *Saccharomyces cerevisiae*, filamentous organisms like the fungi *A. niger* and *T. reesei*, form three-dimensional structures with connected cells (Weuster-Botz and Takors, 2018). Therefore, their growth on cellular (micromorphology) as well as three-dimensional level (macromorphology) is described in detail in the following.

Micromorphology

The growth of filamentous organisms usually starts from dormant spores, which were either distributed through the air (in natural environments) or stored as a cryoculture (in laboratory context). As soon as environmental conditions are favorable, the two-phase germination process commences. First, the spores begin to swell isotropically and change their surface to enable adhesion to other spores or substrate particles (Osherov and May, 2001). Subsequently, the swollen spores form germ tubes, which start polarized growth and mature into hyphae (Hayer et al., 2013). The process of germination is influenced by various environmental parameters, such as temperature, pH, CO_2 concentration or the presence of carbon and nitrogen sources (Yanagita, 1957, Hayer et al., 2013, Hayer et al., 2014). For *A. niger*, sugars like glucose and xylose as well as some amino acids were found to be germination triggers. The sprouting and

growth of *T. reesei* is also inducible by cellulose, as cellulolytic enzymes are already secreted in the early stages of germination (Chaudhary and Tauro, 1982).

After maturation of the hyphae, their tips continue to extend along the growth axis. Therefore, cell wall components alongside with proteins and ribosomes are encapsulated in vesicles and transported from the cell's core along the cytoskeleton to the hyphal tip, or apex (Gooday, 1995, Steinberg, 2007). These vesicles accumulate in the so-called Spitzenkörper, from where they are distributed in the hyphal tip or exocytic vesicles are transported outside the cell for the formation of the outer cell wall layers (Bartnicki-Garcia et al., 1989). Additionally, organelles for protein synthesis, like endoplasmic reticulum and the Golgi apparatus, concentrate in the hyphal apex, supporting polarized growth (Steinberg, 2007). Cells are divided during hyphal growth by forming septa. This process appears to be coordinated by the mitotic division of nuclei, yet the exact mechanism is not completely understood (Steinberg et al., 2017). The septa have a centrical pore to ensure the transport of e.g. vesicles towards the apex.

Further expansion of the fungus is achieved by branching. Two main patterns are observed: apical branching near the hyphal tip or, more often, lateral branching at random sites along the hypha (Harris, 2008). Both apical growth and branching lead to exponential growth of the fungus and form the hyphal network, or mycelium, which spreads throughout the surrounding material. Additional connections between the hyphae can be posed by anastomosis tubes for the exchange of organelles, genes or nutrients (Gabriela Roca et al., 2005). Upon exposition to air, the mycelium forms conidia and ultimately conidiospores, which are released into the air and serve for propagation of the fungus (Krijgsheld et al., 2013).

Macromorphology

Filamentous fungi can take different shapes during submerged cultivation, dependent from various parameters (Krull et al., 2013). The growth forms hereby range from freely dispersed mycelium and denser mycelial agglomerates ("clumps") to dense, spherical pellets (Gibbs et al., 2000, Papagianni, 2004). Free mycelial growth describes a widely spread and branched hyphal network without aggregation of cells. This leads to the formation of a highly viscous non-Newtonian broth, impeding homogenization as well as oxygen and mass transfer in a bioreactor. Spherical pellets do not influence the rheological behavior in the same manner (Papagianni, 2004). Pellet formation of coagulating organisms like *A. niger* contains two distinct steps, initial aggregation of conidia immediately after inoculation, and additional aggregation after germination (Metz and Kossen, 1977, Grimm et al., 2004). Subsequently, exponential growth of the pellet

can continue until a critical radius, where mass transfer limitations hamper the transfer of nutrients into the center of the pellet or hydrodynamic forces lead to the fragmentation of the pellet (Nielsen, 1996).

The macromorphological form has a major impact on the formation of desired products. However, the correlations between morphology and productivity are often very complex. For example, various studies suggest growth in small pellets for the production of citric acid with *A. niger* (Papagianni et al., 1994, Papagianni et al., 1998, Pazouki and Panda, 2000), while others recommend the inoculation with dispersed mycelium turning into clumps during cultivation (Paul et al., 1999). On the other hand, the dispersed form appears preferable to produce hydrolytic enzymes like glucoamylases or pectinases (Pazouki and Panda, 2000, Lin et al., 2010, Wucherpfennig et al., 2011, Schäfer et al., 2020). In the case of *T. reesei*, dispersed mycelial growth or the formation of small pellets were reported as favorable for the secretion of cellulolytic enzymes (Lejeune and Baron, 1995, Domingues et al., 2000). Due to this essential influence of macromorphology on product formation, a vast number of studies were investigating various parameters for controlling the fungal morphology in bioproduction processes. As a complete description would go beyond scope, the focus here lies on the organisms used in this work, *A. niger* and *T. reesei*. For both strains, initial spore concentration and pH were identified as key parameters, as both influence the aggregation of spores after inoculation and thus the morphology (Domingues et al., 2000, Grimm et al., 2004). The influence of pH is caused by the pH dependent changes of surface charge of the conidia (Lejeune et al., 1995, Papagianni, 2004, Grimm et al., 2005). Media composition affects the fungal growth in all phases from spore aggregation and germination to exponential growth, with the carbon source, the availability of manganese and the osmolality reported as influential (Kisser et al., 1980, Papagianni et al., 1999, Domingues et al., 2000, Pazouki and Panda, 2000, Papagianni and Mattey, 2004, Wucherpfennig et al., 2011, Bendig and Weuster-Botz, 2013). Shear forces and fluid dynamics introduced by stirrers have an effect on the second stage of spore aggregation (Grimm et al., 2005) as well as on the subsequent vegetative growth of the fungi (Lejeune and Baron, 1995, Papagianni et al., 1998, Kelly et al., 2004, Lin et al., 2010). Driouch et al. pursued an approach to actively engineer the morphology of *A. niger* using micro-particles and succeeded to increase the production of hydrolytic enzymes (Driouch et al., 2010, Driouch et al., 2011, Driouch et al., 2012).

3.1.4. Co-cultivation of microorganisms[1]

In nature, microorganisms do not live isolated but rather appear in company with other species within a habitat. Those microbial consortia are mostly undefined communities of different strains and species that cooperate for a mutual goal, for instance the degradation of lignocellulosic biomass. Such consortia are frequently applied in the field of environmental engineering for wastewater treatment or bioremediation (Watanabe, 2001, Zhang et al., 2017). In contrast, synthetic consortia and co-cultures are non-natural and highly defined combinations of microorganisms, which are artificially designed for a specific purpose, e.g. the production of a chemical compound. Such co-cultivations bear great potential for the improvement of bioproduction processes by synergistic effects of the involved species. Additional advantages of co-cultures are posed by the reduction of process steps (one cultivation instead of two) or possible integration of enzyme production or pretreatment steps.

However, interactions between microorganisms are often complex and must be considered when designing a co-cultivation process. On the one hand, beneficial interactions like mutualism (advantageous for both partners) and commensalism (advantageous for one partner, no effect on the other partner) are desirable within a co-culture. On the other hand, competitive or even antagonistic relations can significantly worsen the process performance and hence should be avoided (Che and Men, 2019).

A variety of interaction mechanisms have been examined and applied to design microbial consortia. So-called consolidated bioprocesses enable the utilization of low-cost resources like plant biomass by the integration of enzyme production, hydrolysis and bioconversion. Fungi are frequently applied as enzyme producers for the degradation of the complex polymeric substrate. The second microorganism subsequently converts the released monomers into the product of choice. An exemplary process has been reported by Schlembach et al. (2020): *Trichoderma reesei* hydrolyzes cellulose into glucose, which is converted to itaconic acid by *Ustilago maydis*. Co-cultures of photoautotrophic and heterotrophic microorganisms are another example for the application of artificial consortia for substrate provision. The photoautotrophic partner uses (sun-)light to fixate CO_2 and to convert it into sugars through the Calvin cycle. Those sugars are then used for the synthesis of the desired product by the heterotrophic strain. Zhang et al. (2020)

[1] Contents from this chapter are published in: Mittermeier, F., M. Bäumler, P. Arulrajah, J. d. J. García Lima, S. Hauke, A. Stock and D. Weuster-Botz (2023). "Artificial microbial consortia for bioproduction processes." Engineering in Life Sciences **23**(1): e2100152.

used this mechanism to produce the platform chemical 3-hydroxypropionic acid with a cyanobacterium and *Escherichia coli* (*E. coli*).

The principle of division of labor can be used to efficiently produce complex molecules. Hereby, the production pathways are divided into two parts with two microbial strains: the upstream strain forms an intermediate compound and secretes it into the medium. The downstream strain subsequently converts this intermediate into the target molecule. Splitting the pathway reduces the metabolic burden on each organism and thus leads to more efficient production. Recent examples have been reported with recombinant *E. coli* cells for the production of the flavonoid sakuranetin (Wang et al., 2020) or the NADH-intensive synthesis of n-butanol (Saini et al., 2017). An anaerobic co-culture of the autotrophic *Clostridium carboxidivorans* and the chain-elongating *Clostridium kluyveri* was established for the production of C2-C6 alcohols and organic acids from carbon monoxide (Bäumler et al., 2021). *C. carboxidivorans* converts CO and CO_2 into acetate and ethanol, which are subsequently elongated to butyrate and hexanoate by *C. kluyveri* and reduced to the respective alcohols again by *C. carboxidivorans*. The process was then improved by implementing a cascade of two stirred-tank reactors with strain-specific reaction conditions (Bäumler et al., 2023). Division of labor among two strains also enables the prevention of metabolite feedback inhibition. The upstream strain potentially forms intermediate products that act inhibitory towards cell growth. The subsequent conversion of that metabolite by the downstream strain can lift the feedback inhibition and hence leads to higher yields of the final product. For instance, a co-culture of *E. coli* and *Saccharomyces cerevisiae* used this approach to produce taxanes, precursors for anticancer drugs (Zhou et al., 2015). Aside from the intermediate taxadienes, *E. coli* forms potentially inhibiting acetate. However, the inhibition is circumvented by the utilization of acetate by *S. cerevisiae*, which converts the taxadienes to taxanes.

The co-cultivation of naturally incompatible microorganisms like aerobic and anaerobic species enables the production of typically anaerobic products like solvents under aerobic conditions. Aside from other interactions like substrate provision, the growth of the aerobic partner depletes the oxygen dissolved in the medium and creates anaerobic conditions for the second strain. An exemplary consortium of the aerobic *Bacillus cereus* and the anaerobic *Clostridium acetobutylicum* increased the productivity of acetone-butanol-ethanol (ABE) fermentation while decreasing the total costs compared to conventional ABE fermentation (Wu et al., 2016). The cellulolytic anaerobic *Clostridium phytofermentans* and either *S. cerevisiae* or *Candida molischiana* were combined for ethanol production. The anaerobic partner provides soluble cellodextrins from cellulose, and the yeast converts those cellodextrins to ethanol while protecting

C. phytofermentans from oxygen (Zuroff et al., 2013). Shahab et al. (2018) applied a similar mechanism for the production of lactic acid from lignocellulosic material using a membrane bioreactor. *T. reesei* formed a biofilm on the surface of an oxygen permeable membrane and produced enzymes to hydrolyze the lignocellulosic substrate. Simultaneously, *Lactobacillus sp.* in the bulk phase was shielded from oxygen and converted the released glucose into the final product lactic acid.

Fungal consortia can be of value for the degradation of lignocellulosic biomass by producing complementing enzyme mixtures (Zoglowek et al., 2016). *T. reesei* is known for its capability to secrete large amounts of cellulases, but has deficiencies regarding other hydrolytic activities like amylase and β-glucosidase (Herpoël-Gimbert et al., 2008, Peterson and Nevalainen, 2012). Those weaknesses can be compensated for by, for example, *Aspergillus* strains producing these enzymes. Several studies have described the synergistic effects of a co-culture of *Aspergillus spp.* and *T. reesei* for efficient degradation of plant material (Ahamed and Vermette, 2008, Kolasa et al., 2014, Zhao et al., 2018). However, co-cultures do not only offer advantages but also provoke reactions of the organisms to one another. Especially the production of secondary metabolites like antibiotics can be triggered by co-cultivation (Boruta et al., 2021). Such a reaction was also described for the combination of *A. niger* and *T. reesei* by Daly et al. (2017), who observed biomass reduction in the mixed cultures as well as several changes on transcriptomic level. In both strains, the formation or modification of secondary metabolites was induced by the presence of the other organism. Additionally, *A. niger* was affected in its cell wall synthesis and sporulation, although *T. reesei* did not show signs of direct antagonism. An explanation approach therefor was provided by a comparative genome analysis, reporting that *T. reesei* had lost its mycoparasitism capacity (Kubicek et al., 2011).

The potential negative interactions between different microorganisms and their unfavorable effects on bioprocesses necessitate the observation and control of population dynamics. Therefore, several methods were developed for the analysis of population distribution and dynamics in microbial consortia (Schlembach et al., 2021). Classical offline methods like microscopy or plate-counting, e.g. described by Brou et al. (2018) demand a high labor effort, while more advanced technologies like quantitative PCR or flow cytometry with fluorescent reporter strains or fluorescence in situ hybridization (FISH) require special and costly equipment (e.g. applied by Daly et al. (2017), Liu et al. (2018), Bäumler et al. (2021)). Online analysis methods include online-flow cytometry (Conacher et al., 2020) or headspace mass spectrometry, where volatile signature metabolites of the strains are measured (Sovová et al., 2013). More recently,

computational metabolic or thermodynamic modelling methods (Bekiaris and Klamt, 2021, García-Jiménez et al., 2021) as well as automated high-throughput cultivation methods (Jo et al., 2021) have been introduced to minimize the demand in time and labor for the development of artificial consortia.

3.2. Technical background on stirred-tank bioreactors

3.2.1. Microbial growth in bioreactors

Microbial growth describes the increase of the total cell mass over cultivation time, caused by the division of cells. The speed of this growth is known as the specific growth rate and is defined as the timely change of the total biomass concentration (Weuster-Botz and Takors, 2018):

$$\mu \equiv \frac{1}{c_X}\frac{dc_X}{dt} \tag{3.1}$$

This growth can generally be divided into growth phases, which are displayed in Figure 3.1 (Weuster-Botz and Takors, 2018).

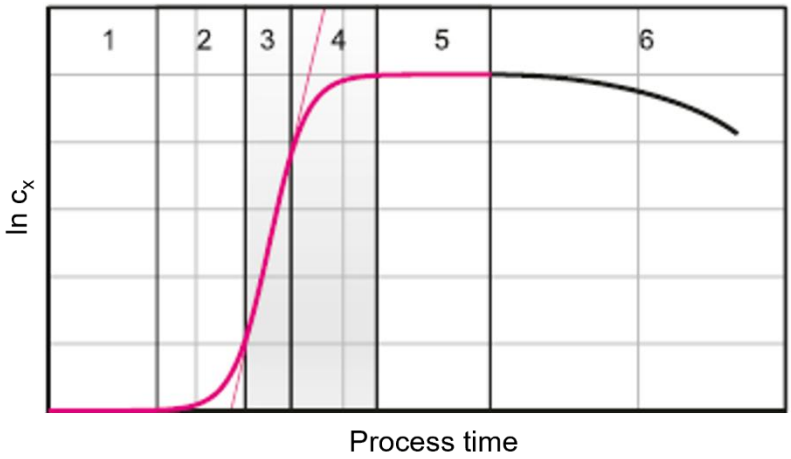

Figure 3.1: Growth curve of microorganisms under ideal conditions, displayed as the logarithmic biomass concentration over time (adapted from Weuster-Botz and Takors (2018)). 1: Lag phase, 2: acceleration phase, 3: exponential growth phase, 4: retardation phase, 5: stationary phase, 6: decline phase.

In the first phase directly after inoculation, the cells have to adapt to the new environment and the present conditions. During this so-called lag-phase (1), no increase in biomass can be observed. Growth commences after adaptation and increases during the acceleration phase (2), until it reaches an exponential rise of cell mass during the exponential phase (3). In this phase, the cells can grow without any limitations, and the maximum growth rate μ_{max} can be reached under ideal conditions (temperature, pH, medium composition). Growth subsequently decelerates again in the retardation phase

(4) until no more increment in biomass is registered (stationary phase, 5). When the process is continued even further, the cells begin to die off (decline phase, 6). Several reason can cause the stop of exponential growth, like changed reaction conditions, the accumulation of inhibiting products or the depletion of substrates (Weuster-Botz and Takors, 2018). The case of substrate limitation and the correlation with the growth rate can be described by various approaches, whereof the approach of saturation kinetics of Monod is probably the most prominent one (Monod, 1949):

$$\mu = \mu_{max} \cdot \frac{c_S}{K_S + c_S} \tag{3.2}$$

with c_S being the substrate concentration and K_S as the nutrient concentration where $\mu = 0.5\ \mu_{max}$. More advanced models also consider the occurrence of substrate excess inhibition (Andrews, 1968) or product inhibition (Levenspiel, 1980).

An ideal stirred-tank bioreactor can be mathematically described by the following balance equation under the assumption of complete ideal homogenization:

$$\frac{dm_i}{dt} = \frac{d(c_i \cdot V)}{dt} = \dot{V}_{in} \cdot c_{i,in} - \dot{V}_{out} \cdot c_i + r_i \cdot V \tag{3.3}$$

with m_i as the mass of component i, t as a time interval, c_i as the concentration of component i, V as the reaction volume, $\dot{V}_{in}$ and $\dot{V}_{out}$ as the flow rates coming in and out of the reactor, respectively, $c_{i,in}$ as the concentration of component i in the stream flowing into the reaction, and r_i as the reaction rate of component i in the reaction. In this work, all cultivation experiments in stirred-tank bioreactors were conducted as batch processes. In this mode of operation, all necessary components are present in the reactor at the beginning of the cultivation. Only air and titration agents pass through the sterile barrier and are continuously added during the cultivation for aeration and pH control. The volumes taken out for sampling and added in for pH control are assumed as neglectable for an ideal stirred-tank reactor. Consequently, $\dot{V}_{in}$ and $\dot{V}_{out}$ in equation 3.3 equal zero and the balance equation is simplified to:

$$\frac{dm_i}{dt} = \frac{dc_i}{dt} \cdot V = r_i \cdot V \tag{3.4}$$

and even more easily to:

$$\frac{dc_i}{dt} = r_i \tag{3.5}$$

When applied to the biomass concentration within the process, the balance equation gives:

$$\frac{dc_X}{dt} = \mu \cdot c_X \tag{3.6}$$

Analogously, the masses of substrate and product can be balanced as follows:

$$\frac{dc_S}{dt} = -q_S \cdot c_X \tag{3.7}$$

$$\frac{dc_P}{dt} = q_P \cdot c_X \tag{3.8}$$

with q_S and q_P as the specific substrate uptake rate and specific product formation rate, respectively (Takors and Weuster-Botz, 2018).

Aside from batch processes, two characteristic modes of operation can be applied: fed-batch processes and continuous processes. In fed-batch processes media components (e.g. carbon source) are fed into the reactor over process time, increasing the reaction volume. This form of process enables the adjustment of the specific growth rate to avoid substrate inhibition or byproduct formation. During continuous bioprocesses, the reaction volume remains constant by setting identical flow rates in and out of the reactor. This leads to a state of equilibrium and allows for prolonged process times compared to the fed-batch mode. Continuous processes can be designed with or without cell retention. The residence times of cells and medium are decoupled in the former case, whereas they are equal in the latter one (Takors and Weuster-Botz, 2018).

3.2.2. Oxygen input and transfer

The supply of oxygen for the cells is essential for aerobic processes and is thus viewed in detail in the following. Oxygen provision in stirred-tank bioreactors is typically realized by injection and dispersion of air through suitable spargers and stirrers (Takors and Weuster-Botz, 2018). Various models are known for the description of oxygen transfer in the medium, whereof the two-film theory, the penetration model and the theory of surface renewal are described here. The two-film theory of Lewis and Whitman (1924) assumes two laminar boundary layers on both sides of the interface. The oxygen concentration converges towards an equilibrium concentration at the interface within these boundary films, whereas the concentration remains constant in the bulk phases. This concentration profile is graphically explained in Figure 3.2.

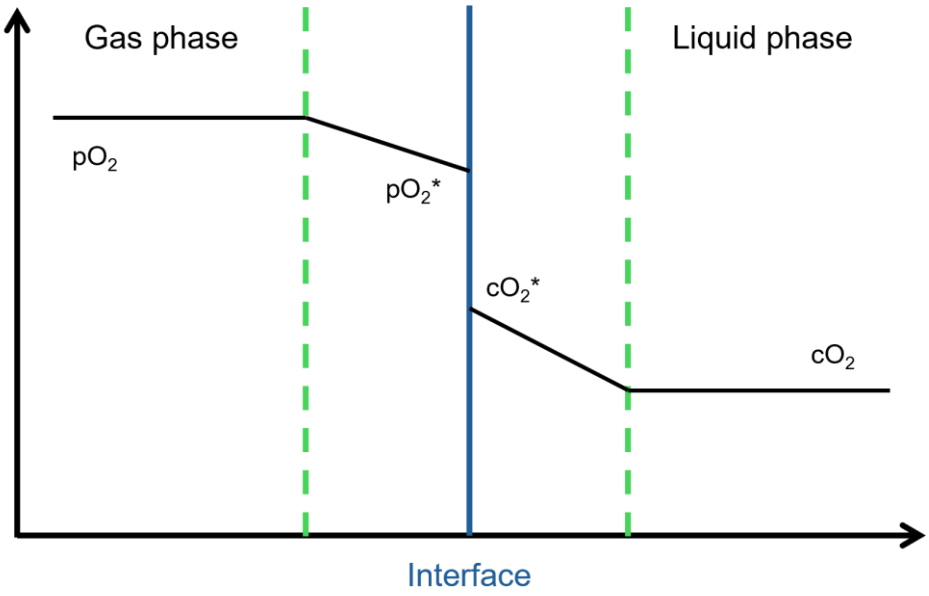

Figure 3.2: Schematic depiction of the oxygen concentration profile on the gas-liquid interface following the two-film theory of Lewis and Whitman (1924).

This model was renewed in 1935, when Higbie proposed the penetration model based on the time-dependency of the diffusion into the laminar boundary layer (Higbie, 1935, Sideman, 1966). The theory of surface renewal discards the assumption of a stagnant liquid film at the interface and instead supposes a continuous replacement of the liquid by turbulent flows (Danckwerts, 1951).

Based on the two-film theory of Lewis and Whitman, the oxygen transfer rate (OTR) can be described as:

$$OTR = \frac{\dot{n}_{O_2,L}}{V_L} = k_L \frac{A}{V_L} \cdot \left(c^*_{O_2,L} - c_{O_2,L}\right) = k_L a \cdot \left(c^*_{O_2,L} - c_{O_2,L}\right) \tag{3.9}$$

with $\dot{n}_{O_2,L}$ as the molar oxygen current across the interface, V_L as the liquid volume, k_L as the mass transfer coefficient, A as the exchange surface, and $c_{O_2,L}$ and $c^*_{O_2,L}$ as the oxygen concentrations in the liquid phase in the bulk phase and boundary layer, respectively. The expression $k_L \frac{A}{V_L}$ can subsequently be summarized to the volumetric oxygen transport coefficient $k_L a$, which is frequently used as a description parameter for the oxygen input in bioreactors (Takors and Weuster-Botz, 2018). The calculation of the $k_L a$ requires detailed knowledge of the reactor systems as well as empirical parameters which depend on the medium, the stirrer configuration, and other variables (Takors, 2014). Because these parameters are seldomly known and the calculation still is imprecise, a dynamic measurement method for the determination of the $k_L a$ during fermentation became established (Bandyopadhyay et al., 1967, Chmiel and Walitza, 2018). This practical approach only requires measurement of the dissolved oxygen

concentration (DO) in the medium at various times and consists of two phases: the non-gassing phase (depletion phase) and the aeration phase (saturation phase). The air flow into the reactor is terminated for the non-gassing phase, leading to a linear DO reduction by oxygen consumption of the cells:

$$\frac{dc_{O_2}}{dt} = -OUR \tag{3.10}$$

OUR is the oxygen uptake rate of the cells during this depletion phase. Afterwards, the aeration is switched on again, and the DO rises again following a saturation curve. In this phase, the change in oxygen concentration can be described as:

$$\frac{dc_{O_2}}{dt} = k_L a \cdot \left(c^*_{O_2} - c_{O_2}\right) - OUR \tag{3.11}$$

or after rearrangement:

$$c_{O_2} = -\frac{1}{k_L a}\left(\frac{dc_{O_2}}{dt} + OUR\right) + c^*_{O_2} \tag{3.12}$$

with $c^*_{O_2}$ as the oxygen equilibrium concentration and c_{O_2} as the oxygen concentration in the bulk phase, represented by the DO. Equation 3.12 now allows the determination of the $k_L a$ via linear regression. Alternatively, equation 3.12 can be integrated and the $k_L a$ can subsequently be calculated directly via non-linear regression (Garcia-Ochoa et al., 2010). Oxygen depletion can also be realized by stripping with nitrogen for $k_L a$ determination in absence of cells.

The concentrations of oxygen and carbon dioxide in the exhaust gas are often observed via off-gas analysis. These data can be recorded continuously on-line and thus provide real-time information about the metabolic activity in the fermentation (Musaalbakri and Webb, 2018). The oxygen molar fluxes in and out of the reactor can be balanced as follows:

$$\dot{n}_{O_2} = \dot{n}_{O_2,in} - \dot{n}_{O_2,out} = \frac{p}{RT}\left(\dot{V}_{g,in} \cdot x_{O_2,in} - \dot{V}_{g,out} \cdot x_{O_2,out}\right) \tag{3.13}$$

with $\dot{n}_{O_2}$ as the respective molar oxygen flux, p as the pressure (assumed as constant), R as the ideal gas constant (8.314 J mol^{-1} K^{-1}), T as the temperature (assumed as constant), $\dot{V}_g$ as the respective air flow rate and x_{O_2} as the respective oxygen concentrations in the inlet gas (in) and the exhaust gas (out) (Takors and Weuster-Botz, 2018). It is further assumed that the air flow only contains oxygen, carbon dioxide and nitrogen (considered inert). Consequently, the oxygen uptake rate can be calculated following:

$$OUR = \frac{\dot{n}_{O_2}}{V_L} = \frac{\dot{V}_{g,in}}{V_L V_m}\left(x_{O_2,in} - \frac{1 - x_{O_2,in} - x_{CO_2,in}}{1 - x_{O_2,out} - x_{CO_2,out}} \cdot x_{O_2,out}\right) \quad (3.14)$$

with V_m being the molar volume of an ideal gas (22.4 L mol^{-1}). In consideration of the CO_2 concentrations in inlet and exhaust gas, the carbon dioxide evolution rate (CER) can be calculated analogously:

$$CER = -\frac{\dot{V}_{g,in}}{V_L V_m}\left(x_{CO_2,in} - \frac{1 - x_{O_2,in} - x_{CO_2,in}}{1 - x_{O_2,out} - x_{CO_2,out}} \cdot x_{CO_2,out}\right) \quad (3.15)$$

The respirational quotient RQ is defined as the quotient of CO_2 evolution rate and oxygen uptake rate:

$$RQ = \frac{CER}{OUR} \quad (3.16)$$

Aerobic cells during exponential growth on e.g. glucose display a RQ of 1. Changes in the metabolism, for instance for the formation of products, however, can affect the RQ. Therefore, the RQ is a potential on-line signal to evaluate the process quality when known for the desired product (Takors and Weuster-Botz, 2018).

3.2.3. Cultivation of filamentous organisms

The cultivation of filamentous organisms like fungi brings certain distinctive features differing from bacterial fermentations. In contrast to single cell organisms, fungal cells do not separate from each other but grow into hyphal networks (see Chapter 3.1.3). As described above, filamentous organisms only grow at their free hyphal tips. Cells close to the tip and cells distant from the tip do not contribute equally to the growth rate. Thus, a structured model is necessary to mathematically describe fungal growth. A simple model was proposed by Nielsen (1993), subdividing the cells into an apical, a subapical and a hyphal compartment (displayed in Figure 3.3).

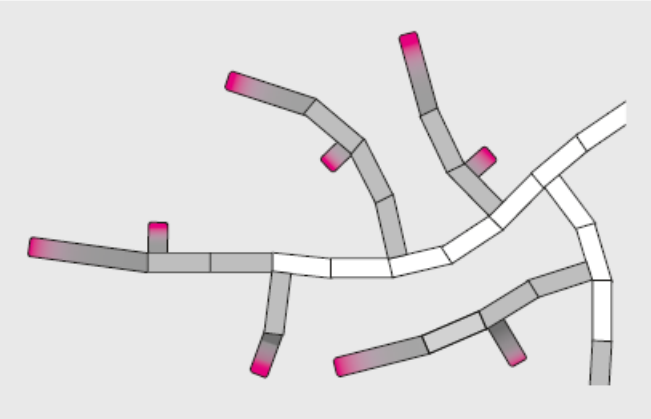

Figure 3.3: Schematic depiction of the compartments in the growth model of Nielsen (1993) (from Weuster-Botz and Takors (2018)). Apical compartments: red and dark gray, subapical compartments: light gray, hyphal compartments: white.

The mass fractions of the compartments summarize to the total biomass:

$$z_A + z_S + z_H = 1 \tag{3.17}$$

with z_A , z_S and z_H as the mass fractions of the apical, subapical and hyphal compartments, respectively.

Only apical and subapical compartments actively contribute to the growth of the organism. Therefore, the total growth rate can be represented via the growth rates of those compartments and their respective mass fractions:

$$\mu = \mu_A \cdot z_A + \mu_S \cdot z_S \tag{3.18}$$

The simplest case for the growth kinetics of filamentous growth hence is given by the assumption of a substrate limitation following Monod (1949):

$$\mu = \left(\mu_{max,A} \cdot z_A + \mu_{max,S} \cdot z_S\right) \cdot \frac{c_S}{K_S + c_S} \tag{3.19}$$

Furthermore, the kinetics of morphogenesis, i.e. the transition of cells to the next compartment during growth must be included to describe the mass fraction changes within the mycelium:

$$\frac{d}{dt}\begin{pmatrix} z_A \\ z_S \\ z_H \end{pmatrix} = \begin{pmatrix} k_1 \cdot z_S - k_2 \cdot z_A + (\mu_A - \mu) \cdot z_A \\ -k_1 \cdot z_S + k_2 \cdot z_A - k_3 \cdot z_S + (\mu_S - \mu) \cdot z_S \\ k_3 \cdot z_S - \mu \cdot z_H \end{pmatrix} \tag{3.20}$$

It is presumed that the morphogenesis reactions are 1st order reactions with the rate constants k_i (Weuster-Botz and Takors, 2018). When other characteristic aspects of filamentous growth, like sporulation, hydrodynamics or morphology, were taken into account, it becomes clear that a complete mathematical description of growth, substrate uptake and product formation of filamentous fungi is highly complex and would go beyond the scope of this thesis.

The macromorphological characteristics of fungal growth also affect the process level. Pelleted growth does not influence the rheological behavior of the fermentation broth, whereas mycelial growth results in increased viscosity and non-Newtonian flow properties (Riley et al., 2000). A structural-viscose or shear-thinning behavior is observed, where increased shear rates lead to decreasing viscosity. This behavior is presumably caused by the disentanglement of mycelial aggregates and alignment of hyphal strings along the flow direction (Nienow, 1990). In stirred-tank bioreactors, the rheological characteristics of fungal broths decrease homogeneity within the fermentation. Cells in the vicinity of the stirrers are exposed to high shear rates, whereas hyphae distant to the stirrers experience low shear rates and form highly viscous areas, where homogenization and oxygen provision are hampered to the point of “dead zones” with no fluid motion (Chmiel and Walitza, 2018). On the other hand, the introduction of shear forces changes the morphology and hence can influence the product formation (Pazouki and Panda, 2000). Because of these complex interactions and the resulting effects, it is of essential importance to find optimal cultivation parameters which ensure sufficient homogenization and avoid oxygen limitation while considering the shear sensitivity of the organisms.

3.2.4. Process scale-up

Usually, bioprocesses are developed and improved in small-scale bioreactors in laboratories. Afterwards, a successful scale-up to industrial-scale production reactors with volumes of several m^3 is essential for the economic realization of such processes (Chmiel et al., 2018). The scale-up is conducted by creating comparable growth environments for the cells to achieve similar process performance. This can be reached by various approaches, which differ in complexity (Garcia-Ochoa and Gomez, 2009). Fundamental and semi-fundamental methods are based on detailed knowledge of hydrodynamics and mass transfer in the reactor. Computational fluid dynamics (CFD) simulations can be applied for the analysis of flow patterns and prediction of scale-up results (Dhanasekharan et al., 2005). The equations from the fundamental model are simplified for the semi-fundamental approach and applied to approximate the process (Garcia-Ochoa and Gomez, 2009), nevertheless still remaining highly complex. The dimensional analysis comprises the description of a bioprocess based on rates or time constants (Garcia-Ochoa and Gomez, 2009). For a subsequent analysis, those parameters, e.g. mixing and circulation times, are kept constant to achieve comparable process conditions, in this case a similar mixing efficiency (Pollard et al., 2007). The most commonly applied scale-up approach is, however, the rule of thumb method (Garcia-Ochoa and Gomez, 2009). Those criteria rest upon easily measurable or determinable

values that are set to remain constant throughout the process transfer. The most used criteria are a constant volumetric power input, a constant volumetric oxygen transfer coefficient k_La or a constant stirrer tip speed (Margaritis and Zajic, 1978). Other potentially useful criteria are geometrical similarity of the reactors or a constant volumetric aeration rate (Chmiel et al., 2018).

The specific characteristics of filamentous fungi in cultivation processes can have a tremendous effect on the scale-up. Increased viscosity of a fungal fermentation broth can lead to insufficient mixing and oxygen limitations in larger bioreactors (Gibbs et al., 2000). Another challenge is posed by the complex interactions between shear forces, fungal morphology and product formation. Thus, the choice of the scale-up criteria and the consideration of the biological responses are essential, and detailed knowledge of the requirements and limitations of the process at hand are necessary (Pollard et al., 2007). A simple approach that has been proven successful for fungal fermentations is the criterion of constant stirrer tip speed (Chmiel et al., 2018):

$$\pi \cdot n_1 \cdot d_1 = \pi \cdot n_2 \cdot d_2 \tag{3.21}$$

with n_i as the stirring rate and d_i as the stirrer diameter in the respective reactor. This approach aims for constant maximum shear forces in the reactor, preventing excessive cell damage or changes in morphology. Nevertheless, this method also results in reduced volumetric power input and oxygen transfer (Garcia-Ochoa and Gomez, 2009). A constant volumetric power input, on the other hand, increases the maximum energy dissipation introduced into the fermentation broth, with potentially detrimental effects. Scale-up criteria based on aeration parameters, like constant volumetric aeration rates or oxygen transport coefficients k_La, are promising approaches for aerobic fermentations that are potentially subject to oxygen limitation (Pollard et al., 2007). The method of a constant specific oxygen transfer coefficient k_La was exemplary applied successfully with the cultivation of *Aspergillus terreus* for the production of itaconic acid (transfer from 5 L to 50 L) (Shin et al., 2013) or *Glarea lozoyensis* for pneumocandin production (different reactors from 70 L to 57 m^3) (Pollard et al., 2007). In this case, the criterion was chosen after a regime analysis suggested oxygen transfer as the limiting step. This further underlines the need for detailed knowledge of the process to select the criteria for efficient scale-up.

3.3. Wheat bran as agricultural residue

3.3.1. Origin, abundance and traditional usage

Wheat is one of the most important cereals in the world, with an annual global production of more than 760 million tons in 2020. Most of it is processed into flour for the food industry (Prueckler et al., 2014). The most important byproduct of this process is wheat bran, which consists of the outer layers of the wheat grain, aleurone layer, testa and pericarp as well as parts of the endosperm (Koutinas et al., 2005). These fractions comprise ~25% of the wheat grain's mass (Neves et al., 2006), leading to potentially 150-200 million tons wheat bran piling up worldwide each year. For the most part, it is currently used as animal feed, and small amounts are applied in human nutrition, mainly in bakery and cereal products (Prueckler et al., 2014). Wheat bran is assumed to have several beneficial health effects on the human body and thus is part of a whole grain nutrition. These positive effects are based on the one hand on its high dietary fiber content, on the other hand on a variety of biologically active compounds like antioxidants, flavonoids or phenolic acids (Apprich et al., 2014, Prueckler et al., 2014).

3.3.2. Structure and composition

The composition of wheat bran is heterogenous and depends on various factors, amongst others processing methods, wheat cultivar as well as growth location and conditions (Prueckler et al., 2014). In general, wheat bran is mostly formed from plant cell walls. These consist of a primary scaffolding network formed by cellulose, a polysaccharide formed by linear chains of β-1,4-linked glucose monomers (Carpita, 1996). Hydrogen bonds between the single chains connect them to crystalline microfibril structures, which can be interspersed with amorphous regions (Figure 3.4).

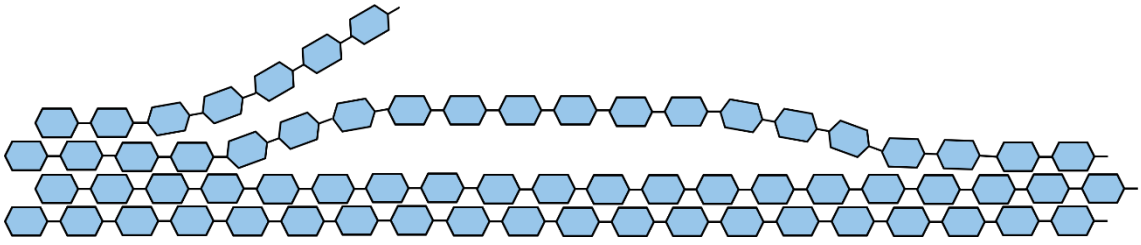

Figure 3.4: Schematic depiction of the structure of cellulose.

In grasses and cereal plants, these cellulose fibers are embedded in a hemicellulose matrix mostly formed by glucuronoarabinoxylans and arabinoxylans (Carpita and McCann, 2002). These comprise a backbone of β-1,4-bonded xylose units bearing arabinose, glucuronic acid or acetyl side chains, as schematically shown in Figure 3.5. Additionally, the arabinose residues can be esterified with ferulic acid molecules (Carpita,

1996, Izydorczyk and Dexter, 2008). These feruloyl residues can form cross-linkers to other xylan chains as well as the phenylpropanoid lignin network via dimerization, hence contributing to the stabilization of the cell walls (Iiyama et al., 1994, Carpita and McCann, 2002). The number and sites of saccharide side chains depends on the histological source of the arabinoxylan and influences the development of hydrogen bonds between xylan chains. The outer layers, pericarp and testa, contain a complex hemicellulose network with a rather high ratio of arabinose to xylose embedded into a lignin matrix, while the aleurone layer is mainly composed by linear arabinoxylans with low arabinose content and monomeric phenolic residues (Prueckler et al., 2014).

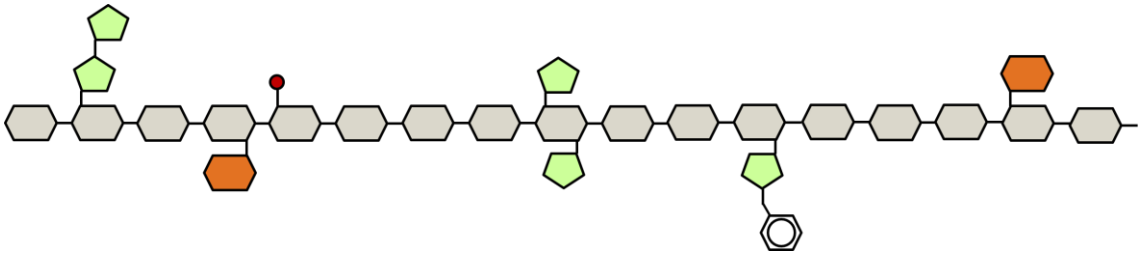

Figure 3.5: Schematic depiction of the structure of arabinoxylan. : xylose, : arabinose, : glucuronic acid, : ferulic acid, : O-acetyl group.

As mentioned above, parts of the starch-containing endosperm end up in the wheat bran, as a complete separation of the kernel layers during processing is not feasible (Apprich et al., 2014). Starch is a glucose homopolymer and exists in the form of unbranched α-1,4-linked amylose helices or as branched amylopectin (schematically displayed in Figure 3.6). In wheat, starch is found in granules that differ in size and properties (Xie et al., 2008).

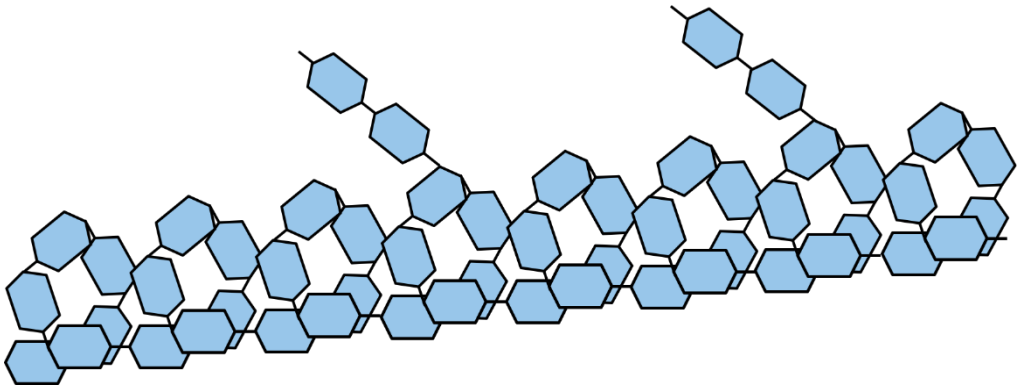

Figure 3.6: Schematic depiction of the structure of starch.

The aleurone layer additionally contains β-glucans, proteins and minerals.

Altogether, wheat bran has a quite complex composition of different biopolymers. Literature as well as analytics conducted by the project partners from the Werner Siemens Chair for Synthetic Biotechnology (WSSB, TUM, Garching, Germany) state a

carbohydrate content of ~55-60%, together with 13-18% protein and 3.5% fat (Apprich et al., 2014). The distribution of the three major polysaccharides may differ within the carbohydrate fraction. Starch contents of 14-24%, arabinoxylan contents of 11-26% and a cellulose content of 11% are described in literature (Dornez et al., 2006, Hemery et al., 2007, Apprich et al., 2014). The detailed monomer analysis by WSSB resulted in (w/w of total carbohydrates): 40.7% glucose, 24.4% xylose and 34.9% other sugars, assumably mostly arabinose. Nandini and Salimath (2001) reported weight percentages of 26%, 27% and 37% for glucose, xylose and arabinose, respectively.

3.3.3. Enzymatic degradation of wheat bran

The complex structure and composition of wheat bran complicates its enzymatic degradation. Therefore, the hydrolysis of the three main polysaccharides in wheat bran should be described in detail in the following chapter.

The heterogenous structure of hemicellulose requires multiple different enzyme activities for its complete and efficient depolymerization. Many microorganisms, including the filamentous fungi *A. niger* and *T. reesei*, produce a spectrum of xylanolytically active enzymes for its degradation (Wong et al., 1988). Generally, xylanases can be classified according to their activities into endoxylanases, β-xylosidases and enzymes acting on the side chains. Endoxylanases mainly hydrolyze the glycosidic bonds on specific sites in the xylan backbone, dependent on properties of the substrate molecule, e.g. the chain length or the presence of branching points (Wong et al., 1988, Polizeli et al., 2005). The second group, β-xylosidases, further cleave the products of endoxylanase activity by releasing xylose monomers from the non-reducing ends of xylooligosaccharides (Polizeli et al., 2005). Exoxylanases prefer the reaction on longer oligomers, while β-xylobiase cleaves dimers into two xylose molecules. As these xylan fragments are assumed to inhibit the activity of endoxylanases, the collaboration of endoxylanases and β-xylosidases is essential for efficient degradation of hemicellulosic substrates (Wong et al., 1988). Side chains sterically hinder the activities of endo- and exoxylanases, therefore enzymes cleaving off the substitutes are of great importance (Polizeli et al., 2005). Debranching xylanases, arabinases and arabinosidases are able to remove arabinose residues from the xylan backbone (Kaji, 1984, Tagawa and Kaji, 1988, Wong et al., 1988). The less frequent side groups glucuronic acid, O-acetyl and ferulic acid are released by specific hydrolases and esterases, namely glucuronidase, acetyl xylan esterase and feruloyl esterase (Biely et al., 1985, Puls et al., 1987, Tenkanen et al., 1991).

Starch-degrading amylases can be found in bacteria, fungi, plants and animals throughout all kingdoms. Three different groups are described in literature, distinguishable by the respective enzymatic mechanism (Saranraj and Stella, 2013). The first group is posed by α-amylases, or endoamylases. These enzymes cleave α-1,4-glycosidic bonds in the amylose chains on random sites, resulting in oligomers of differing chain lengths down to dimers or branched α-limit dextrins (Van Der Maarel et al., 2002). Enzymes from the second group, β-amylases, act on the non-reducing ends of starch chains and cleave off maltose units. Glucoamylases, also called γ-amylases, and α-glucosidases both release single glucose monomers from the non-reducing ends of glucooligomers like maltose or maltotriose, as well as from longer glucan chains (Chiba, 1997). These two groups are distinguished by the detailed reaction mechanism: the hydrolytic reaction of α-glucosidases is retaining the anomeric α-configuration of the glucose molecule, whereas the hydrolysis with a glucoamylase forms β-glucose via an inverting mechanism (Chiba, 1997). Additionally, glucoamylases can cleave the α-1,6-glycosidic bonds on the branching points of amylopectin (Saranraj and Stella, 2013).

Cellulose is the most recalcitrant polysaccharide found in plant biomass. Its hydrolytic degradation hence requires highly specialized enzymes, which exist in noncomplexed or complexed systems (Lynd et al., 2002). Aerobic fungi like *T. reesei* produce free, noncomplexed cellulase systems, consisting of three main enzyme types: endo-glucanases, exo-glucanases and β-glucosidases (Bhat and Bhat, 1997). The endo-glucanases attack amorphous, accessible regions of the cellulose fibers. The resulting non-reducing ends are subsequently removed by endo-glucanases or cellobio-hydrolases, releasing cellobiose units (Wood and Bhat, 1988). Other cellobiohydrolases show a preference towards reducing ends, and glucanohydrolases can directly release glucose from longer glucan chains (Lynd et al., 2002). The β-glucosidases eventually cleave the disaccharidic cellobiose into glucose monomers. The cellulolytic system of *T. reesei* is also described in detail in Chapter 3.1.2. Complexed cellulase systems or cellulosomes are predominantly formed by anaerobic bacteria. In these complexes, the hydrolytically active enzymes are attached to the bacterial cell wall via dockerin domains and a scaffoldin protein carrying cohesin moieties (Lynd et al., 2002). Additionally, cellulosomes usually possess carbohydrate-binding modules, binding the cell with the enzymatic complex to the cellulose microfibrils. The subsequent reactions of endo- and exo-glucanases resemble those of fungal cellulases. Instead of cellobiose cleavage by β-glucosidases, many anaerobic bacteria take up cellobiose and cellodextrins for intracellular conversion by respective phosphorylases (Lynd et al., 2002). Well-studied examples for microorganisms possessing cellulosomes are the clostridia *C. thermocellum* and *C. cellulolyticum* (Bayer et al., 1994, Bélaich et al., 1997).

3.3.4. Biotechnological approaches for utilization

Agricultural byproducts and residues pose an abundant and largely untapped resource for carbohydrates and other valuable compounds. Therefore, they came into focus of studies investigating their utilization. Hereby, the greater goal is the establishment of a circular and waste-free bioeconomy (Velasco-Muñoz et al., 2022, Yaashikaa et al., 2022). As already mentioned above, wheat bran is globally generated in vast quantities and thus possesses great potential for further valorization. Some components can be used directly, while other approaches pursue the conversion into valuable products using biorefinery concepts (Apprich et al., 2014). Examples for direct utilization are the carbohydrates starch, arabinoxylan or β-glucan, which mainly find application in the food industry (Li et al., 2006, Xie et al., 2008, Sun et al., 2011). Other studies explored the extraction of ferulic acid or wheat bran protein and oil as food/feed additives (Roberts et al., 1985, Buranov and Mazza, 2009, Brandolini and Hidalgo, 2012). Modern biorefinery concepts aim for more value-added products like platform chemicals (Apprich et al., 2014). These processes require the pretreatment of the bran to release convertible sugars, mainly glucose and xylose, by for instance extrusion, steam explosion or enzymatic hydrolysis (Reisinger et al., 2013, Jiang and Guo, 2016, Aktas-Akyildiz et al., 2020). Thereafter, the hydrolysate can be utilized in a broad variety of bioconversion processes. Common platform chemicals produced from wheat bran hydrolysate are organic acids like lactic acid, a precursor for bioplastics (Li et al., 2010, Tirpanalan et al., 2015). The application of wheat bran-based hydrolysates in ABE (acetone – butanol – ethanol) fermentation with clostridia or yeasts offers a great potential for the biofuel production (Palmarola-Adrados et al., 2005, Favaro et al., 2013, Cripwell et al., 2015, Farkas et al., 2019). As many other microorganisms are able to utilize glucose and xylose, a large variety of further products, e.g. bulk and fine chemicals or microbial lipids, appears feasible from wheat bran hydrolysate.

4. Material and Methods

4.1. Microorganisms

Six strains of *Aspergillus niger* were tested for initial strain selection. These strains and their characteristic properties are listed in Table 4.1. All strains were assumed from a former project and were stored at the institute in the form of cryo cultures. All strains were used in initial shaking flask experiments. The strains *A. niger* N402, *A. niger* NRRL 3122 and *A. niger* NRRL 2270 were cultivated in a subsequent cultivation in parallel bioreactors for final selection. All following co-cultivation experiments were conducted with the strain *A. niger* NRRL 2270.

Table 4.1: Description of *A. niger* strains for initial strain selection.

Strain	Description	References
N400	Wild-type strain, high gluconic acid producer	(Moyer et al., 1940, Blom et al., 1952)
N402	Mutant of N400, lab strain for mitotic studies	(Bos et al., 1988, Debets et al., 1993)
NRRL 3122	Mutant, industrial producer of glucoamylase	(Van Lanen and Smith, 1968, van Dijck et al., 2003)
CBS 513.88	Mutant of NRRL 3122, high glucoamylase producer	(Pel et al., 2007, Andersen et al., 2011)
NRRL 328	Wild-type strain, citric acid producer	(Currie, 1917, Andersen et al., 2011)
NRRL 2270	Mutant of NRRL 328, improved citric acid production	(Perlman et al., 1946, Dai et al., 2004)

The second organism in this work was *Trichoderma reesei* RUT-C30. It was obtained from the project partners at WSSB (TUM, Garching, Germany) on agar plates. Spores were harvested after sufficient cultivation at 30 °C and cryo cultures were prepared as described in Section 4.3.

4.2. Media and buffers

Spore preparation medium

The fungi were cultivated on agar plates to produce spores for either storage at –80 °C or as preculture for processes with spore inoculation. *A. niger* spores were grown on 39 g L^{-1} potato extract dextrose agar supplemented with 10 g L^{-1} yeast extract and 1 mL L^{-1} trace element solution. Potato extract dextrose agar and yeast extract were

suspended in deionized water (ddH_2O) and dissolved during autoclaving at 121 °C for 20 min. The trace element solution (Table 4.4) was added aseptically after cooling to < 60 °C. The agar was poured into petri dishes and stored at room temperature after cooling. Spores of *T. reesei* were cultivated on potato extract dextrose agar plates (39 g L^{-1}) without any supplements.

Spore suspension solution

The spore suspensions for inoculation were prepared and diluted with a solution of 8.9 g L^{-1} sodium chloride and 0.05% (v/v) Tween 80. The components were dissolved in ddH_2O and autoclaved at 121 °C for 20 min.

Minimal medium

All cultivations in shaking flasks and bioreactors were conducted using a minimal salt medium. The composition of this basal medium is listed in Table 4.2. Stock solutions of the nitrogen source (289 g L^{-1} $(NH_4)_2SO_4$), the potassium salt solution (75 g L^{-1} KH_2PO_4 and 25 g L^{-1} KCl, titrated to pH 4.5), magnesium sulfate (250 g L^{-1} $MgSO_4 \cdot 7\ H_2O$), the trace element solution (Table 4.4) and antifoaming agent (10% polypropylenglycol P2000) were prepared separately, autoclaved at 121 °C for 20 min and stored at 4 °C until usage. For the final cultivation media, the minimal salt media components were mixed accordingly and supplemented to the respective carbon source.

Table 4.2: Composition of the minimal salt medium for the cultivation of *A. niger* and *T. reesei*.

Component		Concentration	
Nitrogen source	$(NH_4)_2SO_4$	23.1	g L^{-1}
Salts	KH_2PO_4	1.5	g L^{-1}
	KCl	0.5	g L^{-1}
	$MgSO_4 \cdot 7\ H_2O$	0.5	g L^{-1}
Trace element solution		1	mL L^{-1}
Antifoaming agent	PPG P2000	1	mL L^{-1}

Preculture medium

The preculture medium contained 10 g L^{-1} yeast extract and 10 mM of each xylose, maltose and lactose. The yeast extract solution as well as the sugar solution were prepared and autoclaved separately before mixing and supplementation with the minimal media components (Table 4.2).

Synthetic wheat bran medium

A defined synthetic wheat bran medium was used to imitate the carbon composition of wheat bran. The carbon sources and their respective concentrations in the final medium are listed in Table 4.3. The components were weighed in, suspended and autoclaved in a separate glass bottle (0.7 L scale) or the reactor vessel (3 L and 25 L scale) before supplementation with the minimal media components. Birch wood xylan was used as xylan unless stated otherwise.

Table 4.3: Carbon sources in the synthetic wheat bran medium.

Component	Concentration	
Xylan	7	g L^{-1}
Starch	10	g L^{-1}
Microcrystalline cellulose (Avicel)	3	g L^{-1}
Glucose	1	g L^{-1}

Wheat bran medium

For cultivation experiments using wheat bran as the substrate, 30 g L^{-1} of wheat bran were suspended in water in the respective reactor before *in-situ* sterilization. The milled and pre-dried wheat bran (provided by the project partners Bayerischer Müllerbund e.V. (Munich, Germany)) was stored at −20 °C and dried at 50 °C for minimum 48 h before use. The bran's composition was analyzed by the project partners of WSSB (TUM, Garching, Germany) via total acidic hydrolysis and HPLC. A total sugar content of 0.555 g g^{-1} was determined, thereof 0.225 g g^{-1} glucose, 0.135 g g^{-1} xylose and 0.193 g g^{-1} other sugars. Other notable components were 0.145 g g^{-1} total protein and 0.080 g g^{-1} total ash.

Trace element solution

The trace element solution added to the minimal salt medium was assumed from Vishniac and Santer (1957). The components for a stock solution (1000×, Table 4.4) were dissolved in ddH_2O, and the pH was set to pH 4.0 before thermal sterilization. The solution was stored at 4 °C until use.

Table 4.4: Composition of the trace element solution (1000×).

Component	Concentration	
EDTA · 2 H_2O	10	g L^{-1}
$ZnSO_4$ · 7 H_2O	4.4	g L^{-1}
$MnCl_2$ · 4 H_2O	1.01	g L^{-1}
$CoCl_2$ · 6 H_2O	0.32	g L^{-1}
$CuSO_4$ · 5 H_2O	0.32	g L^{-1}
$(NH_4)_6Mo_7O_{24}$ · 4 H_2O	0.22	g L^{-1}
$CaCl_2$ · 2 H_2O	1.47	g L^{-1}
$FeSO_4$ · 7 H_2O	1	g L^{-1}

Buffer for hydrolysis and analysis

Sodium acetate (NaAc) solution was used as buffer for the hydrolysis processes. Trisodium acetate dihydrate was dissolved in ddH_2O, and the pH was titrated to pH 4.5. The concentration of the NaAc solution was individually adapted for each experiment to achieve the desired final concentration after addition of the enzyme solution.

4.3. Cultivation of fungi

4.3.1. Preparation and storage of spore suspensions

Spores were prepared by inoculation of agar plates with 30 µL of the cryo cultures and cultivation at 30 °C for 5 and 7 d for *A. niger* and *T. reesei*, respectively. Afterwards, the spores were suspended in 10 mL sterile spore suspension solution using sterile single-use spatulas, filtered through sterile cotton wool and washed via centrifugation and resuspension in 10 mL fresh spore suspension solution. The spore concentration was determined by measuring the extinction at 600 nm (OD_{600}) in a microtiter plate photometer (Multiskan FC, Thermo Fisher Scientific Inc., Waltham, USA), based on a strain-specific linear correlation. Further proceedings depended on the purpose of the spores.

For new cryo cultures, the resulting spore suspension was mixed with 30% sterile glycerol, aliquoted into sterile 2 mL reaction tubes and stored at −80 °C.

For the inoculation of cultivation experiments, the spore suspensions were diluted with spore suspension solution to the desired spore concentration and stored at 4 °C until usage.

4.3.2. Cultivation in shaking flasks

Shaking flask cultivation experiments with *A. niger* were conducted for strain selection. Unbaffled 1 L shaking flasks were filled with 200 mL minimal medium (Table 4.1) containing 1 g L^{-1} glucose and 20 g L^{-1} of either xylan or starch, inoculated with 500 µL spore suspension (OD_{600} = 0.2) and cultivated for 96 h at 30 °C and a shaking rate of 180 min^{-1} (eccentricity 25 mm).

T. reesei was also cultivated in 1 L shaking flasks with 200 mL minimal medium (Table 4.1). Five carbon sources (microcrystalline cellulose, wheat bran, carboxymethyl-cellulose, lactose, glucose) were used at a concentration of 20 g L^{-1}, each batch was additionally supplemented with 1 g L^{-1} glucose. The flasks were inoculated with 390 µL spore suspension and incubated for 99 h at 30 °C and a shaking rate of 180 min^{-1} (eccentricity 25 mm).

Samples for evaluation of enzyme formation were taken from the flasks at the end of cultivation, and the supernatant containing the enzymes was separated via centrifugation and sterile-filtration before storage at −20 °C.

4.3.3. Preculture preparation in shaking flasks

Vegetative precultures were cultivated in 1 L shaking flasks without baffles filled with 200 mL preculture medium. *A. niger* NRRL 2270 precultures were started by inoculation with 10^9 spores L^{-1} and were incubated at 30 °C and a shaking rate of 180 min^{-1} for 48 h. *T. reesei* RUT-C30 precultures were inoculated with 0.2 × 10^9 spores L^{-1} and were incubated at the same conditions for 72 h. Repeated cultivations were conducted to determine the achievable biomass concentrations and thus to enable the calculation of preculture volumes necessary for inoculation. The cells were subsequently drawn into sterile syringes or mixed in a sterile glass bottle for inoculation of processes on the 3 L and 25 L scale, respectively.

4.3.4. Batch co-cultivation in parallel stirred-tank reactors on the 0.7 L scale

Cultivations on the 0.7 L scale were conducted in a parallel bioreactor system with four identical glass stirred-tank reactors with a maximum volume of 1.2 L (DASGIP, Eppendorf AG, Hamburg, Germany). All vessels were equipped with probes for pH, temperature and dissolved oxygen concentration (DO), an L-shaped gassing sparger, a sampling tube and a stirrer axis with one inclined blade stirrer (80 mm above vessel bottom) and one Rushton turbine (30 mm above vessel bottom). The geometrical features of the reactor vessel are listed in Table 4.5.

Table 4.5: Geometrical features of the 0.7 L stirred-tank bioreactor. ↓: stirrer pumping downwards, H_{Liquid}: liquid height in the reactor, $d_{Reactor}$: inner diameter of the reactor, $d_{Stirrer}$: diameter of the Rushton impellers.

Bottom geometry	Flat bottom
Stirrer configuration	1 × inclined blade stirrer ↓
	1 × Rushton impeller
Baffles	0
Ratio $H_{Liquid}/d_{Reactor}$	0.9
Ratio $d_{Stirrer}/d_{Reactor}$	0.5

Temperature control was carried out via heating or cooling of the reactor block. Metabolic activity was observed indirectly by exhaust gas composition analysis (O_2 and CO_2, BlueVary, BlueSens gas sensors GmbH, Herten, Germany). The software DASware® control (Eppendorf AG, Hamburg, Germany) was used for process control, data monitoring and recording.

Figure 4.1: Parallel bioreactor system for cultivation experiments on the 0.7 L scale (Photo: Tobias Haase, TUM).

After assembling and pH probe calibration, the reactors were filled with ddH_2O and autoclaved. Subsequently the water was removed, and 700 mL of synthetic wheat bran medium was filled into the reactors under sterile conditions. The vessels were set into the reactor block, and temperature, pH and aeration were adjusted to their respective

starting values for DO probe calibration. Cultivation experiments were eventually started by inoculation with either spore suspensions or vegetative shaking flask precultures.

In the case of spore inoculation, the desired spore concentrations were transferred into the reactor via syringes and the sampling tube. 0.2×10^9 spores L^{-1} of *T. reesei* were used for inoculation, and 10^9 spores L^{-1} of *A. niger* were added either simultaneously or with a certain delay. The monocultures were inoculated with the respective spore concentrations individually. The reactors were not actively aerated and stirred at a low agitation rate of 250 min^{-1} during the first 6 h to prevent spore loss. Afterwards, gassing and stirring rates were increased to their respective setpoints.

Cultivations with shaking flask precultures were started by inoculation with the respective volumes of expanded cells via syringes and the sampling tube. A total initial biomass concentration of 1.2 g L^{-1} was used with varied initial biomass ratios of the strains. Unlike with spore inoculation, no phase of lowered aeration and agitation was necessary.

The temperature of all cultivation processes was held constant at 30 °C. The pH was controlled at pH 4.5 by automatic titration with 1 M H_2SO_4 or 3 M KOH. The agitation rate remained constant at the respective setpoint throughout process time, and the aeration rate could be gradually increased to the respective maximum value to keep the DO above the critical threshold of 30%. Cultivations were conducted for 72-96 h, and samples were taken regularly through the sampling tube to analyze enzyme activities as well as extracellular metabolite concentrations over time.

Processes were terminated by stopping the process control software. The enzymes in the supernatant were harvested by centrifugation and sterile-filtration and stored at −20 °C until usage for hydrolysis experiments.

4.3.5. Batch co-cultivation in a stirred-tank bioreactor on the 3.0 L scale

A 7.5 L stirred-tank bioreactor with three baffles (Labfors, Infors HT, Bottmingen, Switzerland) was applied for cultivation experiments on the 3.0 L scale. The reactor was equipped with temperature, pH and DO sensors, a gas sparger and a sampling tube reaching down to the bottom of the vessel. Homogenization was realized by a stirrer configuration of (from top to bottom) one downward pumping inclined blade stirrer (160 mm above vessel bottom), one upward pumping inclined blade stirrer (90 mm above vessel bottom) and one Rushton turbine (30 mm above vessel bottom). Table 4.6 lists the geometrical details of the bioreactor.

Table 4.6: Geometrical features of the 3.0 L stirred-tank bioreactor. ↓: stirrer pumping downwards, ↑: stirrer pumping upwards, H_{Liquid}: liquid height in the reactor, $d_{Reactor}$: inner diameter of the reactor, $d_{Stirrer}$: diameter of the Rushton impellers.

Bottom geometry	Round bottom
Stirrer configuration	1 × inclined blade stirrer ↓
	1 × inclined blade stirrer ↑
	1 × Rushton impeller
Baffles	3
Ratio $H_{Liquid}/d_{Reactor}$	1.3
Ratio $d_{Stirrer}/d_{Reactor}$	0.37

The reactor was controlled by the integrated control station, and process data were recorded by the control software eve® (Infors HT, Bottmingen, Switzerland). Off-gas analysis (BlueVary, BlueSens gas sensors GmbH, Herten, Germany) was used to monitor oxygen uptake and CO_2 evolution.

The reactor was assembled and filled with 2 L ddH_2O containing the carbon components of the synthetic wheat bran medium (Table 4.3), and the pH probe was calibrated prior to sterilization. Afterwards, sedimented particles were resuspended by immediate stirring, and the medium was complemented with all other media components through a peristaltic pump. Temperature, gas flow and pH were set to the respective setpoints before the DO probe and the exhaust gas analyzer were calibrated.

For experiments with spore inoculation, 0.2×10^9 spores L^{-1} of *T. reesei* RUT-C30 were injected into the reactor through the sampling tube. No active aeration and a lowered agitation rate of 250 min^{-1} were applied for 6 h after inoculation to avoid spore drag-out. *A. niger* NRRL 2270 spores were added to a concentration of 10^9 spores L^{-1} after 16.5 h process time.

Vegetative fungal cells from shaking flask precultures were prepared in syringes for inoculation with an initial total biomass concentration of 1.2 g L^{-1} (1.0 g L^{-1} *A. niger* NRRL 2270, 0.2 g L^{-1} *T. reesei* RUT-C30) and added to the reactor via the sampling tube.

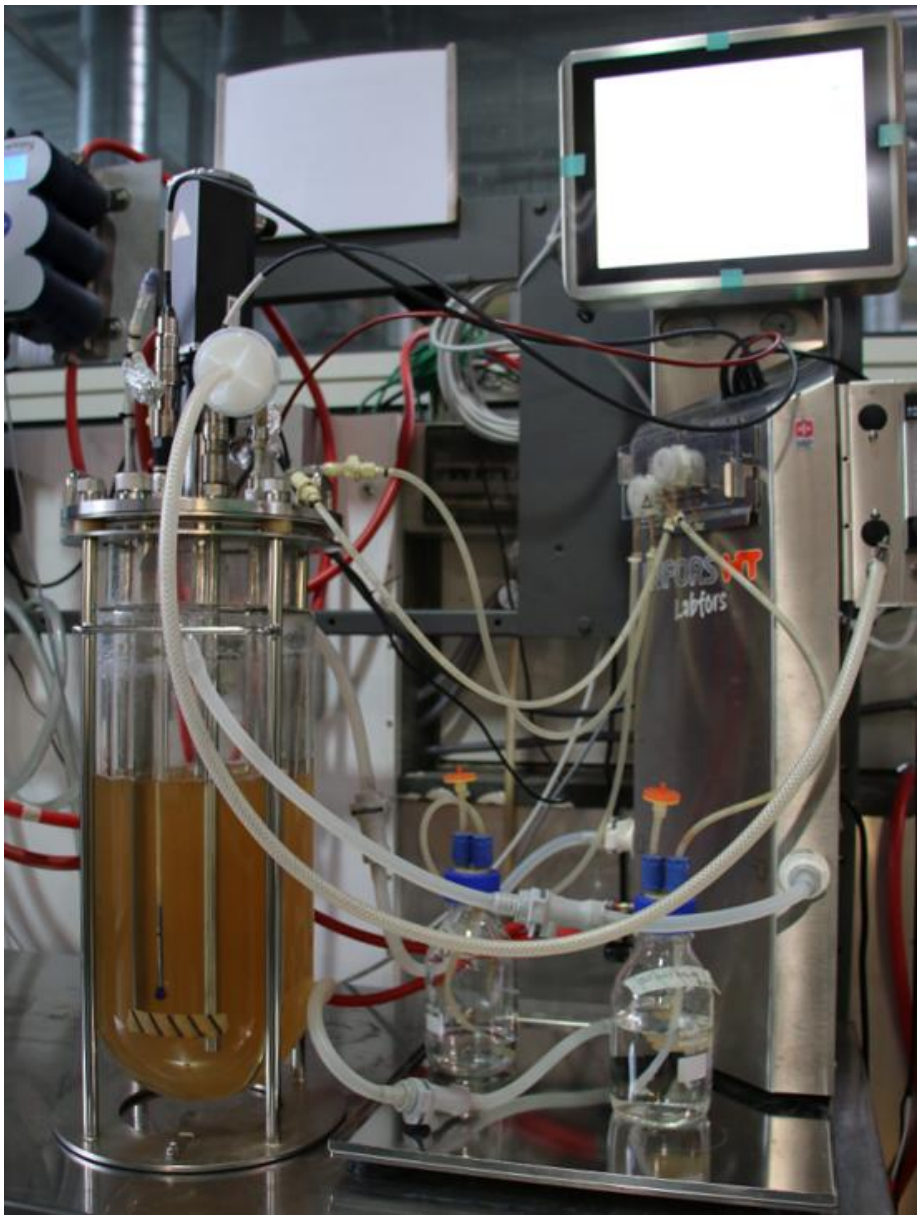

Figure 4.2: Stirred-tank bioreactor for cultivation experiments on the 3.0 L scale.

A temperature of 30 °C was kept constant throughout all cultivations, and pH 4.5 was maintained by automated addition of 1 M H_2SO_4 or 3 M KOH. The agitation rate was set to 660 min^{-1}, and the aeration rate of initially 0.6 L min^{-1} (0.2 vvm) was increased in steps of 0.6 L min^{-1} up to a maximum of 6 L min^{-1} when necessary to keep DO concentration above 30%. The batch cultivations were carried out for 65-86 h and were sampled regularly throughout the process time.

At the end of the process, the fermentation broth was pumped out of the reactor through the sampling tube. The supernatant containing the enzymes was separated from the biomass by centrifugation and sterile-filtration and stored at −20 °C until further usage.

4.3.6. Batch co-cultivation in a stirred-tank bioreactor on the 25 L scale

Batch cultivation processes on the 25 L scale were carried out in a stainless steel stirred-tank bioreactor (Techfors, Infors HT, Bottmingen, Switzerland) with four baffles and a maximum working volume of 42 L. Either three Rushton impellers or a setup of (from top to bottom) one downward pumping inclined blade stirrer, one upward pumping inclined blade stirrer and one Rushton turbine served for homogenization of the fermentation broth. The reactor's geometrical features are summed up in Table 4.7.

Table 4.7: Geometrical features of the 25 L stirred-tank bioreactor. ↓: stirrer pumping downwards, ↑: stirrer pumping upwards, H_{Liquid}: liquid height in the reactor, $d_{Reactor}$: inner diameter of the reactor, $d_{Stirrer}$: diameter of the Rushton impellers.

Bottom geometry	Rounded bottom
Stirrer configuration	3 × Rushton impellers or: 1 × inclined blade stirrer ↓ 1 × inclined blade stirrer ↑ 1 × Rushton impeller
Baffles	4
Ratio $H_{Liquid}/d_{Reactor}$	1.8
Ratio $d_{Stirrer}/d_{Reactor}$	0.41

Probes for temperature, pH and DO as well as the steam-sterilizable sampling valve were mounted at the bottom of the vessel; a pressure sensor, the anti-foam probe and inlets for media components and titration agents were installed at the reactor lid. A part of the off-gas stream was branched off after the cooler and a foam trap into an exhaust gas analyzer measuring O_2 and CO_2 content (EasyLine, ABB Automation, Zurich, Switzerland). Process control, data monitoring and recording was realized by the IRIS® Control Software (Infors HT, Bottmingen, Switzerland).

The pH and DO probes were set into the reactor, and the sampling valve and the mechanical seal were steam-sterilized. The reactor was filled with 20 L water and either the carbon components of the synthetic wheat bran medium (Table 4.3) or 750 g (30 g L^{-1}) wheat bran prior to *in-situ* sterilization (120 °C, 20 min). The reactor was cooled to 30 °C afterwards, before the tubes for titration agents and media components were connected and the medium was completed aseptically. The cultivation parameters were adjusted to the respective initial values (pH 4.5, agitation rate 330 min^{-1}, aeration rate 5 L min^{-1}) before calibration of DO probe and off-gas analysis.

The processes were started by inoculation with vegetative fungal cultures with an initial total biomass concentration of 1.2 g L^{-1}, divided into 1.0 g L^{-1} *A. niger* NRRL 2270 and 0.2 g L^{-1} *T. reesei* RUT-C30. The precultures were collected in a sterile glass bottle and aseptically pumped into the reactor.

Figure 4.3: Stirred-tank bioreactor for cultivation experiments on the 25 L scale (Photo: Tobias Haase, TUM).

The cultivation temperature was 30 °C, and pH 4.5 was held automatically by titration with 1 M H_2SO_4 or 3 M KOH. The DO was kept above 30% by gradually increasing the

aeration rate from 5 L min^{-1} (0.2 vvm) to the technical maximum of 43 L min^{-1} (1.72 vvm), and the pressure was set to 1.2 bar overpressure at a suitable process time. Cultivations were either conducted with a constant agitation rate of 330 min^{-1} or with an agitation rate controlled between 330-600 min^{-1}. In the latter case, the stirring rate was controlled by an asymmetrical proportional controller. The proportionality factor for the reduction of the stirring rate was double the increasing factor to avoid excessive shear stress. The formation of foam was counteracted by a control sequence reducing the aeration and adding anti-foaming agent when triggered. Samples from the process were taken regularly through the steam-sterilizable sampling valve.

Separate enzyme production processes on the 25 L scale were stopped by quitting the process control and emptying the reactor. When the integrated hydrolysis of wheat bran followed up, the end of the enzyme production process was indicated by a rapid increase in DO, and the process was transitioned to the hydrolysis phase as described in detail below (Chapter 4.4.4).

4.3.7. Preculture preparation for cultivation on the 1000 L scale

The precultures for 1000 L scale processes were cultivated simultaneously in two separate stirred-tank bioreactors.

***Aspergillus niger* NRRL 2270**

The *A. niger* NRRL 2270 preculture was cultivated in a stirred-tank bioreactor with a maximum working volume of 50 L (LP75L, Bioengineering, Wald, Switzerland) at the TUM Pilot Plant for Industrial Biotechnology (Garching, Germany). The reactor was equipped with four baffles and two six-blade Rushton impellers for homogenization, a ring sparger for gassing and sensors for pH, DO, temperature (at the vessel bottom) and pressure (in the lid), and was controlled via the BioSCADALab software (Bioengineering, Wald, Switzerland).

The reactor was prepared and filled with 40 L ddH_2O and 500 g (10 g L^{-1}) yeast extract before *in-situ* sterilization (120 °C, 20 min). Sampling valve and mechanical seal were sterilized manually during the procedure, and the missing medium components were pumped into the reactor afterwards. DO calibration was carried out after adjusting the cultivation parameters to their setpoints. The preculture was started by inoculation with 1.2 L cells from shaking flasks, resulting in a total cultivation volume of 50 L.

The cultivation temperature was constant at 30 °C, and a constant pH 4.5 was held by automated titration with 1 M H_2SO_4 and 3 M KOH. The broth was homogenized with a constant stirring rate of 200 min^{-1}, the aeration rate was controlled between 25-

67 L min^{-1} and 0.7 bar overpressure was applied. The preculture was incubated for 22 h before being used for inoculation of the 1000 L process.

Figure 4.4: Stirred-tank bioreactor for preculture preparation of *A. niger* NRRL 2270 (Photo: Andreas Heddergott, TUM).

Trichoderma reesei RUT-C30

T. reesei RUT-C30 precultures for the 1000 L process were prepared in the same stirred-tank bioreactor used for co-cultivation experiments (Techfors, Infors HT, Bottmingen,

Switzerland, see Chapter 4.3.6). The reactor was assembled and prepared the same way as described above. 19 L ddH_2O and 250 g (10 g L^{-1}) yeast extract were filled into the vessel prior to *in-situ* sterilization, and the medium was complemented thereafter.

The reactor preculture was inoculated with 0.8 L shaking flask preculture at a total working volume of 25 L. The cultivation was conducted at 30 °C and a constant pH 4.5, titrated automatically with 1 M H_2SO_4 or 3 M KOH. Oxygen supply and homogenization were realized by the stepwise increasable gassing rate (5-40 L min^{-1}), 0.6 bar overpressure after 13 h process time, and the dynamically controlled agitation rate (330-475 min^{-1}). After a process duration of 34 h, the broth was transferred into sterile plastic containers for transport to the TUM Pilot Plant for Industrial Biotechnology and inoculation of the 1000 L process.

4.3.8. Batch co-cultivation in a stirred-tank bioreactor on the 1000 L scale

A stirred-tank bioreactor with a maximum working volume of 1000 L (LP1500, Bioengineering, Wald, Switzerland) at the TUM Pilot Plant for Industrial Biotechnology was used for the co-cultivation processes on the 1000 L scale. It was equipped with four equidistant baffles, a stirring axis with three Rushton turbines and a ring sparger at the vessel bottom. The geometrical details of the reactor vessel are shown in Table 4.8.

Table 4.8: Geometrical features of the 1000 L stirred-tank bioreactor. ↓: stirrer pumping downwards, ↑: stirrer pumping upwards, H_{Liquid}: liquid height in the reactor, $d_{Reactor}$: inner diameter of the reactor, $d_{Stirrer}$: diameter of the Rushton impellers.

Bottom geometry	Rounded bottom
Stirrer configuration	3 × Rushton impeller
Baffles	4
Ratio $H_{Liquid}/d_{Reactor}$	1.9
Ratio $d_{Stirrer}/d_{Reactor}$	0.40

Sensors for pH, DO and temperature as well as a sampling valve were installed near the bottom of the reactor, and the lid contained a pressure sensor, a larger opening (diameter 60 mm) for substrate addition and ports for the connection of lines for medium components, titration agents or inoculum. The processes were controlled, monitored and recorded by the BioSCADALab software (Bioengineering, Wald, Switzerland).

Figure 4.5: Stirred-tank bioreactor for cultivation experiments on the 1000 L scale (Photo: Andreas Heddergott, TUM).

The reactor was filled with 750 L ddH_2O after pH calibration and mounting of the probes, and 30 kg (30 g L^{-1}) pre-dried wheat bran were added. The reactor was sterilized *in-situ*, meanwhile the sampling valve and mechanical seal were steam-sterilized manually. Other media components (in total 175 L) were autoclaved in a separate medium tank and pumped into the reactor aseptically after cooling to 30 °C. Lines for titration agents and inoculation were connected to the reactor, and the DO probe was calibrated after

the setpoints of the cultivation parameters were reached (temperature 30 °C, pH 4.5, gassing rate 400 L min^{-1}, stirring rate 70 min^{-1}).

The preculture of *A. niger* NRRL 2270 was transferred directly into the reactor via a sterile transfer line and overpressure in the preculture reactor, while the *T. reesei* preculture was pumped from transport containers with a peristaltic pump. The inoculum consisting of 50 L *A. niger* preculture and 25 L *T. reesei* preculture corresponded to an initial total biomass concentration of 1.2 g L^{-1} and a ratio of 5:1 in favor of *A. niger*.

The temperature was kept constant at 30 °C throughout the cultivation, and pH 4.5 was controlled by automated addition of 1 M H_2SO_4 or 3 M KOH when necessary. A DO control cascade aiming for a DO above 30% air saturation controlled the aeration rate between 400-2000 L min^{-1} (0.4-2 vvm) and the agitation rate (70-200 min^{-1}), an overpressure of 0.7 bar was applied additionally. A foam control sequence triggered the addition of antifoaming agent when necessary. Samples were taken from the process through the sterilizable sampling valve.

A rapid increase in DO marked the end of the enzyme production phase and the start of transition to the integrated hydrolysis.

4.4. Enzymatic hydrolysis of wheat bran

4.4.1. Hydrolysis of wheat bran on the mL scale

Small-scale hydrolysis experiments were performed in 100 mL glass bottles following a method adapted from Schäfer et al. (2020). Wheat bran was dried at 80 °C, and 4 g (100 g L^{-1}) were filled into the bottles together with a magnetic stirrer prior sterilization at 121 °C for 20 min. Afterwards, 40 mL reaction solution consisting of 90% (v/v) sterile-filtered cultivation supernatant and 10% (v/v) sterile 1 M sodium acetate buffer (pH 4.5) were added aseptically. The bottles were placed on a magnetic stirring plate inside an incubator and incubated at 30 °C and a stirring rate of 350 min^{-1} for 163 h. Samples were taken regularly under aseptic conditions using sterile syringes.

4.4.2. Hydrolysis of wheat bran on the 0.5 L scale

A parallel bioreactor system consisting of four stirred-tank glass reactors without baffles (DASGIP, Eppendorf AG, Hamburg, Germany) was used for hydrolysis experiments on the 0.5 L scale. Each vessel had a maximum working volume of 1.2 L and was equipped with one inclined blade stirrer and one Rushton turbine for homogenization. Two sampling tubes were installed for the case of plugging.

The reactors were filled with ddH_2O and autoclaved (121 °C, 20 min); 50 g (100 g L^{-1}) of wheat bran were mixed with 200 mL of 62.5 mM sodium acetate buffer (pH 4.5) and sterilized separately. Subsequently, the water was removed from the reactors under a laminar flow sterile bench, and the sterilized wheat bran suspension was washed into the vessel with an additional 200 mL of sterile buffer.

The reactors were mounted into their sockets and tempered to 50 °C before 100 mL sterile enzyme solution was added through syringes to commence the process. The hydrolysis was conducted at 420 min^{-1} stirring for 45 h, and samples were drawn regularly throughout the process time.

4.4.3. Hydrolysis of wheat bran on the 3 L scale

The hydrolysis experiments on the 3 L scale were conducted in a 7.5 L bioreactor (Labfors, Infors HT, Bottmingen, Switzerland). The reactor had three stirrers (from top to bottom: one downward pumping inclined blade stirrer, one upward pumping inclined blade stirrer, one Rushton impeller), three baffles and two sampling tubes. The initial mass of 300 g (100 g L^{-1}) pre-dried wheat bran was mixed with 2.5 L of 60 mM sodium acetate buffer (pH 4.5) inside the reactor before sterilization (121 °C, 20 min). Afterwards, the temperature was set to 50 °C, and the suspension was homogenized with a stirring rate of 350 min^{-1}. 0.5 L sterile-filtered enzyme solution was added via a peristaltic pump. The hydrolysis was conducted for a total process time of 48-52 h, and samples were taken on a regular basis for analytics.

4.4.4. Integrated hydrolysis process on the 25 L scale

The integrated hydrolysis process on the 25 L scale was initiated after the end of the enzyme production phase by increasing the temperature to 50 °C. At the same time the overpressure was released, the aeration rate was lowered to the minimum value of 5 L min^{-1} to prevent clogging of the sparger, and the agitation rate was fixed at 550 min^{-1}. The reactor lid was opened 1 h later, 2.5 kg (100 g L^{-1}) pre-dried, unsterile wheat bran was added through a funnel, and the reactor was closed again. pH control was paused in the meantime until complete homogenization was reached. The hydrolysis had a duration of 46 h and was sampled on a regular basis. An additional sample of 5 L was drawn at the end of the final integrated process on this scale for further analysis of the solid fraction.

4.4.5. Integrated hydrolysis process on the 1000 L scale

The integrated hydrolysis on the 1000 L scale was initiated analogously to the 25 L scale by rising the temperature to 50 °C and reducing the pressure to atmospheric pressure.

The stirrers were set to 150 min^{-1} and aeration was terminated. When the hydrolysis temperature of 50 °C was reached, the larger opening on the lid was opened and 100 kg pre-dried, unsterile wheat bran was added via a funnel. Meanwhile, pH control was paused to avoid excess titration until complete homogenization. Samples were taken out of the reactor through the sampling valve during the whole hydrolysis time of 46 h.

The control parameters were switched off at the end of the process, and the vessel lid was completely lifted off after 1 h of sedimentation. A hose with a pre-filtering device (quadratic pores, 1.2 × 1.2 mm) mounted at the end was dived into the reactor, and the liquid phase was pumped into a medium tank through a membrane pump (SartoJet, Sartorius AG, Göttingen, Germany), while larger fungal and wheat bran particles were retained by the filter mesh. Smaller particles were removed by pumping the hydrolysate through a plate separator (CSA 8-06-476, GEA Westfalia Separator Group GmbH, Oelde, Germany) at a flow rate of 300 L min^{-1}. Solids were discharged for a period of 200-250 ms every 400-450 s, and the hydrolysate was pumped back into the medium tank. The separator was operated until no more solid discharge was observed. The hydrolysate was subsequently thermally stabilized in the collection tank by heating to 121 °C for 20 min.

4.5. Analytical methods

4.5.1. Sampling and sample treatment

Samples for analysis were drawn from all experiments at various time points and stored on ice until processing. The sampled material was aliquoted into 2 mL micro reaction tubes and centrifuged at 21,000 × g and 4 °C for 20 min. Subsequently, the supernatant was sterile-filtered (0.2 µm) into a fresh 2 mL micro reaction tube and stored at −20 °C until further analysis.

A larger sample of 5 L was taken at the end of the final integrated process on the 25 L scale for detailed analysis of the residual biomass. Hydrolysate and solid biomass were separated by centrifugation (3260 × g, 60 min) and decanting of the supernatant. The solid material was collected in a plastic container and frozen at −20 °C until handover to the Bavarian State Institution for Agriculture (Bayerische Landesanstalt für Landwirtschaft, LfL, Grub/Poing, Germany) for detailed analysis regarding the nutrient composition.

4.5.2. Quantification of total protein concentration in culture supernatants

The total protein concentration in culture supernatants was determined with the Pierce™ Coomassie Plus (Bradford) Assay Kit (Thermo Fisher Scientific Inc., Waltham, USA)

following the Micro Microplate Protocol. The samples as well as the bovine serum albumin (BSA) standards were diluted with 100 mM NaAc (pH 4.5) beforehand. 150 µL of the diluted samples were mixed with 150 µL Bradford reagent in a flat-bottom microtiter plate and incubated for 10 min at room temperature. Subsequently, the absorbance at 595 nm was measured in a microplate reader (Multiskan FC, Thermo Fisher Scientific Inc., Waltham, USA). Each culture sample as well as the standards were measured in triplicates and are displayed as the mean with respective standard deviation.

4.5.3. Determination of hydrolytic enzyme activities in culture supernatants

The hydrolytic enzyme activities in supernatant samples were determined using a colorimetric microplate assay where the sugars released by enzymatic hydrolysis react with 4-hydroxybenzhydrazide (pHBAH) and form a yellow compound, which can be detected by absorption measurement at 415 nm (Lever, 1972). Solutions of the polysaccharides xylan, starch and carboxymethyl cellulose (CMC; each 10 g L^{-1}, in 100 mM NaAc, pH 4.5) were applied as substrates to determine xylanase, amylase and cellulase activity, respectively.

The two assay reagents (Reagent A and B) were prepared beforehand as described in Table 4.9 and stored at room temperature. The assay working solution was prepared immediately before the assay by mixing 10% (v/v) Reagent A and 90% (v/v) Reagent B and was stored on ice.

Xylose (xylanase) and glucose (amylase, cellulase) standards in a range from 2.5 mM to 0 mM were used in triplicates for quantification of the released sugar concentrations and calculation of the enzyme activities.

Table 4.9: Composition of the assay reagents A and B.

	Component	**Concentration**
Reagent A	4-hydroxybenzhydrazide	50 g L^{-1}
	HCl, 37%	50 mL L^{-1}
Reagent B	$CaCl_2 \cdot 2\ H_2O$	1.10 g L^{-1}
	Na citrate $\cdot 2\ H_2O$	12.45 g L^{-1}
	NaOH	20 g L^{-1}

Culture supernatants were diluted with 100 mM NaAc (pH 4.5) before the assay. 100 µL of the diluted samples were mixed with 100 µL of the respective substrate solution in 1.5 mL reaction tubes (in triplicates) and placed on ice. 20 µL from each tube were transferred to a PCR plate on ice as a blank sample. Subsequently, the tubes were

placed in a 50 hermos shaker (ThermoMixer comfort, Eppendorf AG, Hamburg, Germany) at a shaking rate of 1000 min^{-1} and a temperature of 50 °C for 30 min (amylase, cellulase) or 50 min (xylanase). Samples of 20 µL were taken from the tubes regularly and transferred to the PCR plate on ice. 20 µL of the standard solutions were pipetted into the PCR plate for quantification. After the last sample, each sample or standard was mixed with 150 µL assay working solution. The PCR plate was sealed with adhesive film, heated to 96 °C for 6 min for reaction, and cooled on ice immediately afterwards. 125 µL of the standards were transferred to a flat-bottom microtiter plate, and 62.5 µL of the samples were pipetted into wells already filled with 62.5 µL ddH_2O before measuring the absorption at 415 nm in a microplate reader (Multiskan FC, Thermo Fisher Scientific Inc., Waltham, USA).

Enzyme activities were calculated from the slopes of sugar concentration over reaction time. One unit (U) was defined as the enzymatic activity releasing 1 µmol of xylose (xylanase) or glucose (amylase, cellulase) equivalents per minute under assay conditions. The activities of each cultivation sample were determined in triplicates and are plotted as their means with respective standard deviations.

Exceptions from the conditions described above occurred with the activity determination of samples from strain selection experiments (incubation temperature 30 °C, see Chapter 5.1) and during characterization of the co-culture enzyme mixture (see Chapter 6.1) with varying temperatures (20-70 °C) and pH (3.0-7-0).

4.5.4. Quantification of sugars and organic acids

The concentrations of relevant carbohydrates and organic acids in cultivation and hydrolysis samples were measured via high-performance liquid chromatography (HPLC). The HPLC system used (1100 series, Agilent Technologies, Santa Clara, USA) was equipped with a cation exchange column (Rezex ROA-Organic Acid H+ (8%) LC Column, 300 × 7.8 mm) combined with a SecurityGuard Cartridge Carbo-H (4 × 3.0 mm) pre-column (both Phenomenex Ltd., Aschaffenburg, Germany) for separation and a refractive index (RI) detector (1200 Series G1362A, Agilent Technologies, Santa Clara, USA) for detection.

Samples were sterile-filtered before measurement, and hydrolysis samples were diluted with ddH_2O. Sample volumes of 20 µL were injected into a constant flow (0.5 mL min^{-1}) of 5 mM H_2SO_4 and separated at a constant temperature of 65 °C. The substances were detected by the RI detector at 50 °C and were quantified using respective standards in a range of 0-20 g L^{-1}.

4.5.5. Calculation of respirational rates

The calculation of respirational rates during cultivations on 0.7 L, 3.0 L and 25 L scale was enabled by exhaust gas analysis regarding O_2 and CO_2 concentrations. The carbon dioxide evolution rate (CER) and oxygen uptake rate (OUR) were calculated as described in Chapter 3.2.2 (Takors and Weuster-Botz, 2018).

CER and OUR were calculated with time intervals of 10 min and plotted over the total process time.

4.5.6. Secretome analysis via sodium dodecylsulfate polyacrylamide gel electrophoresis

Secretome analysis via sodium dodecylsulfate polyacrylamide gel electrophoresis (SDS-PAGE) was conducted during investigations of spore ratios and inoculation times. Samples were prepared by mixing 40 µL culture supernatant with 10 µL 5× Laemmli sample buffer (Laemmli, 1970) prior to denaturation at 95 °C for 10 min. The samples were loaded onto a 12.5% polyacrylamide gel (pH 8.8) and separated via electrophoresis (35 mA, 60 min). The gel was stained afterwards with the method of Fairbanks et al. (1971). Results regarding strain dominance within the co-cultures were concluded by comparing protein band patterns of mono- and co-cultures.

4.5.7. Microscopic analysis of morphology

The macromorphology of fungal cultures was documented during the studies on agitation and aeration rates (see Chapter 5.3). A sample volume of 50 µL was placed on a glass slide and viewed using a light microscope (Axioplan, Carl Zeiss Microscopy GmbH, Oberkochen, Germany) with 1.25 × magnification and a 3.3-megapixel micro-scope camera (Axiocam ICc3, Carl Zeiss Microscopy, Oberkochen, Germany).

4.5.8. Determination of biomass concentration

The biomass concentration (cell dry weight) was determined gravimetrically. However, different methods were applied for cell dry weight determination for strain selection experiments (see Chapter 5.1) and for the preculture preparation in shaking flasks or bioreactors.

Samples of 10 mL were taken at the end of shaking flask cultivations for strain selection. The broth was filtrated through pre-dried and pre-weighed filter paper (Whatman grade 1, pore size 11 µm, diameter 70 mm), which were subsequently placed in glass petri dishes for drying at 80 °C for 48 h. The filters were weighed again after cooling to room

temperature, and the biomass concentration was calculated from the mass difference and the sample volume.

Biomass concentrations from vegetative precultures were determined in 2 mL reaction tubes which were dried at 80 °C for at least 48 h and weighed beforehand. A sample volume of 1 mL was pipetted into the tube and centrifuged at 21.000 × g and 4 °C for 20 min. The supernatant was discarded, and the remaining pellet was dried at 80 °C for at least 48 h. The filled tubes were weighed again after cooling, and biomass concentrations were calculated from the mass difference and the sample volume.

All measurements for biomass concentrations were conducted in triplicates.

4.5.9. Determination of the volumetric oxygen transfer coefficient (k_La)

The volumetric oxygen transfer coefficient (k_La) was determined dynamically by repeated alternations of oxygen saturation and depletion phases (Bandyopadhyay et al., 1967).

Measurements on the 0.7 L and 3.0 L scale were conducted with the nitrogen stripping method, where the dissolved oxygen is displaced with nitrogen. A 0.2% xanthan gum solution was identified as a suitable model fluid by comparison of flow curves with increasing shear rates (0-500 s^{-1}) in a rotational rheometer (RheolabQC, Anton Paar GmbH, Graz, Austria) with a cylinder measuring system (DG42, Anton Paar GmbH, Graz, Austria).

The measurements on the 3.0 L and 25 L scale were conducted during cultivation experiments when the DO has declined to 70% air saturation after inoculation. Depletion phases were initiated by interrupting the aeration. Gassing was switched on again when the DO reached ~20% for saturation. Afterwards, the cycle was repeated.

In both cases, the k_La was calculated from the DO data as described in Chapter 3.2.2.

5. Co-cultivation of *A. niger* and *T. reesei* [2]

A co-culture of the two fungal strains *A. niger* and *T. reesei* is applied to produce the hydrolases necessary for the degradation of wheat bran. After selection and characterization of suitable strains, a cultivation process is established in lab-scale stirred-tank bioreactors with a synthetic, defined medium imitating the composition of wheat bran. Therefore, different inoculation strategies and varied initial spore and biomass ratios are studied. Suitable cultivation conditions, with the focus on the mechanical power input by stirring and aeration, were identified thereafter, before the batch process is transferred from the 0.7 L scale to larger stirred-tank reactors based on rational transfer criteria.

5.1. Selection and characterization of fungal strains

Aspergillus niger

Six *A. niger* strains were characterized regarding their growth and enzyme formation to identify a suitable xylanase and amylase producer. The strains and their respective properties are described in Chapter 4.1. Shaking flask cultivations were performed using a minimal medium with 20 g L^{-1} xylan or starch to induce the formation of xylanase and amylase, respectively. The strains were evaluated by the determination of biomass concentrations and hydrolytic enzyme activities at the end of the cultivations after 96 h. Data regarding the biomass concentrations are displayed in Figure 5.1.

The highest biomass concentrations with xylan as carbon source were formed by *A. niger* NRRL 328 with 36.8 g L^{-1}, followed by the lab strains N402 (32.3 g L^{-1}) and *A. niger* N400 (30.6 g L^{-1}). The biomass of the industrial enzyme producer *A. niger* NRRL 3122 corresponded to ~40% of the highest biomass of *A. niger* NRRL 328.

Five of the six strains tested reached biomass concentrations between 20-30 g L^{-1} with starch as carbon source. The only strain with significantly lower biomass formation was *A. niger* CBS 513.88 (8.3 g L^{-1}).

[2] Parts of the data from this chapter are published in: Mittermeier, F., N. Hafner, K. Xypolia Vasila and D. Weuster-Botz (2023). "Co-Cultivation of *Aspergillus niger* and *Trichoderma reesei* Enables Efficient Production of Enzymes for the Hydrolysis of Wheat Bran." Chemie Ingenieur Technik **95**(4): 565-575.

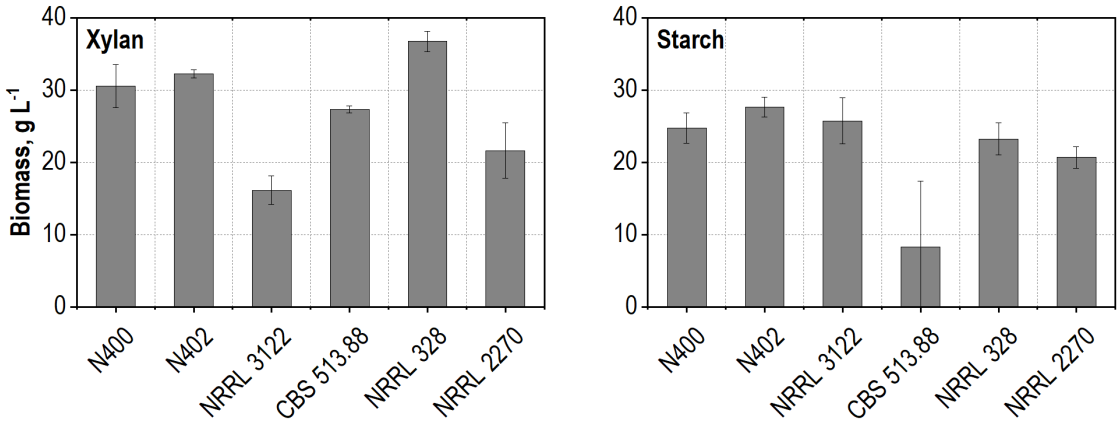

Figure 5.1: Biomass concentrations of different *A. niger* strains after 96 h cultivation time in shaking flasks containing minimal medium with 20 g L^{-1} xylan (left) or starch (right) as carbon source.

The xylanase activities formed during shaking flask cultivations with xylan as well as the amylase activities using starch as carbon source are shown in Figure 5.2.

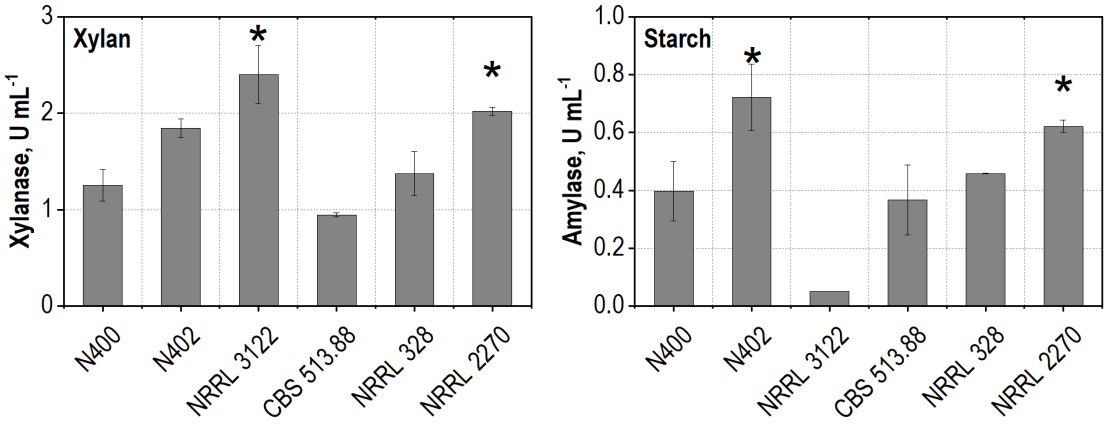

Figure 5.2: Xylanase activity (left) and amylase activity (right) in the supernatant of different *A. niger* strains after 96 h cultivation time in shaking flasks containing minimal medium with 20 g L^{-1} xylan (left) or starch (right) as carbon source. One unit (U) was defined as the amount of enzymatic activity releasing 1 µmol of xylose (left) or glucose (right) equivalents per minute under assay conditions (30 °C, pH 4.5). The strains marked with asterisks were selected for the following experiments.

The highest total xylanase activity was shown by the culture supernatant of *A. niger* NRRL 3122 at 2.40 ± 0.30 U mL^{-1}, followed by *A. niger* NRRL 2270 and *A. niger* N402 with 2.02 ± 0.04 U mL^{-1}, and 1.84 ± 0.10 U mL^{-1}, respectively. Maximum amylolytic activity was observed with the strains *A. niger* N402 at 0.72 ± 0.12 U mL^{-1} and *A. niger* NRRL 2270 at 0.62 ± 0.02 U mL^{-1}, which demonstrated a high potential for both activities. The best xylanase producer *A. niger* NRRL 3122, however, secreted only low total amylase activity. Results from mL scale hydrolysis experiments with the enzyme mixtures from these cultivations are described in Chapter 10.1 in the Supplemental Material.

Following these results, three strains were selected for cultivation in parallel stirred-tank bioreactors for the final selection: *A. niger* N402 as the strain producing the highest amylase activity, *A. niger* NRRL 3122 due to the formation of the highest xylanase activity, and *A. niger* NRRL 2270 as it demonstrated a promising overall performance using both xylan and starch. The batch cultivations were carried out in three parallel bioreactors with 0.7 L synthetic wheat bran medium as described in Chapter 4.3.4. The metabolic activity, represented by the dissolved oxygen concentration in the medium (DO) and the CO_2 evolution rate (CER), as well as the xylanase and amylase activity were used for evaluation of the strains.

The DO and CER are displayed over process time in Figure 5.3.

The exponential growth of *A. niger* N402, observable by the decrease in DO, commenced after ~9 h lag phase. Subsequently, metabolic activity continued to rise and reached its maximum after ~30 h process time, showing a remarkable CER double peak. The DO concentration decreased below 30% air saturation, causing the increase of aeration to the maximum of 1.4 L min^{-1} (2 vvm) to ensure sufficient oxygen supply. An abrupt increase of DO to 90% air saturation and CER approaching zero after 60 h indicated an almost complete stop of metabolic activity and thus the end of growth.

The DO signal of the *A. niger* NRRL 3122 cultivation showed high noise. The decrease in DO started after 30 h and reached the 30% air saturation threshold after 48 h, leading to the increase in aeration to 1.4 L min^{-1} (2 vvm). CER showed its maximum simultaneously, pointing at the maximum metabolic activity. Afterwards, the DO increase and the decline in CER indicated the end of metabolic activity.

The DO In the *A. niger* NRRL 2270 batch process rapidly dropped to nearly zero ~10 h after inoculation and remained constant thereafter, although the gassing rate was increased to its maximum value of 1.4 L min^{-1}. This issue was probably caused by growth of the fungus on the DO probe. The CER, however, strongly resembled the CER of *A. niger* N402, with the maximum after ~30 h process time, a double peak and a slow decrease afterwards until the end of the process.

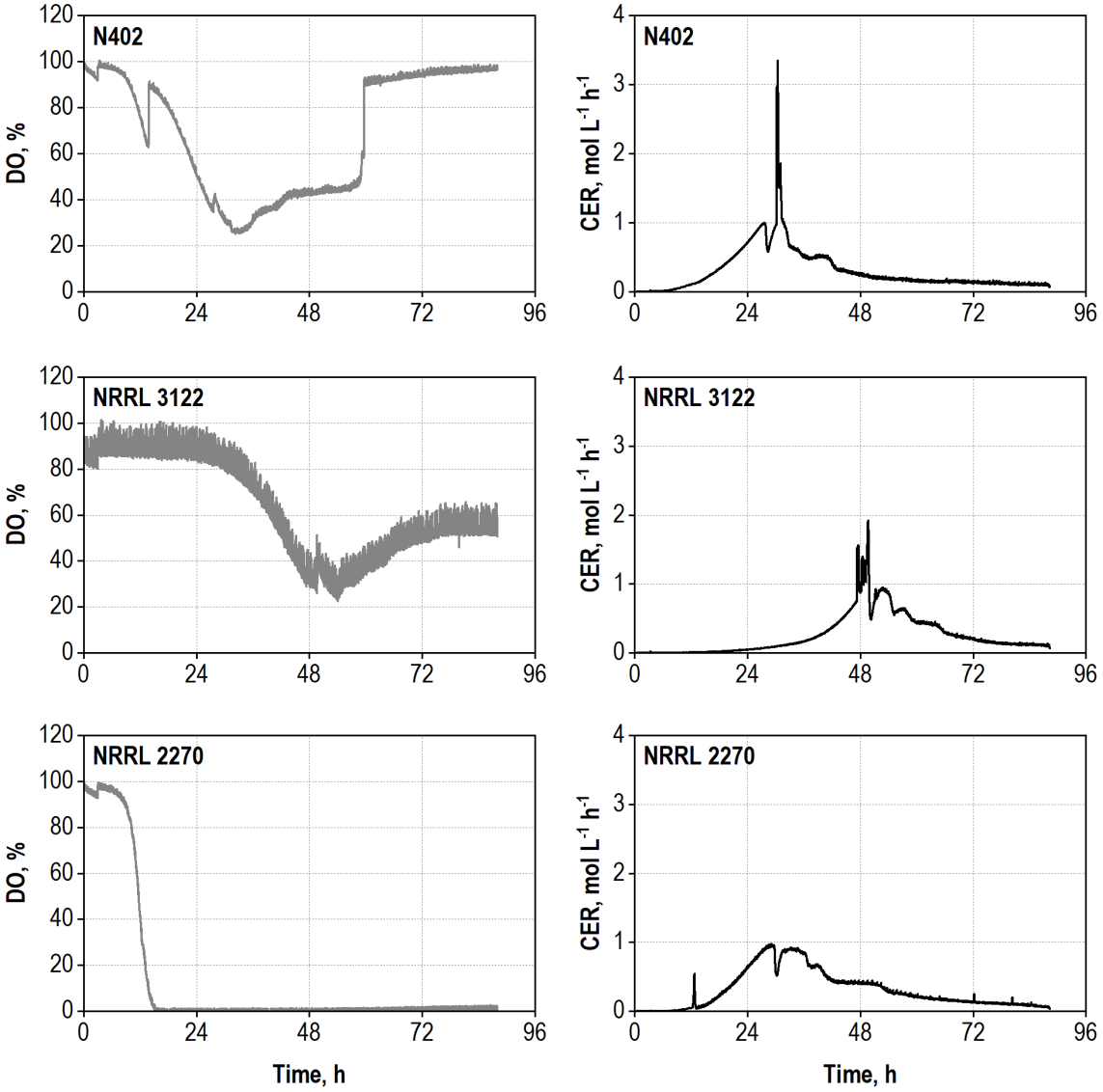

Figure 5.3: Dissolved oxygen concentration (DO, left) and carbon dioxide evolution rates (CER, right), of different *A. niger* strains in a stirred-tank bioreactor on a 0.7 L scale using synthetic wheat bran medium. The batch processes were started by inoculation with spores with an initial concentration of 10^9 spores L^{-1} (agitation rate 600 min^{-1}, aeration rate 0.2-2 vvm, temperature 30 °C, pH 4.5).

Xylanase and amylase activities are depicted in Figure 5.4. The strains *A. niger* N402 and *A. niger* NRRL 2270 demonstrated similar xylanase formation, with the main increase of activity between 24-48 h after process start. In this period, the xylanolytic activity increased to 5.72 ± 1.22 U mL^{-1} with *A. niger* N402 and 5.55 ± 1.55 U mL^{-1} with *A. niger* NRRL 2270. The maximum activities were measured at the end of the process after 88 h (6.63 ± 0.04 U mL^{-1} with *A. niger* N402, 6.26 ± 0.77 U mL^{-1} for *A. niger* NRRL 2270). *A. niger* NRRL 3122 commenced the xylanase production at a later process time, however a comparable final activity of 6.24 ± 0.68 U mL^{-1} was measured.

The amylase formation of all three strains started at an earlier point in the process than the formation of xylanase. The first rise in amylase activity with *A. niger* N402 and *A. niger* NRRL 2270 was observed between 16-24 h process time. *A. niger* NRRL 3122 commenced its amylase formation already within the first 16 h. The amylolytic activity formed by *A. niger* N402 reached its maximum (1.17 ± 0.44 U mL^{-1}) after 48 h and stayed nearly constant for the rest of the cultivation. *A. niger* NRRL 3122 formed the highest amylase activity of the strains tested (2.26 ± 0.28 U mL^{-1}) at the end of the process after 88 h. The maximum activity of *A. niger* NRRL 2270 of 1.59 ± 0.20 U mL^{-1} was measured at the same time.

All three strains demonstrated similar metabolic activities during the characterization in stirred-tank bioreactors with synthetic wheat bran medium and produced the desired enzyme activities. Remarkably, the maximum amylase activity was formed by *A. niger* NRRL 3122, which contrasts with the results of the shaking flask experiments. This discrepancy was probably caused by the improved and controlled growth conditions in the stirred-tank reactors. Nevertheless, this strain showed a longer lag phase, and a delayed xylanase formation compared to the other strains tested. Those strains, *A. niger* N402 and *A. niger* NRRL 2270, had highly similar metabolic activities and xylanase production. The prior one, however, produced 36% less amylolytic activity than *A. niger* NRRL 2270. Overall, *A. niger* NRRL 2270 demonstrated the most suitable features with a combination of high metabolic activity and the secretion of hydrolytically active enzymes. Therefore, this strain was selected for further studies.

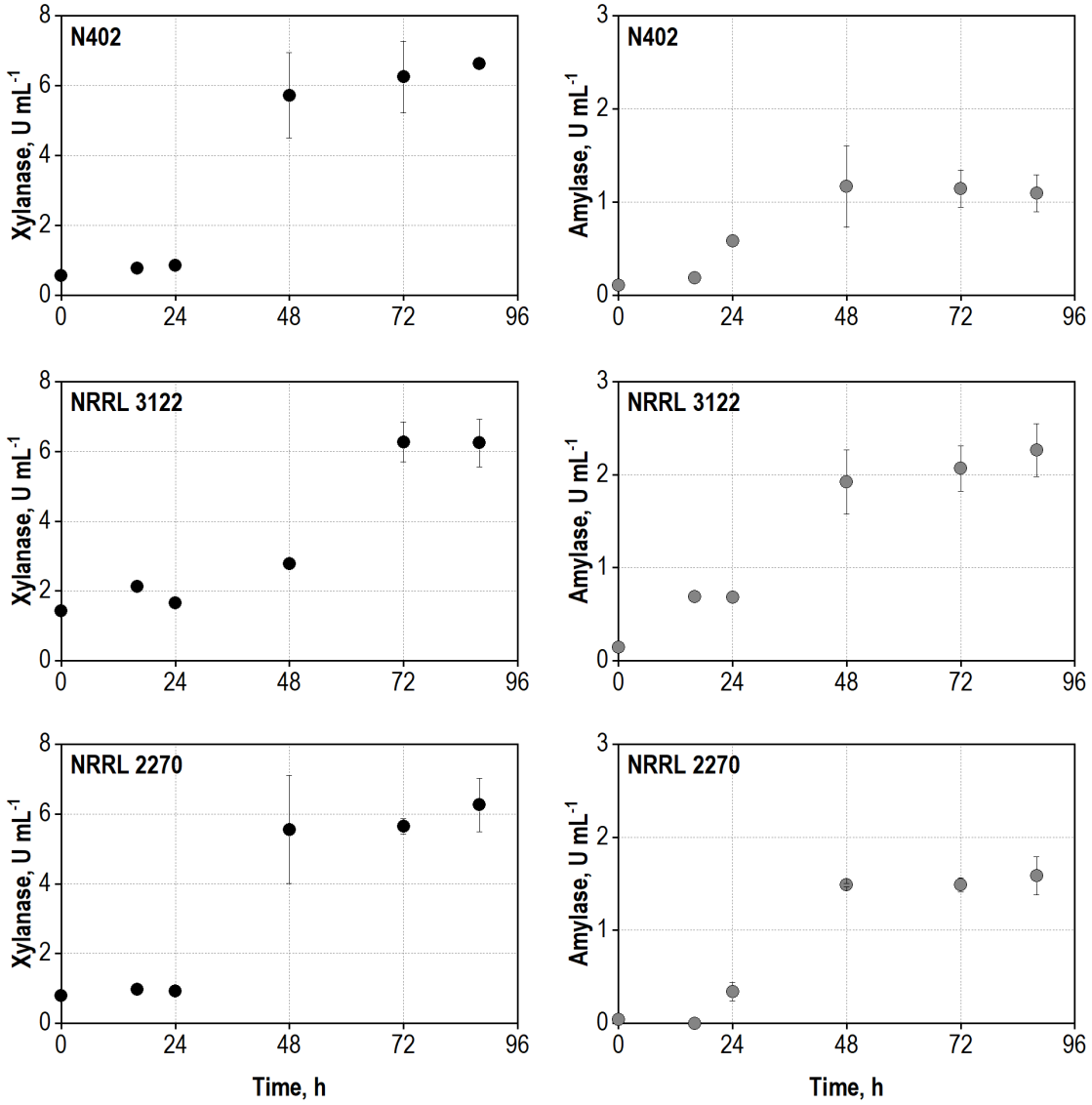

Figure 5.4: Xylanase activity (left) and amylase activity (right) in the supernatant of different *A. niger* strains in a stirred-tank bioreactor on a 0.7 L scale using synthetic wheat bran medium. The batch processes were started by inoculation with spores with an initial concentration of 10^9 spores L^{-1} (agitation rate 600 min^{-1}, aeration rate 0.2-2 vvm, temperature 30 °C, pH 4.5). One unit (U) was defined as the amount of enzymatic activity releasing 1 µmol of xylose (left) or glucose (right) equivalents per minute under assay conditions (30 °C, pH 4.5).

Discussion

Interestingly, the best results regarding the enzyme formation were achieved by the originally citric acid-producing strain *A. niger* NRRL 2270. The strain was already reported as a good producer of hydrolytically active pectinases in previous studies (Schäfer et al., 2020). Although the industrial enzyme-producing strain *A. niger* CBS 513.88 has additional α-amylase genes transferred from *Aspergillus oryzae* as well

as a less stringent regulation (Andersen et al., 2011), less enzymatic activities were measured.

Trichoderma reesei

The second microorganism for the co-culture, *T. reesei* RUT-C30, was selected as the most promising non-recombinant strain from literature data, as it is widely known, described and applied in research as well as in industrial processes. Initial experiments with this strain were conducted in shaking flasks to gain insight into its cellulase formation with different carbon sources.

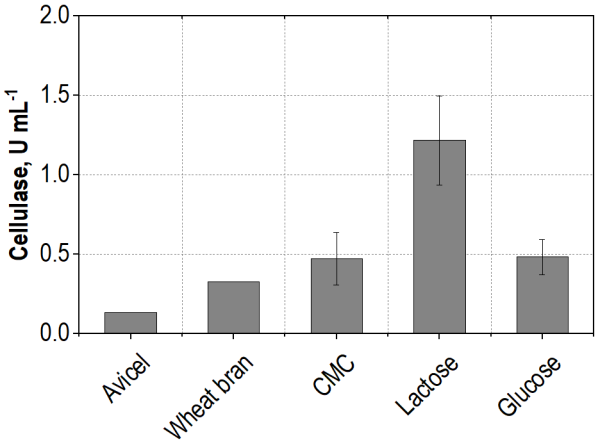

Figure 5.5: Cellulase activity in the supernatant of *T. reesei* RUT-C30 after 99 h cultivation time in shaking flasks containing minimal medium with 20 g L^{-1} microcrystalline cellulose (Avicel), wheat bran, carboxymethyl cellulose (CMC), lactose or glucose as carbon source. One unit (U) was defined as the amount of enzymatic activity releasing 1 µmol of glucose equivalents per minute under assay conditions (30 °C, pH 4.5).

The highest cellulase activity after 99 h cultivation time was measured with lactose as carbon source (1.22 ± 0.28 U mL^{-1}). The inducing effect of lactose on the formation of cellulases by *T. reesei* was already reported by several studies (Seiboth et al., 2005, Lo et al., 2010) and makes it an attractive substrate for the industrial production of cellulases. Activities of around 0.5 U mL^{-1} were measured using the solved substrates CMC and glucose, whereas the insoluble carbon sources Avicel and wheat bran resulted in lower enzyme formation. Nevertheless, *T. reesei* RUT-C30 demonstrated its capability to grow and form cellulases with wheat bran as substrate.

5.2. Inoculation strategies for the co-cultivation process

Two methods of inoculation are mainly used to start fungal bioprocesses: spore inoculation or vegetative precultures.

Inoculation with spores is widely used in small lab-scale processes. The spores are grown on solid media like agar plates or slants, harvested by suspending, e.g., in saline solution, and directly injected into the reactor for inoculation. The spore concentration in the suspension can be determined by measurement of the optical density. Therefore, highly defined initial spore concentrations can be applied for inoculation of bioreactor experiments, leading to high reproducibility. In the case of a co-culture, this high degree of definition allows for a precise adjustment of the ratios of the strains at the beginning of cultivations.

The most important drawback of spore inoculation, however, is the lack of scalability, as the harvest, OD determination and dilution of spore suspensions is rather labor-intensive, and the number of spores is limited by the maximum number of agar plates that can be handled in parallel. Furthermore, the germination of spores to form mycelia leads to prolonged process times.

These disadvantages can be evaded by using already germinated precultures, for example from shaking flasks. The vegetative state of the cells leads to reduced lag-phases at the process start and hence enables shorter process times. In addition, this method is easily scalable as the size of the precultures can be adjusted by the application of larger flasks or bioreactors and the implementation of preculture cascades. However, one issue is posed by the lower degree of definition of vegetative precultures, as the number of fungal cells added to the reactor for inoculation cannot be checked a priori. Thus, it must be ensured that the precultures grow very stable and reproducible to achieve the desired initial biomass concentrations and, in the case of co-cultivation, biomass ratios.

Both inoculation strategies are applied in this work. Spore inoculation is used to study the interactions between the strains used and subsequently find suitable spore ratios and time points for inoculation. The effects of varying initial biomass ratios are analyzed with vegetative precultures from shaking flasks.

5.2.1. Variation of spore ratios and inoculation times

At first, *A. niger* NRRL 2270 and *T. reesei* RUT-C30 were studied in 0.7 L monocultures using spore inoculation to characterize their specific growth behavior. The metabolic activity of the cultures was observed via the carbon dioxide evolution rate (CER) during the process (Figure 5.6).

Both microorganisms showed a characteristic CER over process time. Germination and growth of *A. niger* NRRL 2270 appeared after only a few hours of process time, and the

metabolic activity reached its maximum after ~20 hours with the formation of a characteristic double peak at 24 h process time. This double peak probably indicates a shift in metabolism between different substrates in the medium. Afterwards, the CER decreased until the process end at 72 h.

In the case of *T. reesei*, a lower initial spore concentration was used for inoculation due to a lower number of spores that could be harvested from the agar plates. Therefore, germination was delayed, and metabolic activity was first observed after 24 h. It subsequently reached its maximum at a process time of 40 h, also with a lower CER than *A. niger*.

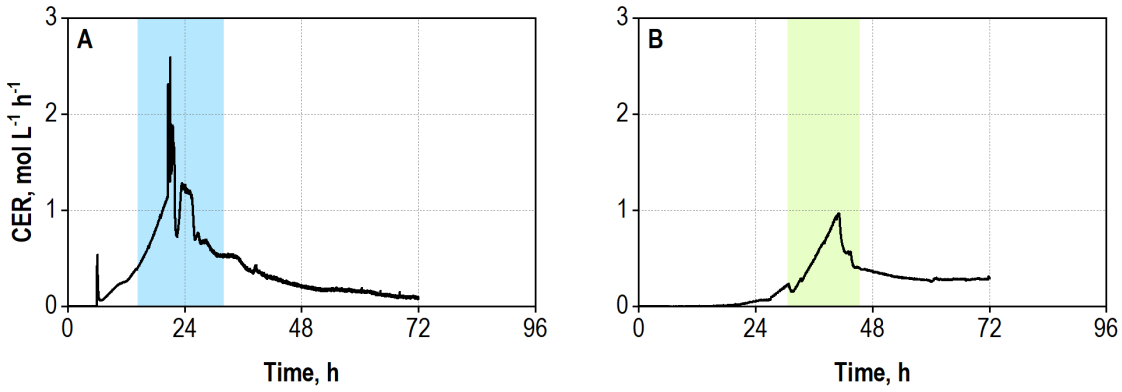

Figure 5.6: Carbon dioxide evolution rates (CER) of *A. niger* NRRL 2270 (A) and *T. reesei* RUT-C30 (B) monocultures in a bioreactor on a 0.7 L scale using synthetic wheat bran medium. *A. niger* NRRL 2270 was inoculated with an initial spore concentration of 10^9 spores L^{-1}, *T. reesei* RUT-C30 was inoculated with an initial spore concentration of 0.2×10^9 spores L^{-1} (agitation rate 600 min^{-1}, aeration rate 0.2-2 vvm, temperature 30 °C, pH 4.5). Colored areas mark the maximum metabolic activity of *A. niger* NRRL 2270 (blue) and *T. reesei* RUT-C30 (green).

The simplest way for inoculation of a co-culture process is to add both strains into the reactor simultaneously. An initial spore concentration ratio of 5:1 in favor of *A. niger* was applied. This ratio was used due to practical reasons, as *A. niger* formed higher spore amounts on the agar plates than *T. reesei*, and the number of agar plates was limited. The CER of this co-cultivation process is displayed over process time in Figure 5.7.

CO_2 production strongly resembled that of the *A. niger* monoculture described above (Figure 5.6), with the characteristic double peak after 24 h process time. This points at a strong dominance of *A. niger* within the co-culture, as it seems to repress germination and growth of *T. reesei*. This conclusion was supported by the results of SDS-PAGE secretome analysis, where the protein band pattern of the co-culture appeared identical to the *A. niger* monoculture (see Supplemental Material, Figure 10.2)

The variation of the initial spore ratios with simultaneous inoculation showed no effects on the metabolic activity (data not shown). Therefore, the ratio of *A. niger* to *T. reesei* of

5:1 was kept for practical reasons, as this ratio required a minimum number of agar plates.

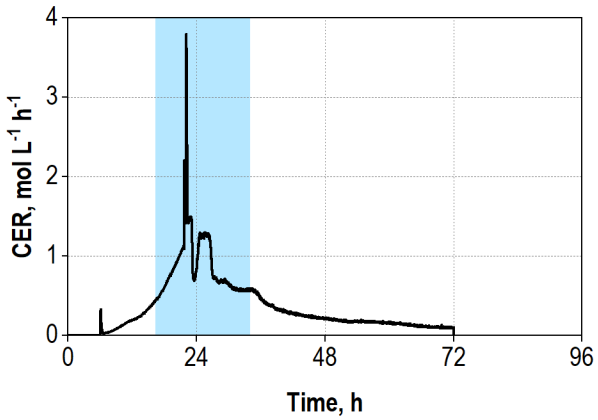

Figure 5.7: Carbon dioxide evolution rate (CER) of a co-culture of *A. niger* NRRL 2270 and *T. reesei* RUT-C30 in a bioreactor on a 0.7 L scale using synthetic wheat bran medium. *A. niger* NRRL 2270 was inoculated with an initial spore concentration of 10^9 spores L^{-1}, *T. reesei* RUT-C30 was inoculated with an initial spore concentration of 0.2 × 10^9 spores L^{-1} (agitation rate 600 min^{-1}, aeration rate 0.2-2 vvm, temperature 30 °C, pH 4.5). The colored area marks the maximum metabolic activity.

Delayed inoculation of the dominant partner within a co-culture is a potential approach to enable growth of both microorganisms in one process. A time delay of 24 h was tested for the addition of *A. niger*. Two distinct metabolic maxima were observed (displayed in Figure 5.8A): the first one at 40 h most probably formed by *T. reesei*, whereas *A. niger* may have produced the second peak at 64 h process time. The latter one is, however, significantly lower than in the *A. niger* monoculture. This pointed at reduced activity of *A. niger*. Two distinct maxima of metabolic activity were observed when the delay for *A. niger* inoculation was decreased to 16.5 h (Figure 5.8B). Again, the first peak most probably was caused by *T. reesei* while the second one stemmed from *A. niger*, with the CER maxima being comparable to the respective monocultures. It was concluded that both fungi were metabolically active and could produce their respective sets of hydrolytic enzymes. These assumptions were confirmed by SDS-PAGE secretome analysis (displayed in Figure 10.2, Supplemental Material), where characteristic protein bands of both strains were visible. Therefore, this delay of 16.5 h for the addition of *A. niger* spores was kept constant for further studies.

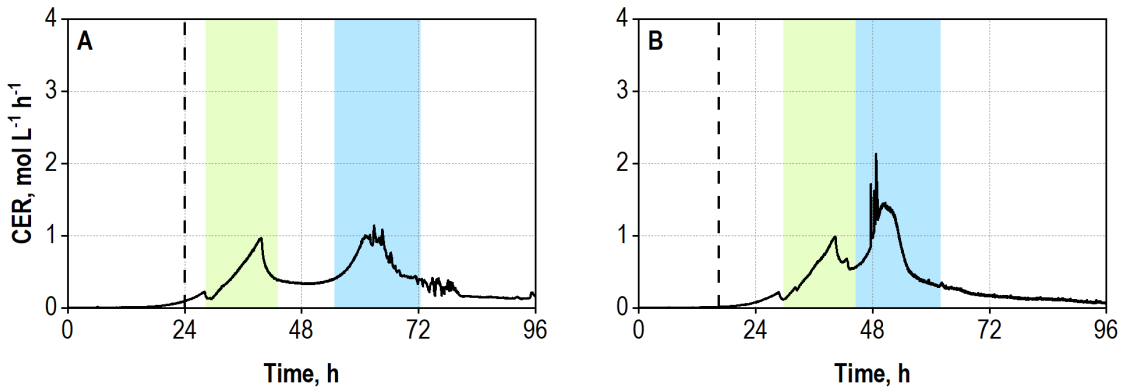

Figure 5.8: Carbon dioxide evolution rates (CER) of co-cultures of *A. niger* NRRL 2270 and *T. reesei* RUT-C30 in a bioreactor on a 0.7 L scale using synthetic wheat bran medium. *T. reesei* RUT-C30 was inoculated with an initial spore concentration of 0.2 × 10^9 spores L^{-1}. *A. niger* NRRL 2270 was added (marked by black dashed lines) after 24 h (A) or 16.5 h (B) with an initial spore concentration of 10^9 spores L^{-1} (agitation rate 600 min^{-1}, aeration rate 0.2-2 vvm, temperature 30 °C, pH 4.5). Colored areas mark the maximum metabolic activity of *A. niger* NRRL 2270 (blue) and *T. reesei* RUT-C30 (green).

A comparative cultivation experiment with monocultures of *A. niger* NRRL 2270 and *T. reesei* RUT-C30 and a co-culture as described above (inoculation with 0.2 × 10^9 spores L^{-1} *T. reesei*, addition of 10^9 spores L^{-1} *A. niger* after 16.5 h) was conducted to evaluate the potential of the co-culture to produce the enzymatic activities necessary for the hydrolysis of wheat bran. Xylanase, amylase and cellulase activities in the supernatant samples of mono- and co-cultures are displayed in Figure 5.9.

It can be seen clearly that neither of the monocultures could sufficiently produce all three enzymatic activities. On the one hand, *A. niger* secreted relatively high xylanase and amylase activities, but only little cellulase activity. On the other hand, *T. reesei* produced the highest cellulase activity, but was not able to form amylases. Aside from the expected cellulases, *T. reesei* also produced the maximum xylanase activity. In contrast to the monocultures, the supernatant of the co-culture contained all three activities. Xylanase and cellulase activities were only slightly lower than those of *T. reesei*, and the activity of amylase was even higher than in the *A. niger* monoculture.

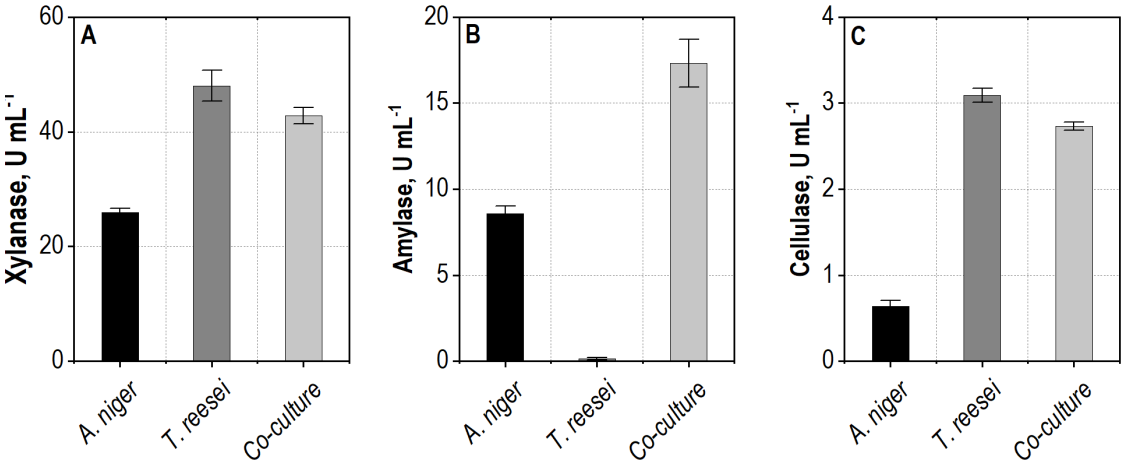

Figure 5.9: A: Xylanase activity, B: Amylase activity, C: Cellulase activity in the supernatant of *A. niger* NRRL 2270 (black) and *T. reesei* RUT-C30 (dark gray) monocultures or a co-culture of *A. niger* NRRL 2270 and *T. reesei* RUT-C30 (light gray) after 86 h in a bioreactor on a 0.7 L scale using synthetic wheat bran medium. The co-culture was started by inoculation with 0.2×10^9 spores L^{-1} of *T. reesei* RUT-C30, and 10^9 spores L^{-1} of *A. niger* NRRL 2270 were added after 16.5 h (agitation rate 600 min^{-1}, aeration rate 0.2-2 vvm, temperature 30 °C, pH 4.5). The monocultures were inoculated with the same respective spore concentrations. One unit (U) was defined as the amount of enzymatic activity releasing 1 µmol of xylose (A) or glucose (B, C) equivalents per minute under assay conditions (50 °C, pH 4.5).

Discussion

It is essential that both *A. niger* and *T. reesei* are able to grow and form their respective enzymes in the intended co-culture. Therefore, germination and growth behavior as well as interactions between the strains came into focus during these initial experiments. *A. niger* showed dominant growth behavior when both strains were inoculated simultaneously, regardless of the initial spore concentration ratios. This indicated a faster germination of *A. niger*, giving the strain an advance that *T. reesei* could not compensate during the process. Hence, the population dynamics within the co-culture needed to be influenced to enable growth of strains, and the time-delayed inoculation of one microorganism was reported in literature as an approach to achieve that goal (Kolasa et al., 2014, Schlembach et al., 2020). Here, this method was used with a delayed addition of spores of the presumably faster-growing *A. niger*. A delay of *A. niger* inoculation of 24 h resulted in reduced metabolic activity (lowered maximum CER) of the strain, although sugars and polysaccharides were evidently still available as carbon sources (HPLC data in Supplemental Material, Figure 10.3). Nevertheless, the limitation of another nutrient could not be excluded. Another potential explanation was described by Daly et al. (2017), who investigated the responses of *A. niger* and *T. reesei* to the presence of other fungi on a transcriptomic level. Equal masses of vegetative fungal cells of both strains were mixed in a culture containing wheat straw as a lignocellulosic carbon

source and analyzed the changes in gene expression by RNA quantification and sequencing. Especially *A. niger* is described to react highly sensitive to the presence of *T. reesei*, inducing genes linked with carbon starvation, autolysis and sporulation as well as the formation of antibiotic-like secondary metabolites, oxidoreductases or transporter proteins. In contrast, *T. reesei* was not affected as much by the presence of *A. niger* and thus did not form toxins or other secondary metabolites. However, the strain could have modified already present metabolites. The authors concluded that *T. reesei* antagonizes other fungal strains like *A. niger*, affecting their growth and product formation.

A finely tuned delay of *A. niger* inoculation of 16.5 h resulted in a co-culture where both strains were metabolically active and could secrete their respective set of enzymes. Consequently, the enzyme solution produced by the co-culture contained all three enzymatic activities (xylanase, amylase, cellulase) in similar or even increased amounts compared to both monoculture enzyme cocktails. This demonstrated the potential of the co-cultivation of *A. niger* and *T. reesei* to produce a suitable enzyme solution for the efficient hydrolysis of wheat bran.

5.2.2. Variation of initial biomass ratios

The inoculation with vegetative fungal precultures from shaking flasks was tested as the second method of inoculation. The preparation of precultures in 1 L shaking flasks using 0.2 L preculture medium was characterized and tested beforehand regarding the cultivation time and the biomass concentration achievable. Reproducibility was checked by repeated cultivations in triplicate. *A. niger* NRRL 2270 reached the end of the exponential growth phase after 48 h with a biomass concentration of 25.9 ± 0.7 g L^{-1} cell dry weight. *T. reesei* RUT-C30 showed exponential growth until 72 h cultivation time and formed a biomass concentration of 12.3 ± 0.7 g L^{-1}. The preculture durations were set at 72 h for *A. niger* and 96 h for *T. reesei* to allow the cells to enter the stationary growth phase. This aimed for a reproducible state of the cells for inoculation of the bioreactor process.

The effects of the initial biomass ratio were investigated in a co-cultivation experiment in parallel stirred-tank reactors on a 0.7 L scale. A total initial biomass of 1.2 g L^{-1} was thereby divided into ratios of *A. niger* to *T. reesei* of 5:1 (1.0 g L^{-1} *A. niger* + 0.2 g L^{-1} *T. reesei*), 1:1 (0.6 g L^{-1} *A. niger* + 0.6 g L^{-1} *T. reesei*), 1:2 (0.4 g L^{-1} *A. niger* + 0.8 g L^{-1} *T. reesei*) and 1:5 (0.2 g L^{-1} *A. niger* + 1.0 g L^{-1} *T. reesei*). The CERs of the co-cultures are displayed in Figure 5.10.

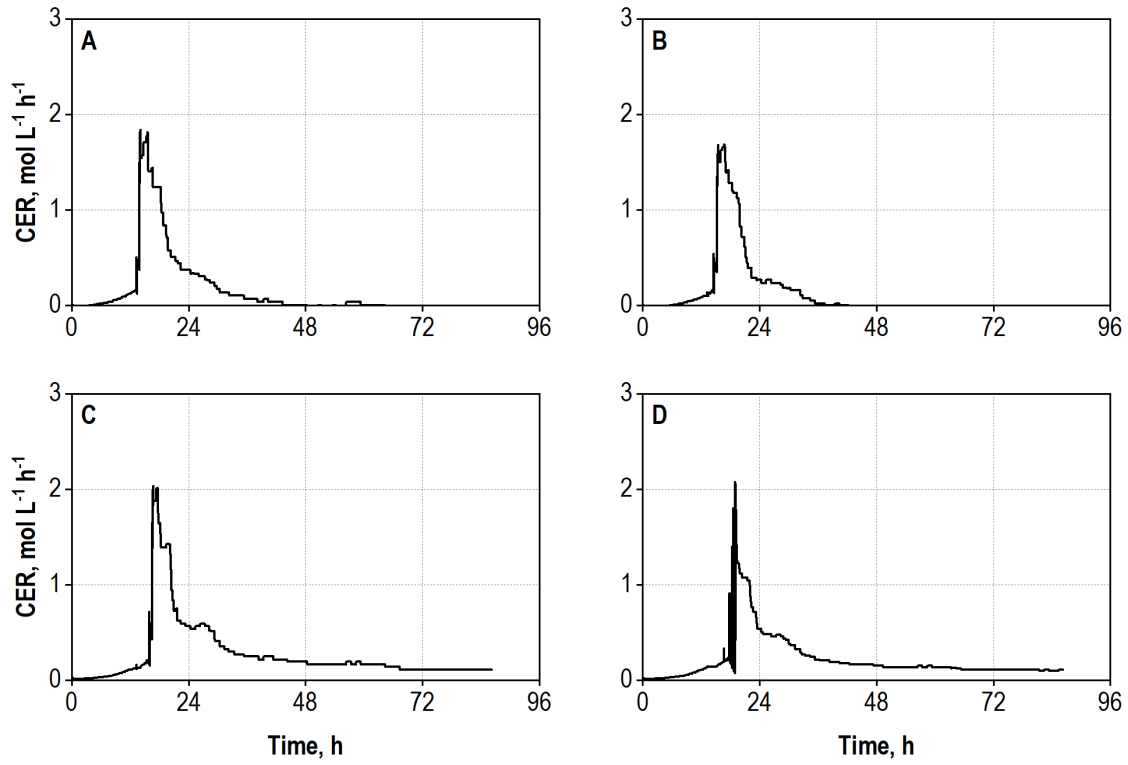

Figure 5.10: Carbon dioxide evolution rates (CER) of co-cultures of *A. niger* NRRL 2270 and *T. reesei* RUT-C30 in a bioreactor on a 0.7 L scale using synthetic wheat bran medium. The processes were started by simultaneous inoculation with vegetative cultures from shaking flasks with an initial biomass concentration of 1.2 g L^{-1} and an initial biomass ratio of *A. niger* to *T. reesei* of 5:1 (A), 1:1 (B), 1:2 (C), and 1:5 (D), respectively (agitation rate 800 min^{-1}, aeration rate 0.2-2 vvm, temperature 30 °C, pH 4.5).

Surprisingly, the variation of the initial biomass ratios did not result in significant differences in metabolic activity. The CER maxima were slightly shifted towards later process times with a decreasing biomass share of *A. niger*. Growth started with a short lag phase after inoculation and reached the exponential phase after a few hours in all reactors. A distinction of metabolic maxima for each strain, as it was seen with spore inoculation, was not possible.

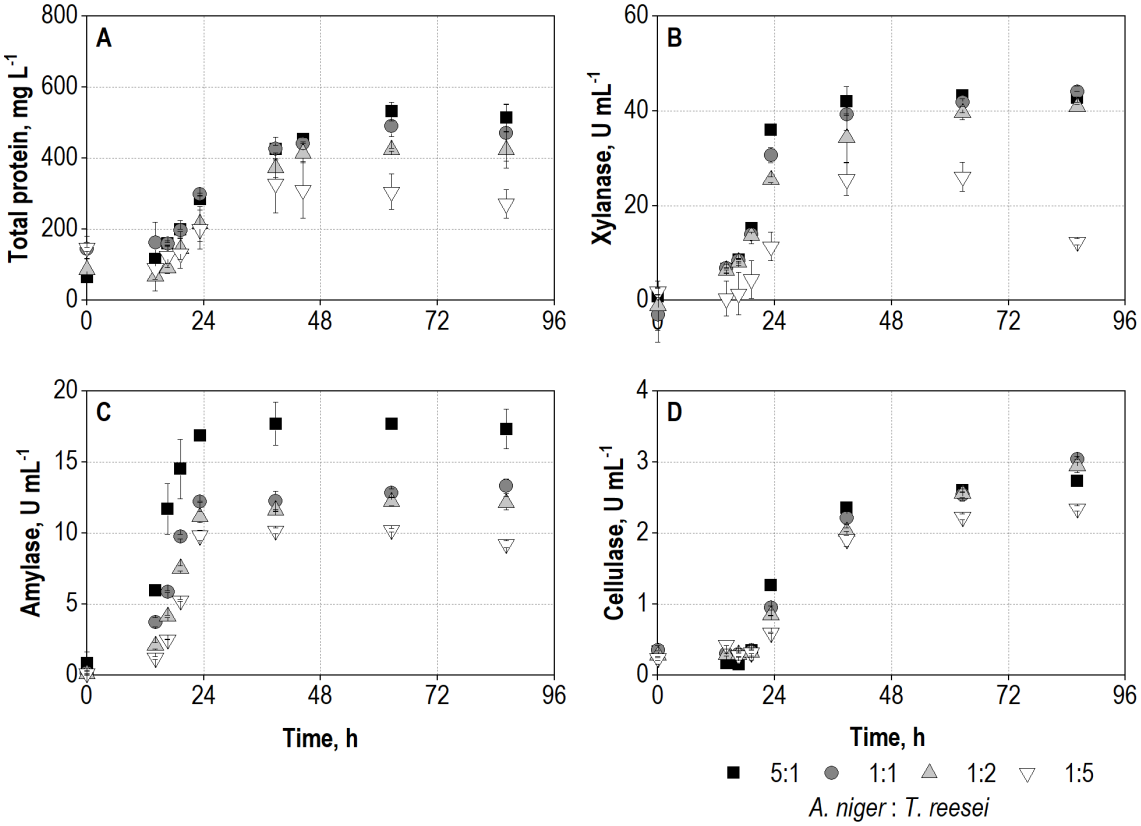

Figure 5.11: A: Total protein concentration, B: Xylanase activity, C: Amylase activity, D: Cellulase activity in the supernatant of co-cultures of *A. niger* NRRL 2270 and *T. reesei* RUT-C30 in a bioreactor on a 0.7 L scale using synthetic wheat bran medium. The process was started by simultaneous inoculation with vegetative cultures from shaking flasks with an initial biomass concentration of 1.2 g L^{-1} and an initial biomass ratio of *A. niger* to *T. reesei* of 5:1, 1:1, 1:2, and 1:5, respectively (agitation rate 800 min^{-1}, aeration rate 0.2-2 vvm, temperature 30 °C, pH 4.5). One unit (U) was defined as the amount of enzymatic activity releasing 1 µmol of xylose (B) or glucose (C, D) equivalents per minute under assay conditions (50 °C, pH 4.5).

In contrast to the CERs, overall protein formation and hydrolytic activities were influenced by the variation of the initial biomass ratios, as shown in Figure 5.11. Lower initial biomass concentrations of *A. niger* resulted in decreasing total protein concentrations in the medium. The highest concentration was measured with a ratio of *A. niger* to *T. reesei* of 5:1 with 514 ± 39 mg L^{-1} after 86 h, followed by the ratios 1:1 and 1:2 with 471 ± 79 mg L^{-1} and 424 ± 51 mg L^{-1}, respectively. With the ratio of 1:5 (in favor of *T. reesei*), protein concentration was nearly halved to 272 ± 40 mg L^{-1}. Xylanase activities of ~40 U mL^{-1} after 86 h were measured in all cultures except with a ratio of 1:5 in favor of *T. reesei*. However, xylanase activity appeared to be formed at a lower rate with smaller initial shares of *A. niger*. A ratio of *A. niger* to *T. reesei* of 1:5 resulted in a strong decrease in xylanase activity towards the end of the process to 12.4 U mL^{-1}. The strongest influence of varying initial biomass ratios was observed regarding the amylase formation. Here, higher initial biomass concentrations of *T. reesei* resulted in decreasing amylase activities. With ratio of 1:2 and 1:5 in favor of *T. reesei*, amylolytic activities were

reduced by 31% and 47%, respectively, compared to a ratio of 5:1 in favor of *A. niger*. No distinct trend was visible in the case of cellulase activity. Remarkably, the lowest activity was achieved in the process with the highest share of the predestined cellulase producer *T. reesei*. With all these aspects considered, an initial biomass ratio of 5:1 in favor of *A. niger* appeared suitable for inoculation with shaking flask precultures.

Discussion

Distinct correlations could be observed between the initial biomass ratios and the enzyme activities expectedly formed by *A. niger*. Reduced initial *A. niger* biomass concentrations resulted in decreased activities of xylanase and amylase (reduction by 71% and 47%, respectively, with a 1:5 dominance of *T. reesei*). Here, the lower initial biomass shares of *A. niger* pose a handicap that cannot be compensated within the process, possibly in connection with the assumed competitive or antagonistic effects described in Chapter 5.2.1 and in literature (Daly et al., 2017). Interestingly, lower *T. reesei* biomass concentrations did not have a similar effect on the cellulase formation. Generally, the inoculation of the enzyme production processes with vegetative precultures brings several advantages, including shorter process times compared to spore inoculation, and easier scalability to larger scales.

5.3. Variation of agitation and aeration

Various combinations of agitation rates between 400-1000 min^{-1} and initial aeration rates of 0.1-0.3 vvm (0.07-0.21 L min^{-1}), which could be increased tenfold, were studied in co-cultivation processes in bioreactors with 0.7 L synthetic wheat bran medium. The cultivations were first inoculated with 0.2×10^9 spores L^{-1} of *T. reesei* RUT-C30, and 10^9 spores L^{-1} of *A. niger* NRRL 2270 were added after 16.5 h process time. The metabolic activities of the cultures, measured by the CER, are displayed in Figure 5.12.

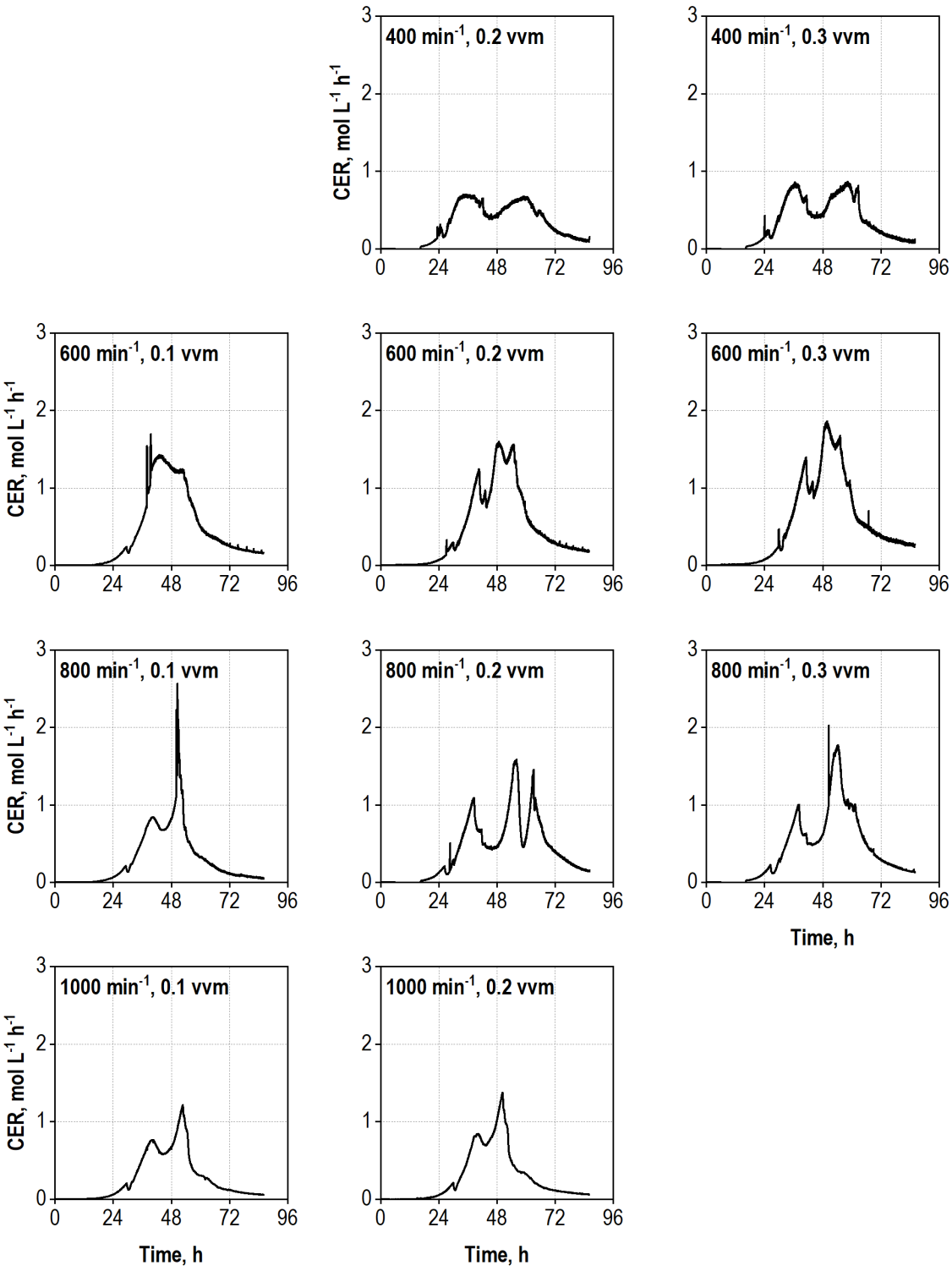

Figure 5.12: Carbon dioxide evolution rates (CER) of co-cultures of *A. niger* NRRL 2270 and *T. reesei* RUT-C30 in a bioreactor on a 0.7 L scale using synthetic wheat bran medium with varying agitation rates (400-1000 min^{-1}) and initial aeration rates (0.1-0-3 vvm). *T. reesei* RUT-C30 was inoculated with an initial spore concentration of 0.2 × 10^9 spores L^{-1}, *A. niger* NRRL 2270 was added after 16.5 h process time with an initial spore concentration of 10^9 spores L^{-1} (temperature 30 °C, pH 4.5).

The CERs of processes with medium agitation (600-800 min^{-1}) in combination with medium to high aeration rates (initially 0.2-0.3 vvm) strongly resembled each other. They showed two distinct CER peaks for both strains (*T. reesei* at ~40 h process time, *A. niger* at 50-60 h) and comparably high maxima. Processes with either 400 min^{-1} stirring rate or 0.1 vvm initial aeration rate demonstrated flattened CER maxima despite the aeration increasing to the respective maximum, indicating a limitation of metabolic activity. The CER maxima in processes with 1000 min^{-1} agitation also remained lower than in other batches.

The results regarding the protein secretion as well as the relevant enzymatic activities are displayed in Figure 5.13. The data can also be found in Table 10.2, Table 10.3, Table 10.4 and Table 10.5 in the Supplementary Material.

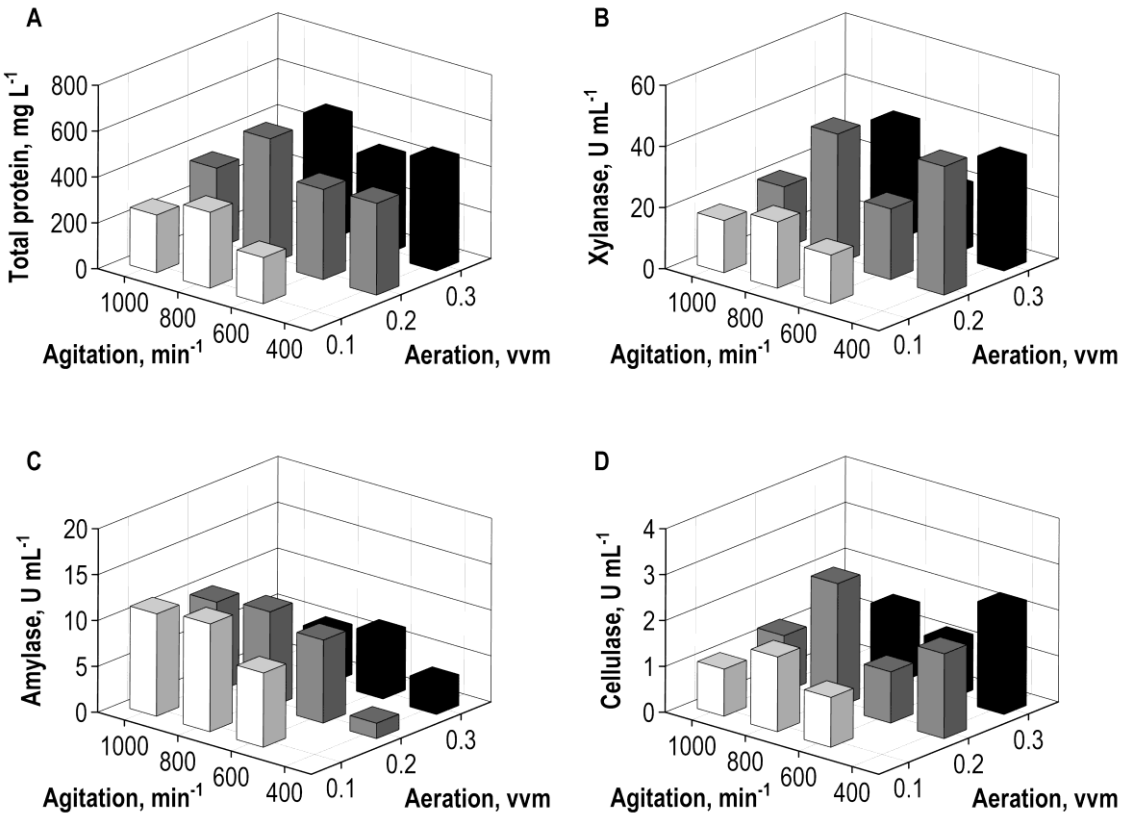

Figure 5.13: A: Total protein concentration, B: Xylanase activity, C: Amylase activity, D: Cellulase activity in the supernatant of co-cultures of *A. niger* NRRL 2270 and *T. reesei* RUT-C30 after 86 h process time in a bioreactor on a 0.7 L scale using synthetic wheat bran medium with varying agitation rates (400-1000 min^{-1}) and initial aeration rates (0.1-0-3 vvm). *T. reesei* RUT-C30 was inoculated with an initial spore concentration of 0.2 × 10^9 spores L^{-1}, *A. niger* NRRL 2270 was added after 16.5 h process time with an initial spore concentration of 10^9 spores L^{-1} (temperature 30 °C, pH 4.5). One unit (U) was defined as the amount of enzymatic activity releasing 1 µmol of xylose (B) or glucose (C, D) equivalents per minute under assay conditions (50 °C, pH 4.5).

Low aeration rates as well as high stirrer speeds seem to be disadvantageous for xylanase and cellulase formation as well as for the overall protein secretion. The maxima of total protein concentration (546 mg L^{-1}), xylanase activity (42.5 U mL^{-1}) and cellulase activity (2.7 U mL^{-1}) were observed at an agitation rate of 800 min^{-1} and an initial aeration rate of 0.2 vvm with an increase to 2 vvm during the batch process. The amylase activity reached its maximum when low aeration rates were combined with intense stirring. However, the amylase activity was only 12% reduced at 800 min^{-1} and 0.2 vvm, the best combination for the other enzyme activities.

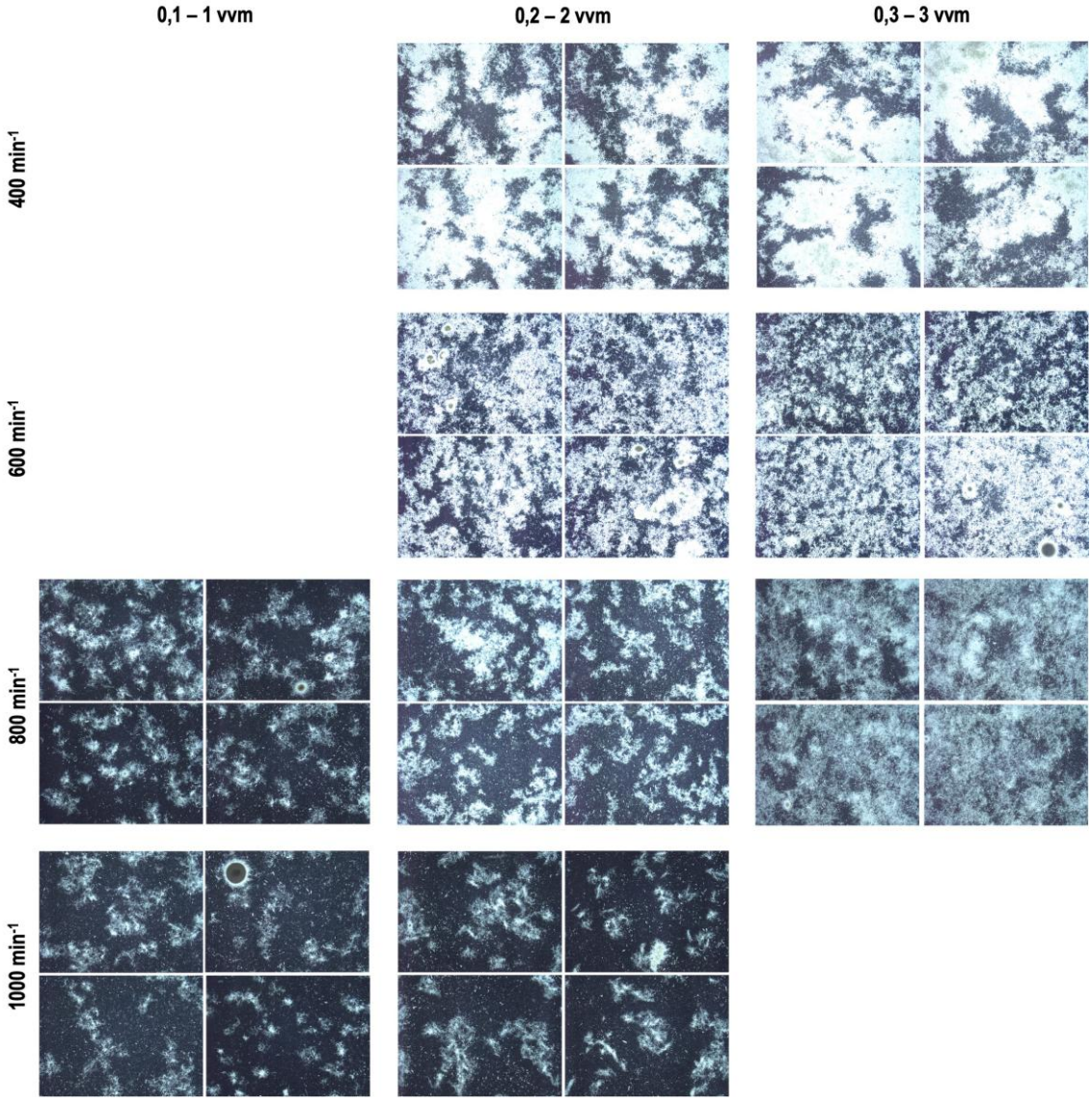

Figure 5.14: Macromorphology of co-cultures of *A. niger* NRRL 2270 and *T. reesei* RUT-C30 after 86 h process time in a bioreactor on a 0.7 L scale using synthetic wheat bran medium at different operating points (agitation rates 400-1000 min^{-1}, initial aeration rates 0.1-0.3 vvm). Identical volumes were analyzed at 1.25 × magnification, and pictures were taken from four different spots on the microscopy slide.

The results described above were also confirmed via microscopy at a 1.25 × magnification, displayed in Figure 5.14. It became visible that high agitation rates resulted in mechanical disruption of the fungal mycelium. Additionally, an apparent decrease in biomass formation was observed with intense stirring.

Consequently, the combination of 800 min^{-1} agitation rate and 0.2-2 vvm aeration rate was selected as a suitable point of operation of the co-cultivation process.

Discussion

Intense agitation of the fermentation broth resulted in a changed macromorphology of the fungi as well as lowered enzyme activities, most probably caused by the introduction of high shear forces into the reactor. This effect was frequently reported for both strains used in this work (Lejeune and Baron, 1995, Kelly et al., 2004, Lin et al., 2010). Those studies describe a change in fungal morphology towards clumped or pelleted growth with high shear forces, resulting in decreasing active biomass and a reduction in the number of enzyme-secreting hyphal tips. This deterioration of enzyme production with high agitation in this work is intensified by the reduced biomass formation, as shown through microscopic analysis (Figure 5.14).

Changes in aeration had different effects on the enzyme formation of the co-culture. The overall protein concentration in the supernatant samples decreased with the lower maximum aeration rate of 0.7 L min^{-1}, as well as the xylanolytic and cellulolytic activities. This was presumably caused by oxygen limitation of the co-cultures, which was observed by flattened CER curves in those processes (Figure 5.12). *T. reesei* is strongly affected by such oxygen-limited conditions and reacts with the termination of growth and protein secretion, especially with genes for cellulase formation being repressed (Bonaccorsi et al., 2006, Rautio et al., 2006). Interestingly, the amylase formation of *A. niger* appears to profit from oxygen-limited conditions. As oxygen limitation is also applied in industrial glucoamylase production, the reasons were investigated in detail by Lu et al., who ascribed this phenomenon to a favorable allocation of reduction equivalents and precursors towards the protein synthesis (Lu et al., 2018). In contrast, *A. niger* is also reported to form various polyols including mannitol, glycerol and erythritol for redox potential balance under oxygen-limited conditions, reducing the carbon available for protein synthesis (Diano et al., 2006).

5.4. Process transfer to the 3 L scale

The co-cultivation process was transferred from the 0.7 L to a 3.0 L bioreactor based on the two criteria (I) constant stirrer tip speed and (II) constant volumetric aeration rate. A constant stirrer tip speed aims to keep the maximum local energy dissipation on the

same level, while the constant volumetric aeration rate serves for a comparable supply with oxygen.

Unfortunately, the stirred-tank bioreactors were not geometrically similar. The geometric features of the 0.7 L and the 3.0 L reactors are listed in Table 4.5 and Table 4.6, respectively. Major differences can be found in the vessel geometry and the number and type of stirrers. These features strongly influence the flow profile inside the vessel, the introduction of shear forces as well as the dispersion and distribution of oxygen in the medium.

The stirrer tip speed of the 0.7 L reactor at the selected agitation rate of 800 min^{-1} was calculated following equation 3.21 at 2.09 m s^{-1} for the inclined blade stirrer and 1.88 m s^{-1} for the Rushton impeller. Consequently, the 3.0 L reactor was operated with a stirring rate of 660 min^{-1}, corresponding with stirrer tip speeds of 2.07 m s^{-1} for the inclined blade stirrers and 1.90 m s^{-1} for the Rushton turbine.

Both stirred-tank reactors were subsequently compared regarding the volumetric oxygen transport coefficient k_La at the chosen operation point at 2 vvm. A 0.2% xanthan solution was applied as a model fluid representing the fungal broth. Almost identical volumetric oxygen transport coefficients of 44.6 h^{-1} were measured.

Subsequently, co-cultivation experiments using synthetic wheat bran medium were conducted in the stirred-tank reactor on the 3.0 L scale. Both methods of inoculation, spores as well as shaking flask precultures were applied.

Inoculation with spores

The 3.0 L process was started by inoculation with 0.2 × 10^9 spores L^{-1} of *T. reesei* RUT-C30 and a following phase of 6 h without active aeration and reduced stirring to prevent the loss of spores. Afterwards, the agitation was increased to 660 min^{-1} and the aeration rate was set to the initial value of 0.6 L min^{-1} (0.2 vvm). *A. niger* NRRL 2270 was added after 16.5 h process time with an initial spore concentration of 10^9 spores L^{-1}. The results are compared with the corresponding co-cultivation process on a 0.7 L scale (from Chapter 5.3, agitation rate 800 min^{-1}, initial aeration rate 0.2 vvm). Overall protein concentrations and enzymatic activities from both processes are depicted in Figure 5.15.

The protein secretion as well as the formation of xylanase, amylase and cellulase in both batch processes commenced at the same process time. The total protein concentration and cellulolytic activity were highly comparable between the two scales, whereas xylanase and amylase activities were even increased by 37% and 23% in the 3.0 L bioreactor, respectively.

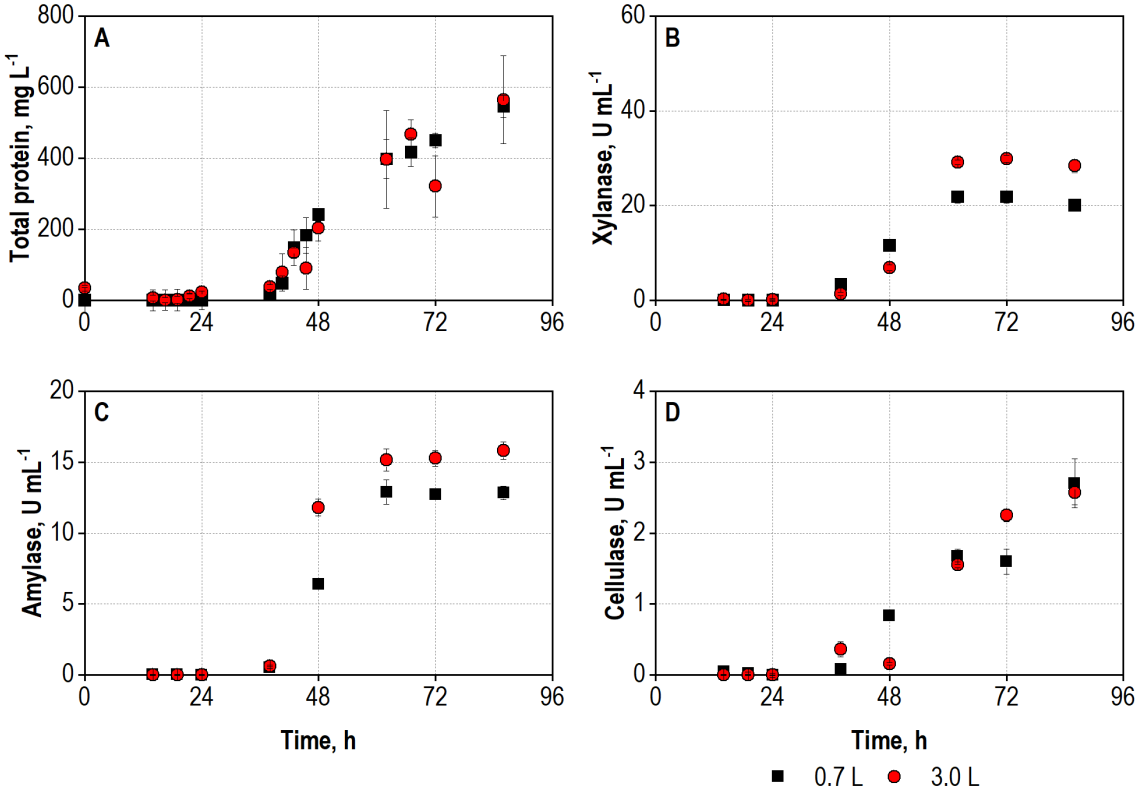

Figure 5.15: A: Total protein concentration, B: Xylanase activity, C: Amylase activity, D: Cellulase activity in the supernatant of co-cultures of *A. niger* NRRL 2270 and *T. reesei* RUT-C30 in a bioreactor on a 0.7 L scale (agitation rate 800 min^{-1}, aeration rate 0.2-2 vvm, black squares) and a bioreactor on a 3.0 L scale (agitation rate 660 min^{-1}, aeration rate 0.2-2 vvm, red circles) using synthetic wheat bran medium. *T. reesei* RUT-C30 was inoculated with an initial spore concentration of 0.2 × 10^9 spores L^{-1}, *A. niger* NRRL 2270 was added after 16.5 h process time with an initial spore concentration of 10^9 spores L^{-1} (temperature 30 °C, pH 4.5). One unit (U) was defined as the amount of enzymatic activity releasing 1 µmol of xylose (B) or glucose (C, D) equivalents per minute under assay conditions (50 °C, pH 4.5).

Inoculation with vegetative cells

The 3.0 L process was inoculated with vegetative cells from shaking flasks precultures with a total initial biomass concentration of 1.2 g L^{-1} (1.0 g L^{-1} *A. niger* NRRL 2270 and 0.2 g L^{-1} *T. reesei* RUT-C30). The agitation rate was constant at 660 min^{-1} and the initial aeration rate of 0.6 L min^{-1} was increased up to 6 L min^{-1} during the cultivation. Figure 5.16 shows the total protein concentrations and enzyme activities compared to the 0.7 L process (from Chapter 5.2.2, ratio of *A. niger* to *T. reesei* of 5:1).

Again, both batch cultivations were highly similar regarding the enzyme activities produced. The overall process time could be shortened from 86 h to 65 h when vegetative cells were applied for inoculation.

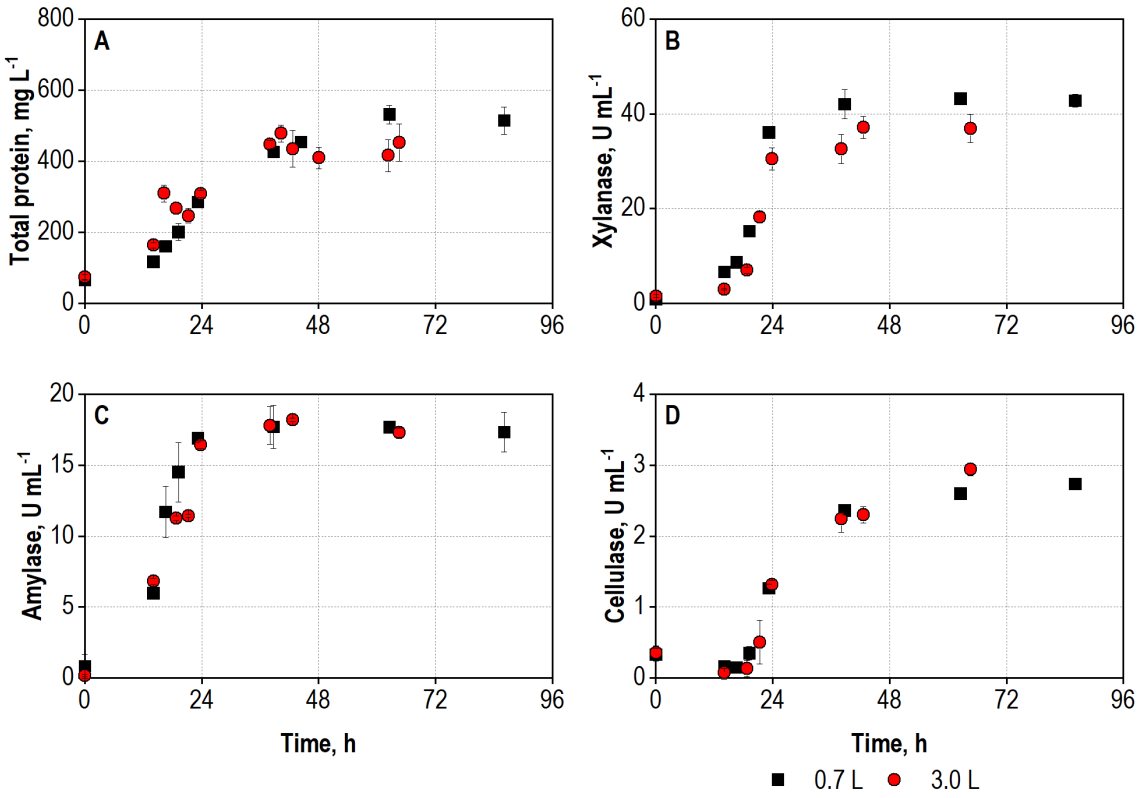

Figure 5.16: A: Total protein concentration, B: Xylanase activity, C: Amylase activity, D: Cellulase activity in the supernatant of co-cultures of *A. niger* NRRL 2270 and *T. reesei* RUT-C30 in a bioreactor on a 0.7 L scale (agitation rate 800 min^{-1}, aeration rate 0.2-2 vvm, black squares) and a bioreactor on a 3.0 L scale (agitation rate 660 min^{-1}, aeration rate 0.2-2 vvm, red circles) using synthetic wheat bran medium. The processes were started by simultaneous inoculation with precultures from shaking flasks with an initial biomass concentration of 1.2 g L^{-1} (1.0 g L^{-1} *A. niger* and 0.2 g L^{-1} *T. reesei*; temperature 30 °C, pH 4.5). One unit (U) was defined as the amount of enzymatic activity releasing 1 µmol of xylose (B) or glucose (C, D) equivalents per minute under assay conditions (50 °C, pH 4.5).

A change in the substrates applied in the synthetic wheat bran medium (corn xylan instead of birch wood xylan, caused by delivery problems) made an additional process on the 3.0 L scale necessary. All other process conditions and parameters remained unchanged. Agitation rate and aeration rate as well as the dissolved oxygen concentration (DO) and the carbon dioxide evolution rate (CER) for processes using both types of xylan are displayed in Figure 5.17.

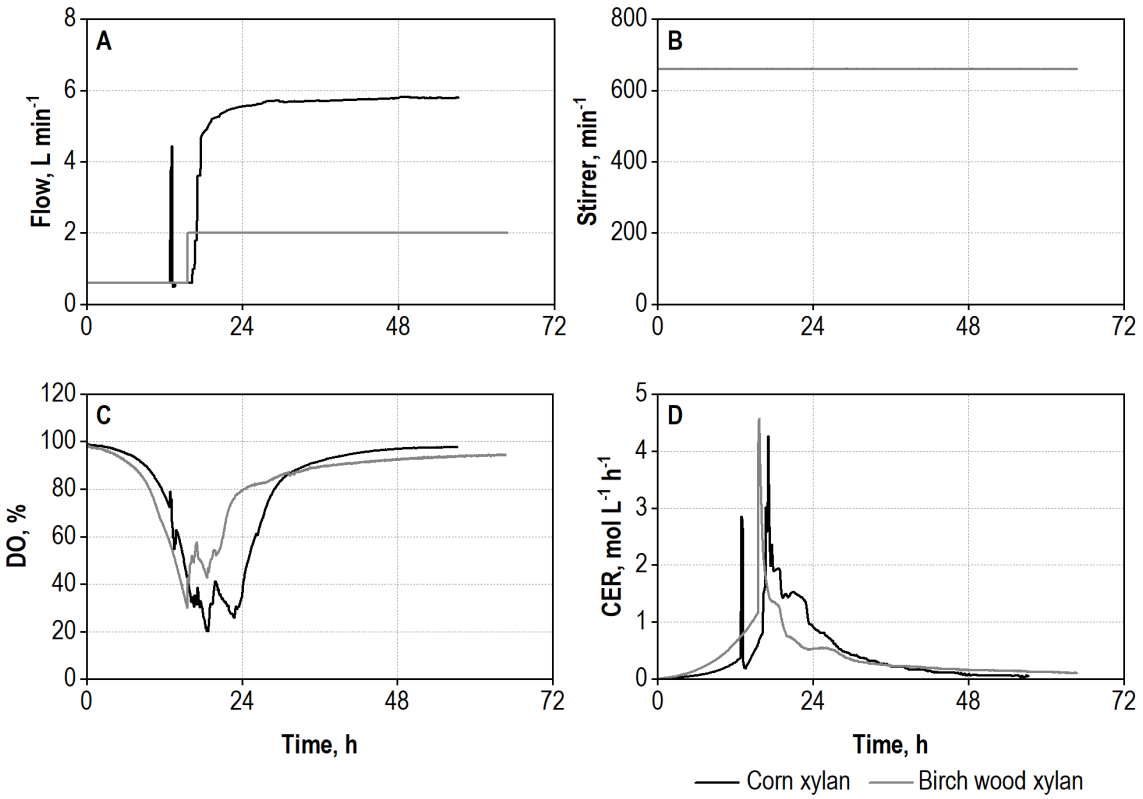

Figure 5.17: A: Air flow rate (Flow), B: Agitation rate (Stirrer), C: Dissolved oxygen concentration (DO), D: Carbon dioxide evolution rate (CER) of co-cultures of *A. niger* NRRL 2270 and *T. reesei* RUT-C30 in a bioreactor on the 3.0 L scale using synthetic wheat bran medium with corn xylan (black lines) and birch wood xylan (gray lines). The process was started by simultaneous inoculation with expanded precultures from shaking flasks with an initial biomass concentration of 1.2 g L^{-1} (1.0 g L^{-1} *A. niger* and 0.2 g L^{-1} *T. reesei*; temperature 30 °C, pH 4.5).

The DO concentration began to drop in both batches shortly after inoculation with 1.2 g L^{-1} vegetative fungal cells. Consequently, the aeration rate increased when the critical DO threshold of 30% was reached. The gassing rate in the process with birch wood xylan settled at 2 L min^{-1}, while it increased to its technical maximum of 6 L min^{-1} (2 vvm) in the process with corn xylan. The maximum metabolic activity in both processes was measured between 16-24 h process time, with a slightly earlier CER decrease with birch wood xylan. The determination of the volumetric oxygen transfer coefficient for the 3.0 L reactor using synthetic wheat bran medium with corn xylan was performed when the DO dropped <80% after ~14 h process time. This resulted in a k_La of 45.5 h^{-1}, which is highly comparable to the k_La determined before using a model fluid (44.6 h^{-1}).

Figure 5.18 compares the overall protein secretion as well as the relevant enzymatic activities produced with corn xylan to the results with birch wood xylan.

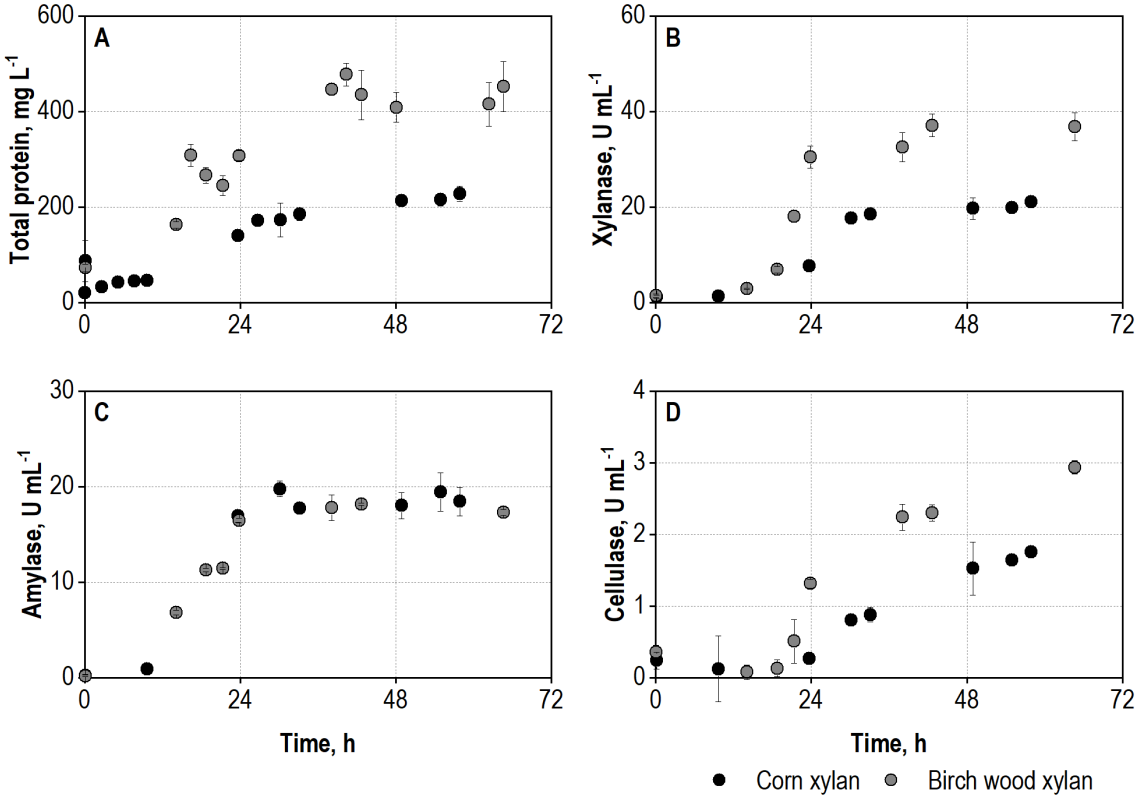

Figure 5.18: A: Total protein concentration, B: Xylanase activity, C: Amylase activity, D: Cellulase activity in the supernatant of co-cultures of *A. niger* NRRL 2270 and *T. reesei* RUT-C30 in a bioreactor on a 3.0 L scale using synthetic wheat bran medium with corn xylan (black circles) and birch wood xylan (gray circles). The processes were started by simultaneous inoculation with precultures from shaking flasks with an initial biomass concentration of 1.2 g L^{-1} (1.0 g L^{-1} *A. niger* and 0.2 g L^{-1} *T. reesei*; temperature 30 °C, pH 4.5). One unit (U) was defined as the amount of enzymatic activity releasing 1 µmol of xylose (B) or glucose (C, D) equivalents per minute under assay conditions (50 °C, pH 4.5).

The total protein concentration with corn xylan reached a maximum of 228 ± 16 mg L^{-1} at the end of the process, being reduced by nearly 50% compared to birch wood xylan (453 ± 52 mg L^{-1}). The maximum xylanase and cellulase activities were also significantly decreased with corn xylan, by 43% (from 37.1 ± 2.3 U mL^{-1} to 21 ± 1 U mL^{-1}) and 40% (from 2.9 ± 0.1 U mL^{-1} to 1.8 U mL^{-1}), respectively. Solely the amylase formation appeared unaffected. Amylolytic enzymes in both processes were mainly formed between ~10-24 h process time and remained at a plateau of 19 U mL^{-1} afterwards.

Discussion

The co-cultivation process with *A. niger* and *T. reesei* was successfully transferred between two geometrically unsimilar reactors by the application of two rational transfer criteria. Constant stirrer tip speeds and volumetric aeration rates enabled comparable growth and enzyme production of the fungi, which were inoculated with either spores or vegetative shaking flask precultures.

A direct comparison of both inoculation methods on the 3.0 L scale made it obvious that the application of precultures is the preferable way of inoculation. It did not only result in higher enzymatic activities (xylanase +24%, amylase +15%, cellulase +12%), but these enzyme activities were reached within 65 h instead of 86 h, allowing shortened process times.

The substrate change from birch wood xylan to corn xylan resulted in a clear shift of the enzyme activities produced, especially of xylanase and cellulase. As those two types of xylan stem from different sources and are assumably processed differently (Ebringerová and Heinze, 2000), they probably offer different structures and composition, and the fungi adapt their enzyme secretion accordingly.

5.5. Process transfer to the 25 L scale

Once again, the reactor vessels at hand were not geometrically similar. Their respective geometric features are listed in Table 4.6 and Table 4.7.

A prominent disparity in reactor geometry is posed by the different stirrer types installed. The lab-scale bioreactors were equipped with inclined blade stirrers, while only Rushton turbines were available for the 25 L reactor. Another important difference is the placement of the probes for pH, DO, temperature and sampling close to the bottom of the vessel instead of the lid. This also affects homogenization as only the four built-in baffles serve for turbulent mixing of the broth near to the reactor wall. The ratio of liquid height to reactor diameter was 1.8, and the ratio of stirrer diameter to reactor diameter was 0.41, both numbers higher than with the 3.0 L reactor. The experiments were conducted using corn xylan as hemicellulosic component of the synthetic wheat bran medium.

As before, the stirrer tip speed and the volumetric aeration rate were kept constant. These criteria resulted in a constant stirring speed of 330 min^{-1} and an initial aeration rate of 5 L min^{-1}. A volumetric oxygen transfer coefficient k_La of 27.7 h^{-1} was determined ~7 h after inoculation, when the DO concentration dropped below 80%, i.e. at the same point in the process than in the 3.0 L cultivation (k_La of 45.5 h^{-1}, see Chapter 5.4). This measurement allowed the assumption of reduced oxygen transfer in the 25 L reactor, even though the metabolic activities (CERs) of the cultures were not identical at the time.

Figure 5.19 displays the agitation rate and the aeration rate as well as DO and CER during the 25 L process.

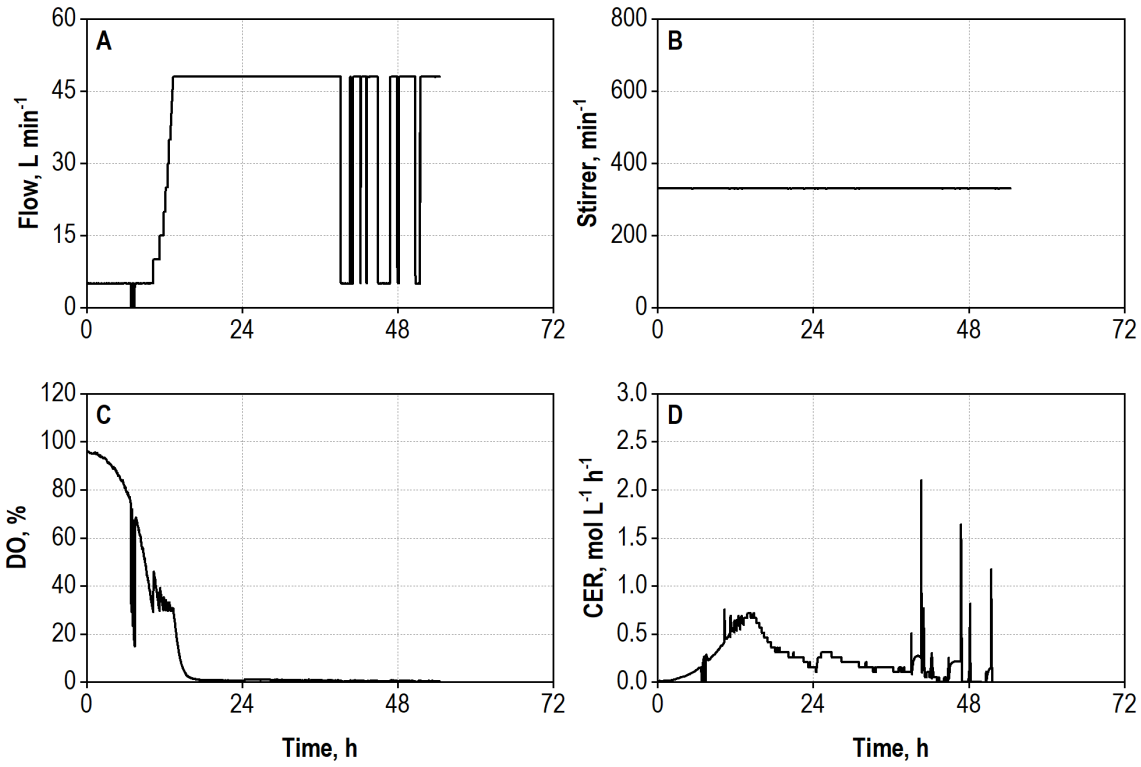

Figure 5.19: A: Air flow rate (Flow), B: Agitation rate (Stirrer); C: Dissolved oxygen concentration (DO), D: Carbon dioxide evolution rate (CER) of a co-culture of *A. niger* NRRL 2270 and *T. reesei* RUT-C30 in a bioreactor on a 25 L scale using synthetic wheat bran medium with corn xylan. The process was started by simultaneous inoculation with precultures from shaking flasks with an initial biomass concentration of 1.2 g L^{-1} (1.0 g L^{-1} *A. niger* and 0.2 g L^{-1} *T. reesei*; temperature 30 °C, pH 4.5).

The stepwise increase of the aeration rate from 5-50 L min^{-1} kept the DO above the threshold of 30% between 10-14 h process time, afterwards the DO dropped to zero until process end, despite the maximum aeration rate and an additional 1.2 bar overpressure in the reactor after 24 h. The aeration of the reactor was repeatedly decreased in a time interval between 39-52 h process time due to the anti-foaming control sequence (described in detail in Chapter 4.3.6). This was, however, triggered by fungal surface growth on the anti-foam probe, consequently the control was inactivated for the remainder of the process.

The data regarding total protein and enzyme formation are depicted in Figure 5.20, in comparison to the respective data from the 3 L reference experiment described above.

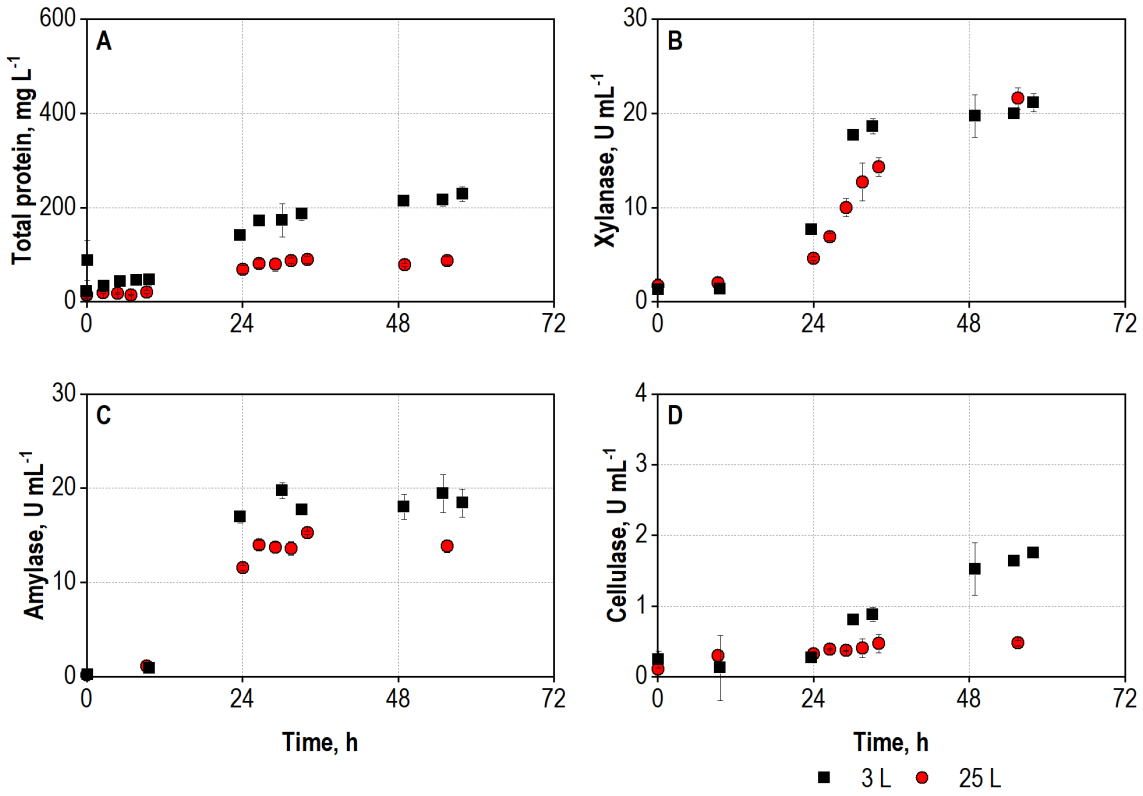

Figure 5.20: A: Total protein concentration, B: Xylanase activity, C: Amylase activity, D: Cellulase activity, in the supernatant of co-cultures of *A. niger* NRRL 2270 and *T. reesei* RUT-C30 in a bioreactor on a 3 L scale (agitation rate 660 min^{-1}, aeration rate 0.2-2 vvm, black squares) and a bioreactor on a 25 L scale (agitation rate 330 min^{-1}, aeration rate 0.2-2 vvm, red circles) using synthetic wheat bran medium with corn xylan. The process was started by simultaneous inoculation with precultures from shaking flasks with an initial biomass concentration of 1.2 g L^{-1} (1.0 g L^{-1} *A. niger* and 0.2 g L^{-1} *T. reesei*; temperature 30 °C, pH 4.5). One unit (U) was defined as the amount of enzymatic activity releasing 1 µmol of xylose (B) or glucose (C, D) equivalents per minute under assay conditions (50 °C, pH 4.5).

The maximum values of the total protein concentration, the amylase and the cellulase activity were significantly decreased by 61%, 23% and 71%, respectively, compared to the 3.0 L process. Xylanase formation did not appear to be affected by the oxygen limitation and rose to a nearly identical maximum activity compared to the 3.0 L scale. However, the oxygen limitation strongly affected the enzyme production, thus lifting this limitation was defined as the main task during the process transfer to the 25 L scale.

A common approach to improve the dispersion and solution of oxygen in the medium is increasing the agitation rate. Here, this was realized by a control cascade after the aeration rate had reached its maximum. The cascade parameters are described in detail in Chapter 4.3.6. Simultaneously, the upper Rushton turbines in the reactor were replaced by inclined blade stirrers (middle stirrer: upward-pumping, upper stirrer: downward-pumping) to avoid excess shear stress at the stirrer tips at higher agitation rates. The gassing and stirring rate during the co-cultivation process on a 25 L scale are

displayed in Figure 5.21, together with the resulting dissolved oxygen concentration and the CO_2 evolution rate.

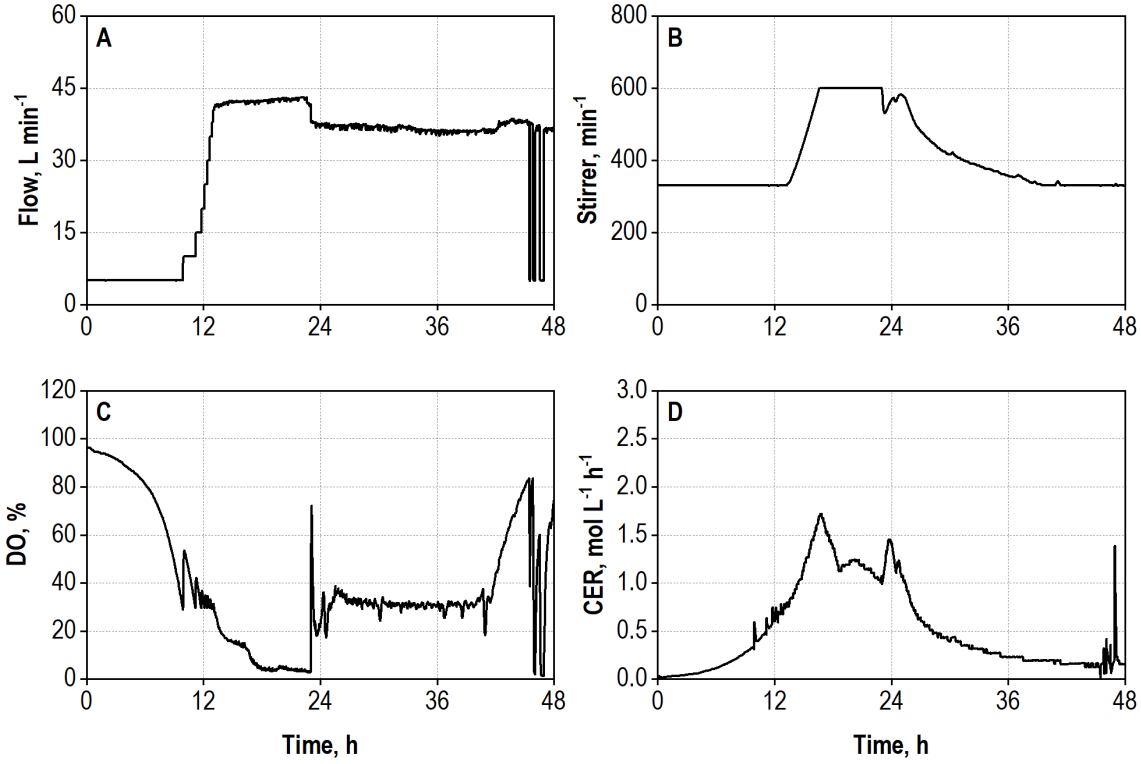

Figure 5.21: A: Air flow rate (Flow), B: Agitation rate (Stirrer), C: Dissolved oxygen concentration (DO), D: Carbon dioxide evolution rate (CER) of a co-culture of *A. niger* NRRL 2270 and *T. reesei* RUT-C30 in a bioreactor on a 25 L scale using synthetic wheat bran medium with corn xylan. A stirrer control cascade was applied for DO control, and 1.2 bar overpressure were added after 23 h process time. The process was started by simultaneous inoculation with precultures from shaking flasks with an initial biomass concentration of 1.2 g L^{-1} (1.0 g L^{-1} *A. niger* and 0.2 g L^{-1} *T. reesei*; temperature 30 °C, pH 4.5).

As before, fungal growth started without a significant lag phase and DO reached the critical threshold of 30% air saturation already after 10 h process time. Subsequently, the stepwise increasement of the aeration rate kept the DO above 30% within the next 3 h, afterwards the stirring rate increased to its maximum after 17 h. Nevertheless, the DO dropped to around 5% air saturation. At 23 h process time, 1.2 bar overpressure was applied, causing the dissolved oxygen concentration to stabilize at 30% air saturation again, and the stirring rate was slowly decreased to the initial value of 330 min^{-1}. A further, rapid increase in DO after 42 h indicated the depletion of accessible substrates and thus the end of the enzyme production process.

The overall protein concentration and the corresponding hydrolytic enzyme activities are shown in Figure 5.22.

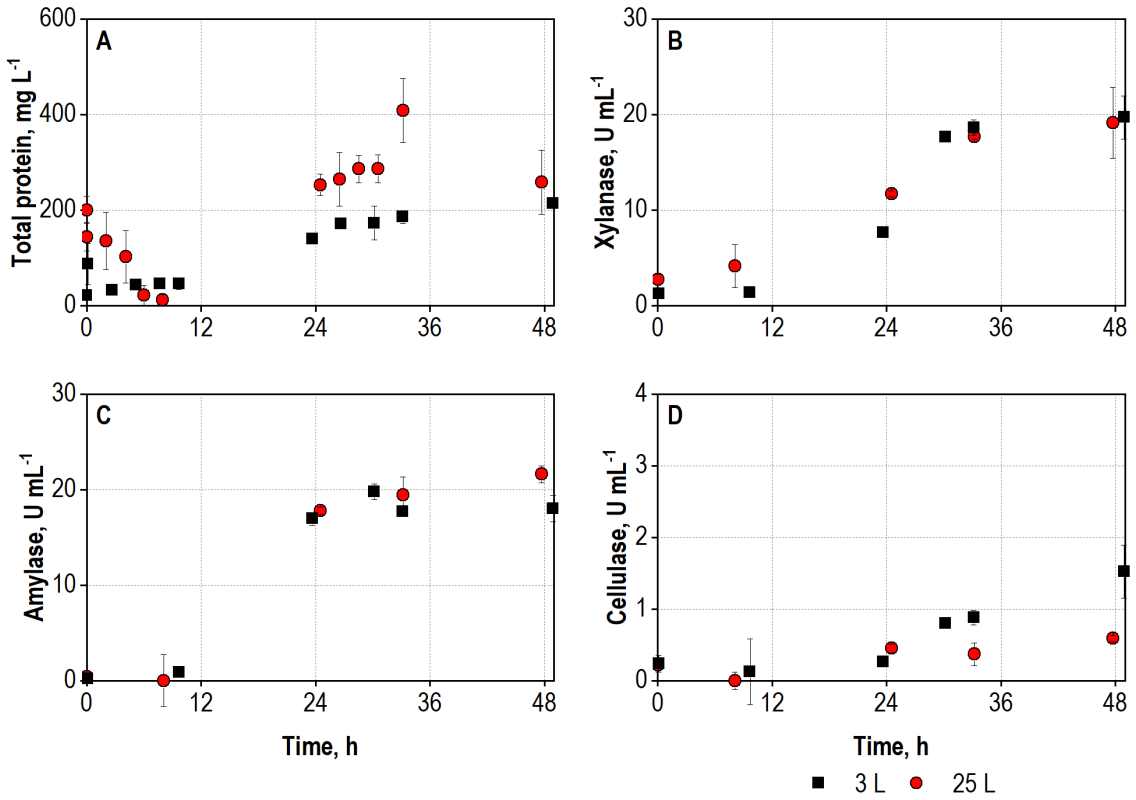

Figure 5.22: A: Total protein concentration, B: Xylanase activity, C: Amylase activity, D: Cellulase activity, in the supernatant of a co-culture of *A. niger* NRRL 2270 and *T. reesei* RUT-C30 in a bioreactor on a 3 L scale (agitation rate 660 min^{-1}, aeration rate 0.2-2 vvm, black squares) and a bioreactor on a 25 L scale (agitation rate 330 min^{-1}, aeration rate 0.2-2 vvm, red circles) using synthetic wheat bran medium with corn xylan. A stirrer control cascade was applied for DO control. The process was started by simultaneous inoculation with expanded precultures from shaking flasks with an initial biomass concentration of 1.2 g L^{-1} (1.0 g L^{-1} *A. niger* and 0.2 g L^{-1} *T. reesei*; temperature 30 °C, pH 4.5). One unit (U) was defined as the amount of enzymatic activity releasing 1 µmol of xylose (B) or glucose (C, D) equivalents per minute under assay conditions (50 °C, pH 4.5).

The implemented DO control enabled enhanced protein secretion and the formation of similar xylanolytic and amylolytic activities compared to the 3.0 L process. A xylanase activity of 19.2 ± 3.7 U mL^{-1} and an amylase activity of 21.6 ± 0.9 U mL^{-1} were measured in the supernatant at the end of the enzyme production after 48 h. Solely the cellulase activity stayed 65% lower than on the 3.0 L scale.

Discussion

The transfer of the co-cultivation process from the 3.0 L to the 25 L scale based on constant stirrer tip speeds and volumetric aeration rate resulted in oxygen limitation of the fungi and consequently decreased enzyme formation. Especially the enzyme production of *T. reesei* appeared to be inhibited by the lack of oxygen. A strong restriction of the cellulase production of *T. reesei* under such conditions was reported in literature (Rautio et al., 2006). The oxygen transfer coefficient k_La was significantly lower than on

the 3.0 L scale, confirming the reduced oxygen transfer in the 25 L reactor. A potential cause could be posed by the viscous and shear thinning character of the fermentation broth. This behavior could hinder the transfer of dispersed gas bubbles to the outer zones of the larger reactor vessel, where areas with diminished mixing and oxygen provision would be created.

A dynamic stirrer control cascade was subsequently applied as a corrective measure. So far, an increasement of the agitation rate was omitted due to the reported disadvantageous effects of high shear forces on the enzyme formation of *A. niger* and *T. reesei* (Lejeune and Baron, 1995, Kelly et al., 2004, Lin et al., 2010). These influences were also observed in earlier experiments (see Chapter 5.3). In return, the shear forces introduced into the broth should be minimized to alleviate those detrimental effects. This was realized on the one hand by replacing two Rushton turbines with inclined blade stirrers, and on the other hand by an asymmetrical stirrer control, where the reduction of the stirring rate happens faster than the increment (described in detail in Chapter 4.3.6). Consequently, the enzyme production on the 25 L scale was enhanced. Xylanolytic and amylolytic activities were on the same level as in the 3.0 L process. Only the cellulase formation remained reduced, possibly caused by the negative impact of increased shear forces on *T. reesei* (Lejeune and Baron, 1995).

6. Enzymatic hydrolysis of wheat bran[3]

The enzyme solution formed in the co-cultivation process with *A. niger* and *T. reesei* is intended for the degradation of wheat bran in a cell-free hydrolysis process. The enzyme mixtures from cultivation experiments are separated from the fungal cells and solid media components by centrifugation and filtration before the application in hydrolysis experiments. Additional purification or stabilization steps (like drying or formulation with supplements) are not necessary. First, the enzyme mixture produced by the selected co-culture is characterized regarding its temperature and pH optima. Afterwards, hydrolysis processes are conducted in stirred-tank reactors on the L scale to compare the co-culture enzymes to those produced in monocultures.

6.1. Characterization of enzyme activities from co-culture

The enzymes produced in the co-culture of *A. niger* and *T. reesei* were characterized regarding their temperature and pH optima in order to find suitable reaction conditions for the hydrolysis of wheat bran. This was done by determining the relevant enzymatic activities, i.e. xylanase, amylase and cellulase activity, with the colorimetric assay (see Chapter 4.5.3) at different reaction temperatures (20-70 °C) and pH 3.0-pH 7.0. The enzyme solution was harvested from a 0.7 L co-cultivation process of *A. niger* NRRL 2270 and *T. reesei* RUT-C30, which was inoculated with spore suspensions (0.2×10^9 spores L^{-1} *T. reesei*, 10^9 spores L^{-1} *A. niger* added after 16.5 h) and was conducted at the cultivation conditions identified in Chapter 5.3 (agitation rate 800 min^{-1}, initial aeration rate 0.2 vvm). The enzyme activities are plotted in Figure 6.1 and additionally listed in Table 10.6, Table 10.7 and Table 10.8 in the Supplementary Material.

The xylanolytic activity showed a clear maximum at a temperature of 60 °C and pH 4.5. Lower temperatures of 30-50 °C led to reduced activity, and at 70 °C the enzymes were obviously inactivated. The amylase activity in the culture supernatant increased with temperature and showed a broad pH optimum < 5.5. The maximum cellulase activity could be observed at 50 °C and around pH 5.0.

[3] Parts of the data from this chapter are published in Mittermeier, F., N. Hafner, K. Xypolia Vasila and D. Weuster-Botz (2023). "Co-Cultivation of *Aspergillus niger* and *Trichoderma reesei* Enables Efficient Production of Enzymes for the Hydrolysis of Wheat Bran." Chemie Ingenieur Technik **95**(4): 565-575.

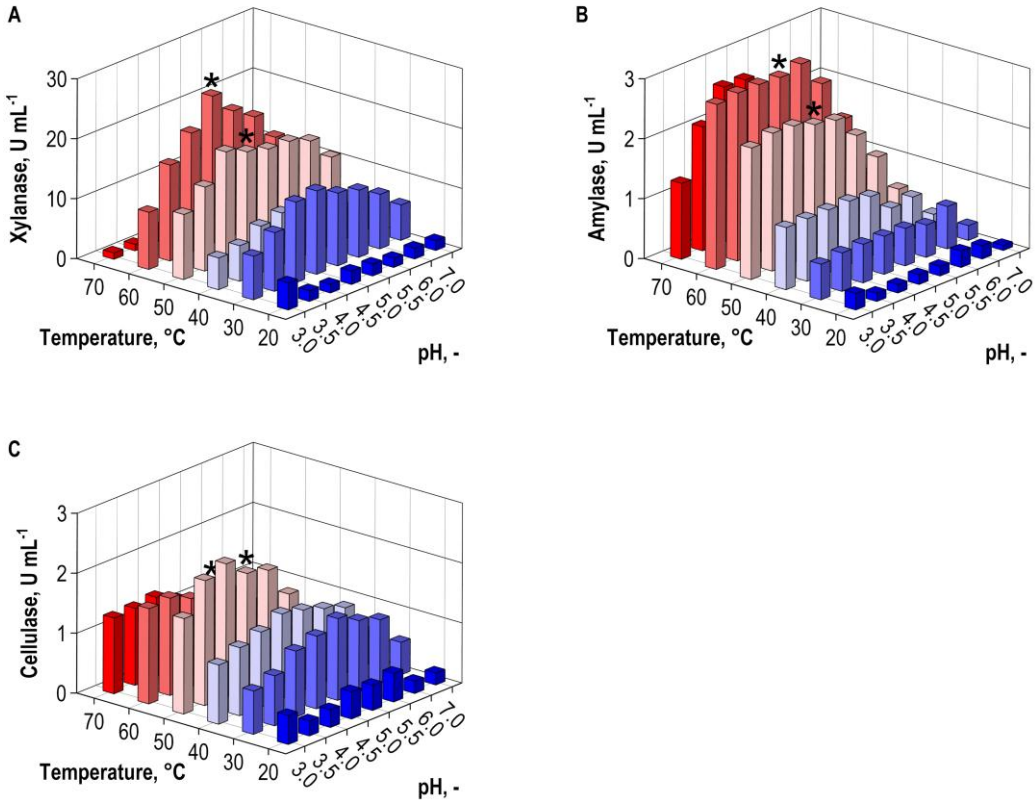

Figure 6.1: A: Xylanase activity, B: Amylase activity, C: Cellulase activity at varying temperatures and pH of the enzyme solution produced by a co-culture of *A. niger* NRRL 2270 and *T. reesei* RUT-C30. One unit (U) was defined as the amount of enzymatic activity releasing 1 µmol of xylose (A) or glucose (B, C) equivalents per minute under assay conditions (50 °C, pH 4.5, reaction time 50 min (xylanase) or 30 min (amylase, cellulase)). The reaction conditions marked with asterisks were selected for the following experiments.

The highest enzyme activities were measured at a temperature of 50 °C (cellulase) and 60 °C (xylanase, amylase) at a pH ~4.0-4.5. Subsequently, these conditions were applied for the hydrolysis of wheat bran on the 40 mL scale in glass bottles. The resulting sugar concentrations over process time are shown in Figure 6.2.

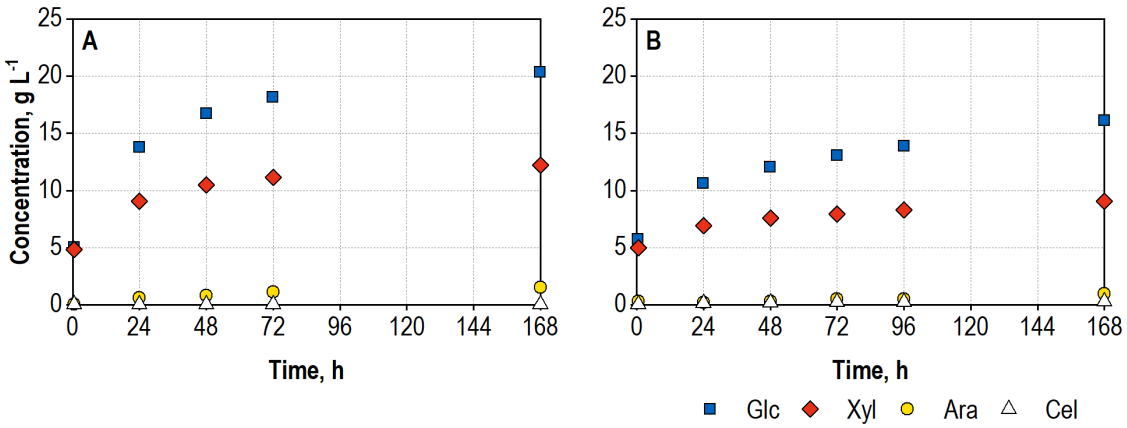

Figure 6.2: Sugar concentrations released from 100 g L^{-1} wheat bran during hydrolysis with enzymes from a co-culture of *A. niger* NRRL 2270 and *T. reesei* RUT-C30. Hydrolysis was performed on the 40 mL scale in glass bottles at 50 °C (A) or 60 °C (B) and pH 4.5, buffered with 50 mM sodium acetate. The wheat bran was sterilized in a dry state at 121 °C for 20 min before a mixture of 10% (v/v) enzyme solution and 90% (v/v) buffer were added. Glc: glucose, Xyl: xylose, Ara: arabinose, Cel: cellobiose.

The released sugar concentrations only reached 26.4 g L^{-1} at 60 °C. At 50 °C, an overall sugar concentration of 34.0 g L^{-1} was measured in the hydrolysate (20.3 g L^{-1} glucose and 12.2 g L^{-1} xylose). The usage of *T. reesei* cellulases at 50 °C and pH 4.8 for cellulose degradation has been described in literature (Reese and Mandels, 1980), however they are also reported to be rather thermostable (Boer and Koivula, 2003, Kupski et al., 2014). *A. niger* α-amylases are also described as resistant up to 105 °C, while the strain's glucoamylases and xylanases apparently have high short-time activities, but are more thermosensitive at longer process times (Wang et al., 2006, McDaniel et al., 2008, Membrillo Venegas et al., 2013). Therefore, 50 °C was set as the temperature for subsequent hydrolysis processes. A variation of the buffer systems used for hydrolysis (sodium acetate, sodium citrate, potassium acetate, potassium citrate, each 50 mM or 100 mM) had no significant influence on the sugar release (data not shown).

6.2. Comparison of hydrolysis with enzymes from monoculture and co-culture

The hydrolytic potential of the enzyme mixture produced by the co-culture of *A. niger* NRRL 2270 and *T. reesei* RUT-C30 was evaluated by comparison with the respective monoculture enzyme solution and a 1:1 mixture of those supernatants. These processes were conducted with a volume of 0.5 L in stirred-tank reactors and a process time of 45 h. 100 g L^{-1} wheat bran provided by the project partners of Bayerischer Müllerbund (Munich, Germany) was used as a substrate. Its composition is described in detail in Chapter 4.2. Figure 6.3 displays the enzymatically released sugar concentrations over time. Due to the sterilization process of the wheat bran suspended in buffer, a total of

8.7-9.6 g L^{-1} sugars were already present before enzyme addition. These initial sugar concentrations were not considered here.

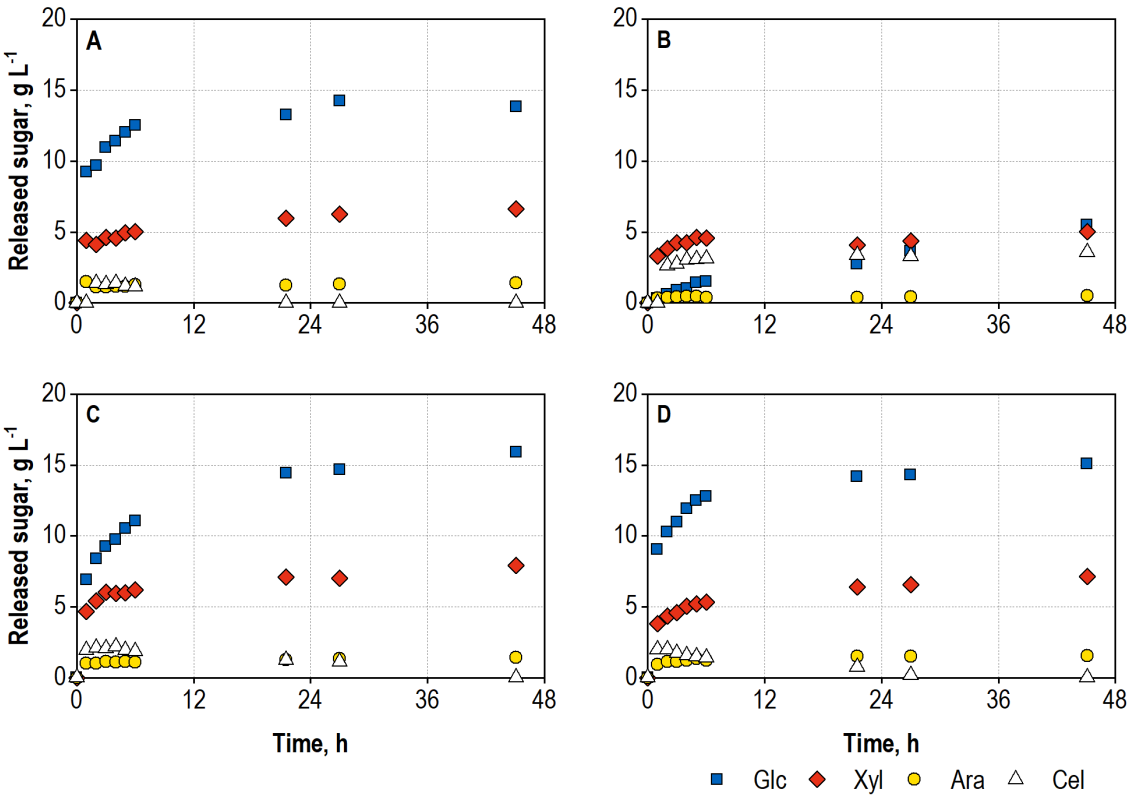

Figure 6.3: Sugars released from 100 g L^{-1} wheat bran during hydrolysis with enzymes from *A. niger* NRRL 2270 (A) and *T. reesei* RUT-C30 (B) monocultures, a 1:1 mixture of these enzymes (C) and enzymes produced in a co-culture of *A. niger* NRRL 2270 and *T. reesei* RUT-C30 (D). Hydrolysis was performed in 0.5 L stirred-tank reactors at 50 °C and pH 4.5, buffered with 50 mM sodium acetate. The wheat bran was suspended in buffer and sterilized at 121 °C for 20 min before 10% (v/v) enzyme solution were added into each reactor. Glc: glucose, Xyl: xylose, Ara: arabinose, Cel: cellobiose.

Most of the sugars were already released within the first few hours. Subsequently, glucose release was observable over the complete process time with the mixed enzymes and the co-culture, whereas it reached a plateau with *A. niger* enzymes after 25 h. *T. reesei* enzymes released significantly less sugar, with a higher share of hemicellulosic sugars and a noteworthy accumulation of cellobiose.

The composition of the hydrolysates at the process end is depicted in Figure 6.4, with the sugars present after sterilization and the sugars released during hydrolysis added up.

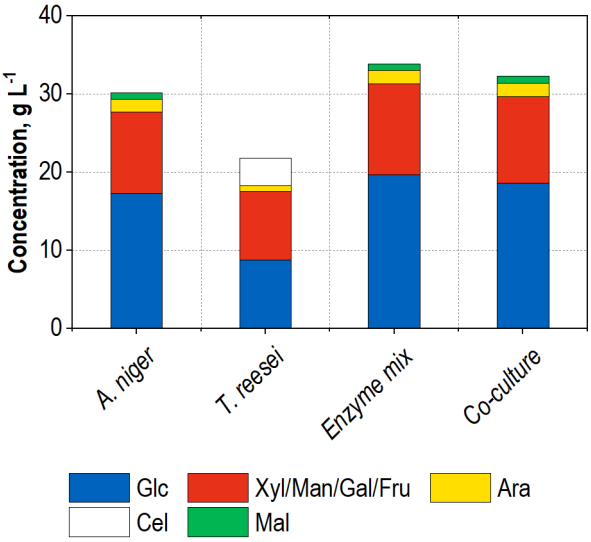

Figure 6.4: Hydrolysate composition after 45 h hydrolysis of 100 g L^{-1} wheat bran using enzymes from *A. niger* NRRL 2270 and *T. reesei* RUT-C30 monocultures, a 1:1 mixture of these enzymes and enzymes produced in a co-culture of *A. niger* NRRL 2270 and *T. reesei* RUT-C30. Hydrolysis was performed in 0.5 L reactors at 50 °C and pH 4.5, buffered with 50 mM sodium acetate. Wheat bran was sterilized at 121 °C for 20 min before 10% (v/v) enzyme solution were added into each reactor. Sugars released after sterilization and after enzymatic hydrolysis are summed up. Glc: glucose, Xyl: xylose, Ara: arabinose, Cel: cellobiose.

Final sugar concentrations of 30.2 g L^{-1} (*A. niger*), 32.4 g L^{-1} (co-culture) and 33.9 g L^{-1} (enzyme mix) were measured after 45 h, respectively. Each of those hydrolysates contained ~57% glucose, ~34% xylose and ~5% arabinose. The *T. reesei* enzymes resulted in a total sugar concentration of only 21.9 g L^{-1}, composed of 40.4% glucose, 40.1% xylose, 3.1% arabinose and 16.4% cellobiose.

The enzymatic hydrolysis process was subsequently transferred to the 3 L scale using a stirred-tank bioreactor with a maximum volume of 7.5 L. Several identical processes were conducted on this scale to produce wheat bran hydrolysate for utilization experiments with oleaginous yeasts (described in the Supplementary Material, see Chapter 10.4). One of these processes is exemplary displayed in Figure 6.5, together with data from the 0.5 L scale for comparison.

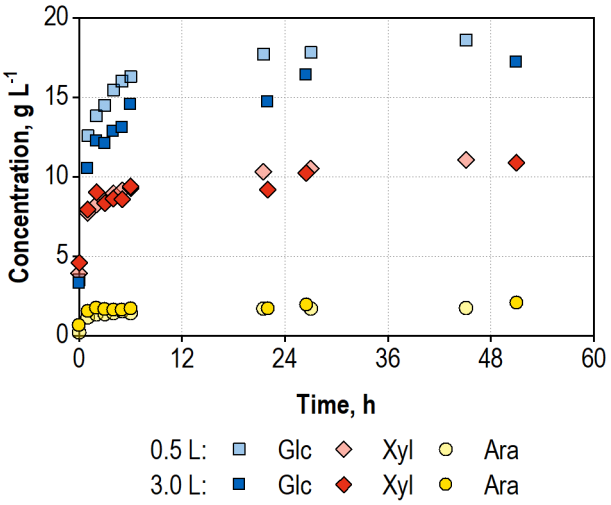

Figure 6.5: Sugar concentrations released from 100 g L^{-1} wheat bran during hydrolysis with enzymes from a co-culture of *A. niger* NRRL 2270 and *T. reesei* RUT-C30. Hydrolysis was performed in a 0.5 L reactor (pale symbols) or a 3.0 L reactor (dark symbols) at 50 °C and pH 4.5, buffered with 50 mM sodium acetate. The wheat bran was suspended in buffer and sterilized at 121 °C for 20 min before 10% (v/v) enzyme solution were added into each reactor. Glc: glucose, Xyl: xylose, Ara: arabinose, Cel: cellobiose.

The sugar concentrations from the 0.5 L scale and the 3.0 L scale strongly resemble each other. An overall concentration of 8.6 g L^{-1} sugars was already released during the sterilization process. Afterwards, the concentrations increased rapidly within the first 6 h of the process up to a total of 25.7 g L^{-1}. When the process was terminated after 51 h, 30.2 g L^{-1} sugars were measured in the hydrolysate, corresponding to 54% of the theoretical yield (0.5 L scale: total sugar concentration 32.4 g L^{-1}, yield 58.4%). Of these sugars, 57% (17.2 g L^{-1}, 0.5 L scale: 18.6 g L^{-1}) were glucose, 36% (10.9 g L^{-1}, 0.5 L scale: 11.1 g L^{-1}) xylose and 7% (2.1 g L^{-1}, 0.5 L scale: 1.8 g L^{-1}) arabinose.

Discussion

The enzyme solutions from an *A. niger* monoculture, a co-culture as well as a mix of monoculture enzymes reached comparable final sugar concentrations and yields of 54.4% (*A. niger* monoculture), 58.4% (co-culture) and 61.1% (enzyme mix). These yields are similar or even higher than those achieved in comparable studies, without using harsh pretreatment methods such as steam explosion extrusion or chemical pretreatment (Jiang and Guo, 2016, Aktas-Akyildiz et al., 2020). Enzymes produced by *T. reesei* released significantly less sugar (21.9 g L^{-1}, corresponding to 39.5% yield), and a remarkable accumulation of cellobiose in the hydrolysate. The most likely cause therefor was a high cellulase activity together with a known deficiency of *Trichoderma* β-glucosidases (Ryu and Mandels, 1980).

The co-culture of *A. niger* NRRL 2270 and *T. reesei* RUT-C30 proved to be able to produce a suitable enzyme solution for the degradation of wheat bran. It reached improved total sugar yields compared to the respective monoculture enzymes and showed the highest space-time yield with 4.8 g L^{-1} h^{-1} in 4 h (*A. niger* and enzyme mix: 4 g L^{-1} h^{-1}). Additionally, an initial accumulation of cellobiose followed by its rapid cleavage into glucose indicated its high capability of cellulose utilization. Furthermore, co-cultivation brings a procedural advantage: the production of enzymes with a co-culture can be conducted in one process in a single bioreactor, whereas the enzyme mix requires either the availability of multiple bioreactors or two processes with intermediate cleaning and sterilization steps. This leads to either higher investment costs or increased demand in time and labor, especially at larger scales.

7. Process integration of enzyme production and hydrolysis[4]

So far, enzyme production and hydrolysis have been separated processes. The integration of these operations into a one-pot process poses a possibility to reduce the number of work steps, leading to lower process times and costs. Such a one-pot process is divided into two main phases. First, fungi are cultivated in a stirred-tank bioreactor to produce the desired enzymes. Afterwards, it is necessary to inactivate the fungal cells to enable sugar accumulation during the subsequent hydrolysis phase. This can be achieved by changing the reaction conditions to conditions unfavorable for microbial growth, for instance increased temperature or stop of aeration.

According to this, an integrated process for the enzyme production with a co-culture of *A. niger* NRRL 2270 and *T. reesei* RUT-C30, followed by the enzymatic hydrolysis of wheat bran is established. The enzyme production process is conducted as described before, except for a change of substrate from synthetic wheat bran to real wheat bran. The fungal cells are subsequently inactivated by terminating the aeration and increasing the temperature to the hydrolysis temperature of 50 °C, before fresh wheat bran is added for hydrolysis. First experiments are performed in a stirred-tank bioreactor on a 25 L scale, before the complete process is transferred to the 1000 L scale. The solid fraction remaining after the process, consisting of fungal and plant biomass, is additionally analyzed regarding its suitability as animal feed.

7.1. Integration of enzyme production and hydrolysis

The integration of enzyme production and hydrolysis into a one-pot process on a 25 L scale raised a series of challenges that needed to be tackled. As mentioned above, the enzyme-producing fungi must be inactivated prior to the addition of fresh wheat bran for hydrolysis. Additionally, it was technically not feasible to sterilize this wheat bran in a dry state (180 °C, 30 min) beforehand. An autoclaving procedure with suspended wheat bran (for example with buffer) would have resulted in an increased reaction volume, dilution of the substrate and consequently in a lowered yield. Consequently, unsterile wheat bran was added for hydrolysis, potentially bringing additional contaminating microorganisms into the process. It was therefore necessary to prevent the growth of either microorganism during the hydrolysis process. One potential solution was posed by the hydrolysis temperature of 50 °C, as most microorganisms cannot grow at this

[4] Parts of the data from this chapter are published in: Mittermeier, F., F. Fischer, S. Hauke, P. Hirschmann and D. Weuster-Botz (2024). "Valorization of Wheat Bran by Co-Cultivation of Fungi with Integrated Hydrolysis to Provide Sugars and Animal Feed." BioTech **13**(2): 15.

temperature. The second approach pursued was to create anaerobic conditions. To minimize the availability of oxygen in the reactor, the overpressure was released, and the gassing rate was set to 5 L min^{-1}. A complete termination of the aeration would have led to a blockage of the gas sparger by biomass particles in this specific setup, causing excessive and complicated cleaning steps before the reactor could have been used for other purposes. Gassing with nitrogen was technically not possible.

An integrated process on the 25 L scale was conducted using wheat bran for both enzyme production and hydrolysis. A concentration of 30 g L^{-1} wheat bran was applied as carbon source for the co-cultivation of *A. niger* and *T. reesei*, before 100 g L^{-1} fresh wheat bran were added for hydrolysis. The oxygen supply in the process was controlled via the stepwise increase of the aeration, the application of 1.2 bar overpressure after 17 h process time, and a stirrer control cascade as described before (Chapter 5.5). A comparable co-cultivation process on the 25 L scale with synthetic wheat bran medium for enzyme production and 50 g L^{-1} wheat bran for hydrolysis was used as a reference process. Stirring rate and gassing rate as well as the dissolved oxygen concentration and the CO_2 evolution rate of both processes are depicted in Figure 7.1.

The growth of the fungi started shortly after inoculation with shaking flask precultures without a lag phase. Subsequently, the DO control cascade managed to maintain a DO above 30% by stepwise increasing the aeration rate to the technical maximum of 43 L min^{-1} between 11.5-16 h process time. An additional overpressure of 1.2 bar was applied after 17 h, and the DO was controlled by the stirrer speed afterwards. The maximum in metabolic activity was after 20-24 h, indicated by the CER peak. A lower maximum CER as well as a mostly lower stirring rate pointed at a reduced metabolic activity of the fungi with wheat bran compared to synthetic wheat bran medium. The following rapid increase in DO after 35 h indicated the depletion of all accessible carbon sources, hence the enzyme production phase was terminated after 40 h (8 h shortened process time compared to synthetic medium). Consequently, the temperature was increased to 50 °C, the overpressure was released, and the aeration rate was reduced to 5 L min^{-1} to prevent blockage of the sparger openings. The short drop in DO was followed by an increase up to 100% within a few hours due to the inactivation of the fungal cells. The simultaneous peak of the CER can be explained by the reduced air flow, resulting in higher CO_2 concentrations in the exhaust gas. Afterwards no CO_2 production could be detected. The agitation rate was set to 550 min^{-1} to assure sufficient homogenization during hydrolysis before 100 g L^{-1} wheat bran was added.

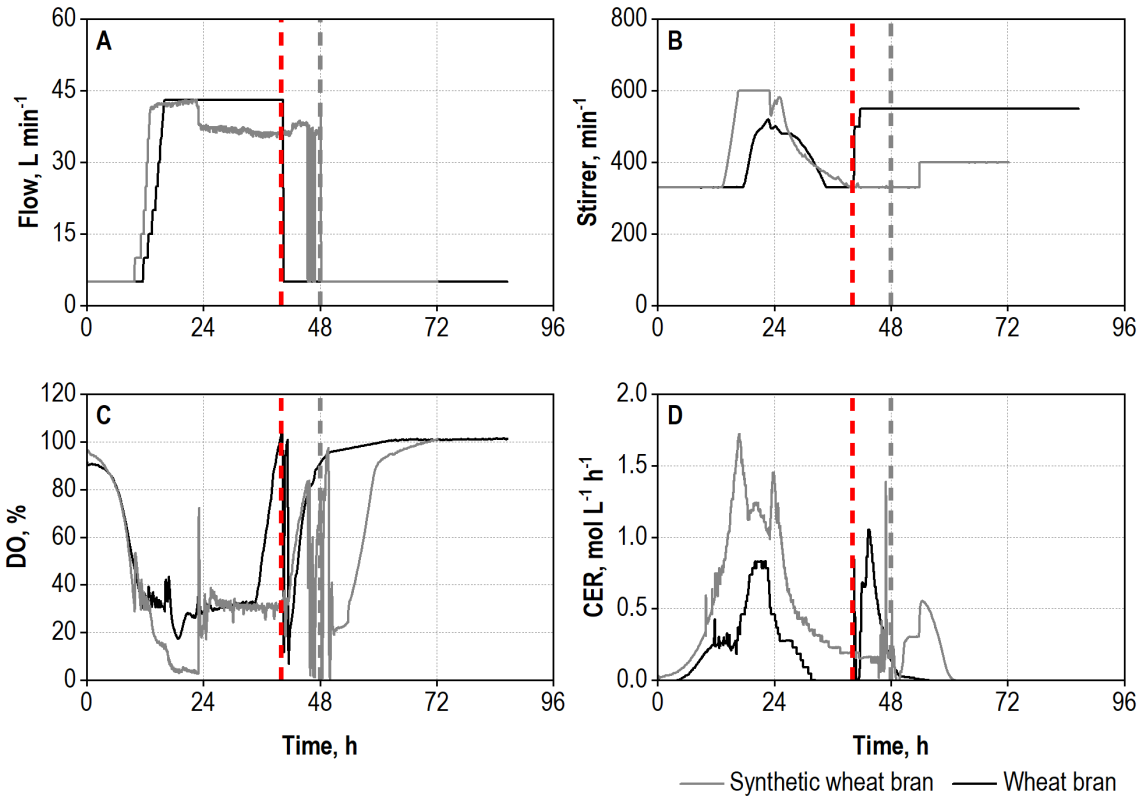

Figure 7.1: A: Air flow rate (Flow), B: Agitation rate (Stirrer), C: Dissolved oxygen concentration (DO), D: Carbon dioxide evolution rate (CER) of a co-culture of *A. niger* NRRL 2270 and *T. reesei* RUT-C30 in a bioreactor on a 25 L scale using synthetic wheat bran (gray) and 30 g L^{-1} wheat bran (black), followed by integrated hydrolysis at 50 °C. A stirrer control cascade was applied for DO control, and 1.2 bar overpressure were added after 23 h (gray) and 17 h (black) process time. The process was started by simultaneous inoculation with precultures from shaking flasks with an initial biomass concentration of 1.2 g L^{-1} (1.0 g L^{-1} *A. niger* and 0.2 g L^{-1} *T. reesei*; temperature 30 °C, pH 4.5). The dashed lines mark the increase of temperature to 50 °C and the addition of wheat bran for the integrated hydrolysis (gray: synthetic wheat bran medium + 50 g L^{-1} wheat bran, red: 30 g L^{-1} wheat bran + 100 g L^{-1} wheat bran).

The enzymatic activities and sugar concentrations in the supernatant samples are displayed in Figure 7.2. The enzyme activities from a comparable process using synthetic wheat bran medium are shown for reference. As the hydrolysis of this reference process was conducted with 50 g L^{-1} wheat bran, the sugar concentrations cannot be compared directly. The dashed lines respectively mark the transition to the hydrolysis phase by increasing the temperature to 50 °C.

Smaller hydrolytic activities were already present at inoculation due to enzymes produced during preculture preparation. Subsequently, xylanase, amylase, and cellulase activities were formed with wheat bran as the substrate as well as with synthetic wheat bran medium. However, the quantity of the different activities was significantly shifted: while the amylase activity at the end of the enzyme production phase was 80% higher with synthetic wheat bran medium, the xylanase and cellulase activities were drastically increased by 270% and 167%, respectively, with 30 g L^{-1} wheat bran as substrate.

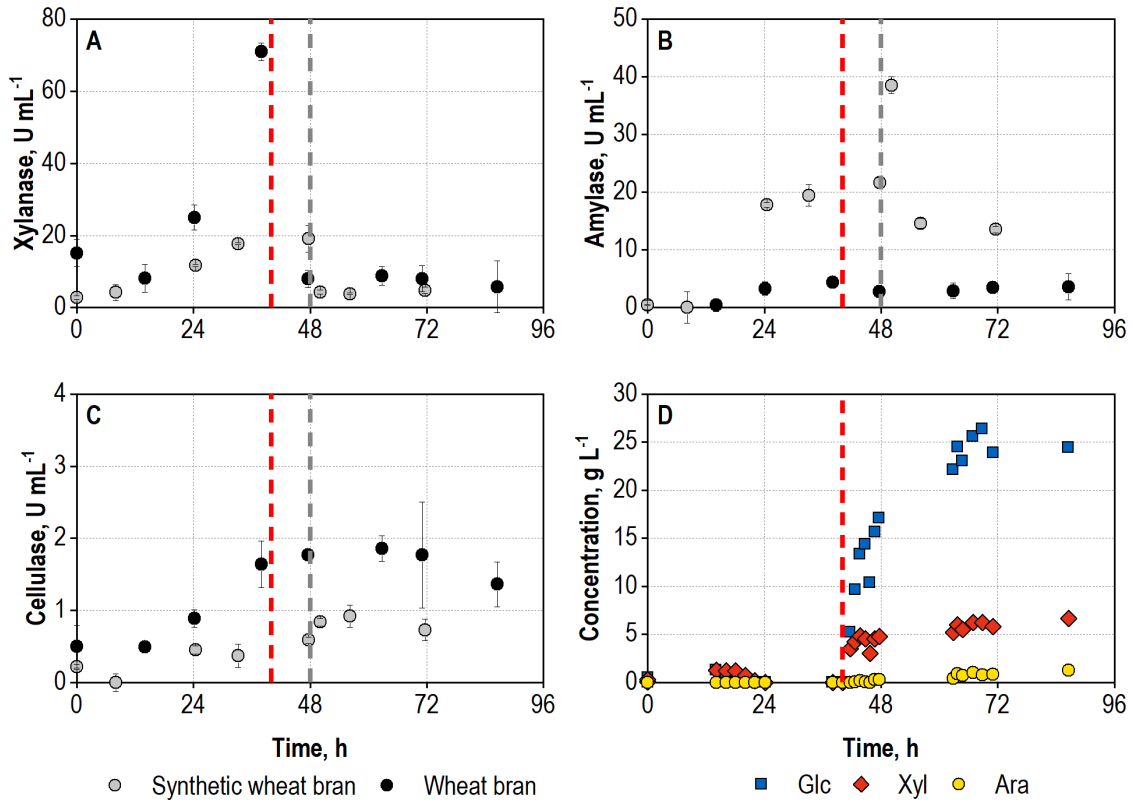

Figure 7.2: A: Xylanase activity, B: Amylase activity, C: Cellulase activity, D: Concentrations of glucose (Glc), xylose (Xyl) and arabinose (Ara), in the supernatant of a co-culture of *A. niger* NRRL 2270 and *T. reesei* RUT-C30 in a bioreactor on a 25 L scale using synthetic wheat bran medium (gray circles) and 30 g L^{-1} wheat bran (black circles), followed by integrated hydrolysis at 50 °C. A stirrer control cascade was applied for DO control. The process was started by simultaneous inoculation with precultures from shaking flasks with an initial biomass concentration of 1.2 g L^{-1} (1.0 g L^{-1} *A. niger* and 0.2 g L^{-1} *T. reesei*; temperature 30 °C, pH 4.5). The dashed lines mark the increase of temperature to 50 °C and the addition of wheat bran for the integrated hydrolysis (gray: synthetic wheat bran medium + 50 g L^{-1} wheat bran, red: 30 g L^{-1} wheat bran + 100 g L^{-1} wheat bran). One unit (U) was defined as the amount of enzymatic activity releasing 1 µmol of xylose (A) or glucose (B, C) equivalents per minute under assay conditions (50 °C, pH 4.5).

The release of sugars in the batch process using wheat bran for enzyme production began almost instantly after the addition of 100 g L^{-1} wheat bran for hydrolysis, with a space-time yield of total sugars of 4.8 g L^{-1} h^{-1} within the first 4 h. 22.2 g L^{-1} total sugars have already accumulated in the hydrolysate after 6 h, and an overall sugar concentration of 32.3 g L^{-1} was measured at the end of the process after 86.6 h (46 h hydrolysis). The hydrolysate consisted of 24.4 g L^{-1} (76%) glucose, 6.7 g L^{-1} (20%) xylose and 1.2 g L^{-1} (4%) arabinose, which corresponded to 58.2% of the theoretical yield.

A larger sample of 5 L was drawn at the end of the final integrated process using wheat bran. The residual solid fraction after saccharification was separated from the hydrolysate and analyzed regarding its nutritional value for animals. The composition of

raw wheat bran and fermented biomass are compared in Table 7.1. Analytics were done by the Bavarian State Institution for Agriculture (Bayerische Landesanstalt für Landwirtschaft LfL, Grub/Poing, Germany) following standardized lab protocols.

Table 7.1: Composition of raw wheat bran and fermentation residues from the integrated enzyme production and hydrolysis process on a 25 L scale using 30 g L^{-1} wheat bran for enzyme production and 100 g L^{-1} wheat bran for the integrated hydrolysis. Bold numbers indicate improved properties for animal nutrition.

		Raw wheat bran	Fermentation residues
Protein	g kg^{-1}	156	**231**
Sugar	g kg^{-1}	29	**84**
Fat	g kg^{-1}	33	**61**
Phosphate (P_2O_5)	g kg^{-1}	33.9	**20.9**
Energy content (ruminants)	MJ kg^{-1}	9.69	**12.52**

The solid fermentation residues differed in several aspects from the original wheat bran. The protein content was 48% higher than in the raw material, and lipids released from wheat bran particles raised the fat content by 85%. Additionally, the sugar content was increased almost threefold (+190%) by the liquid hydrolysate fraction remaining in the residual biomass after separation. This resulted in an increased energy density of the biomass, which rose, e.g., for ruminants from 9.69 MJ kg^{-1} to 12.52 MJ kg^{-1}. An additional beneficial effect is the reduction of phosphate by 38%.

A mass balance was estimated based on the mass fluxes in and out of the process (Figure 7.3):

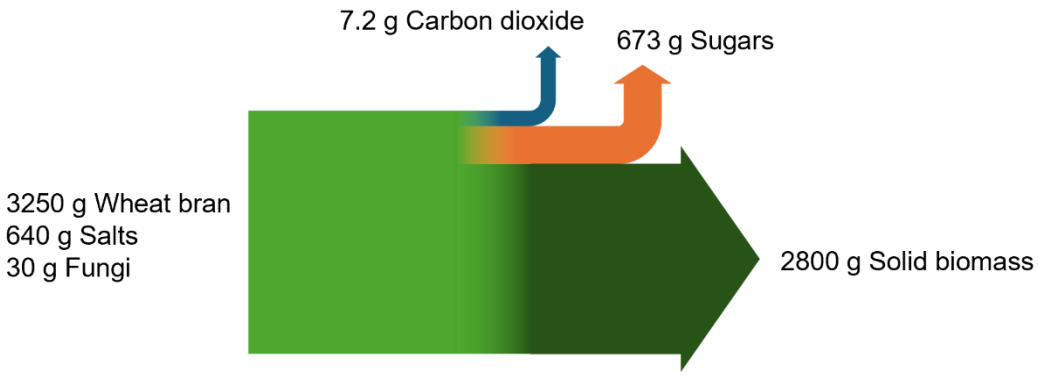

Figure 7.3: Flow diagram displaying masses in and out of the integrated enzyme production and hydrolysis process on a 25 L scale.

The main input was wheat bran with a mass of 3250 g (750 g for enzyme production and 2500 g for hydrolysis). Other relevant inputs in the process were posed by 640 g salts, which were partly assimilated into the biomass, and 30 g of fungal biomass as inoculum.

A total of 7.2 g CO_2, quantified by exhaust gas analysis, was formed by the fungi during growth and enzyme production. The overall sugar mass in the hydrolysate was 673 g (based on HPLC analysis), corresponding to 37.3% yield of the complete integrated process. The larger sample (5 L) taken for solid biomass analysis contained ~3 kg wet biomass after separation with a dry biomass percentage of 18.7% (w/w, data from LfL), accounting for ~2800 g dry biomass when projected on the total reactor volume.

Discussion

So far, enzyme production and hydrolysis have been conducted in two separate processes. This poses the challenge of separation and stabilization of the enzyme solution. Additionally, several sterilization and cleaning steps or the availability of multiple reactor systems became necessary, leading to a high demand in labor and equipment. The integration of the two processes into a single one-pot process could make these steps gratuitous, leading to lowered process times and costs as well as improved overall yields. The feasibility of such an integrated process for enzyme production using wheat bran with a subsequent hydrolysis of wheat bran was demonstrated.

The main carbon source for fermentation was changed from a defined mix of xylan, starch and cellulose to real wheat bran. The fungi demonstrated lower metabolic activity with wheat bran as substrate, indicated by a lower CER. Furthermore, the enzyme spectrum produced by the co-culture with wheat bran changed significantly, with drastically lowered amylase activity, in contrast to strongly increased xylanase and cellulase activity. It was assumed that the carbohydrate composition of synthetic and real wheat bran differed, and the fungi adapted the secretion of enzymes to the substrate present in the reactor. The subsequent hydrolysis phase was initiated by the increase in process temperature from 30 °C to 50 °C. On the one hand, this increased temperature inactivated the fungal cells in the broth (Bonner, 1948) as well as potential contaminants on the wheat bran; on the other hand, it created optimal process conditions for the hydrolytic enzyme mixture produced. Afterwards, 100 g L^{-1} wheat bran were added aseptically. The noteworthy drop of xylanase activity after the addition of wheat bran was most probably caused by the adsorption of the enzymes to the substrate particles in order to cleave the covalent bonds within the hemicellulosic components, leaving only little activity in the supernatant (Pribowo et al., 2012). The sugar concentrations released from wheat bran during the integrated hydrolysis were similar to those from separate processes. The same space-time yield (4.8 g L^{-1} h^{-1}) was determined within the first 4 h of hydrolysis than in separate 0.5 L hydrolysis processes, and the final overall sugar yield of the hydrolysis was highly comparable as well (0.5 L scale: 58.4%, 25 L scale 58.2%). The total yield of the integrated process, considering the wheat bran applied for both

enzyme production and hydrolysis, amounts to 37.3% A comparable integrated process with synthetic wheat bran medium (displayed in Figure 7.2 for comparison) resulted in a total sugar yield of 59.5% from 50 g L^{-1} wheat bran.

The solid fermentation residues, consisting of plant and fungal biomass, had improved properties for animal nutrition compared to untreated wheat bran. The increased contents of sugars, protein and fat resulted in a higher energy density for e.g. ruminants. Additionally, the reduced phosphate content, on the one hand, reduces the phosphate deposition into the environment and thus helps to prevent eutrophication of soils and waters and, on the other hand, enables better animal nutrition in accordance with environmental laws. The fungi applied here were well-known wild-type strains, whose enzymes have been used in a food and feed context for a long time (Ghorai et al., 2009) and are both certified for safe use for human or animal nutrition (Nevalainen et al., 1994, Schuster et al., 2002). Advantageous effects of fungal fermentation and the respective biomass for animals have also been reported regarding the nutrient availability or the content of protein and other functional components (Osama et al., 2013, Chuang et al., 2020), supporting the proposed utilization of the residual biomass of the integrated process for animal nutrition.

7.2. Transfer of the integrated process to the 1000 L scale

The integrated process is transferred from the 25 L scale to the 1000 L scale to study its technical feasibility. Before, the preparation of the precultures must be characterized in two different stirred-tank bioreactors.

7.2.1. Preculture preparation in stirred-tank bioreactors

A two-stage preculture cascade was applied, where shaking flask precultures were used for the inoculation of separate stirred-tank reactors. The *T. reesei* RUT-C30 preculture was prepared in the same reactor that had been applied for the co-cultivation experiments on the 25 L scale. A stirred-tank bioreactor with a working volume of 50 L was used for the preculture of *A. niger* NRRL 2270 to gain enough biomass for the inoculation of the 1000 L process with the initial biomass ratio of *A. niger* to *T. reesei* of 5:1.

Figure 7.4 shows the formation of biomass in both preculture batches as well as the DO concentration of the *T. reesei* preculture over time.

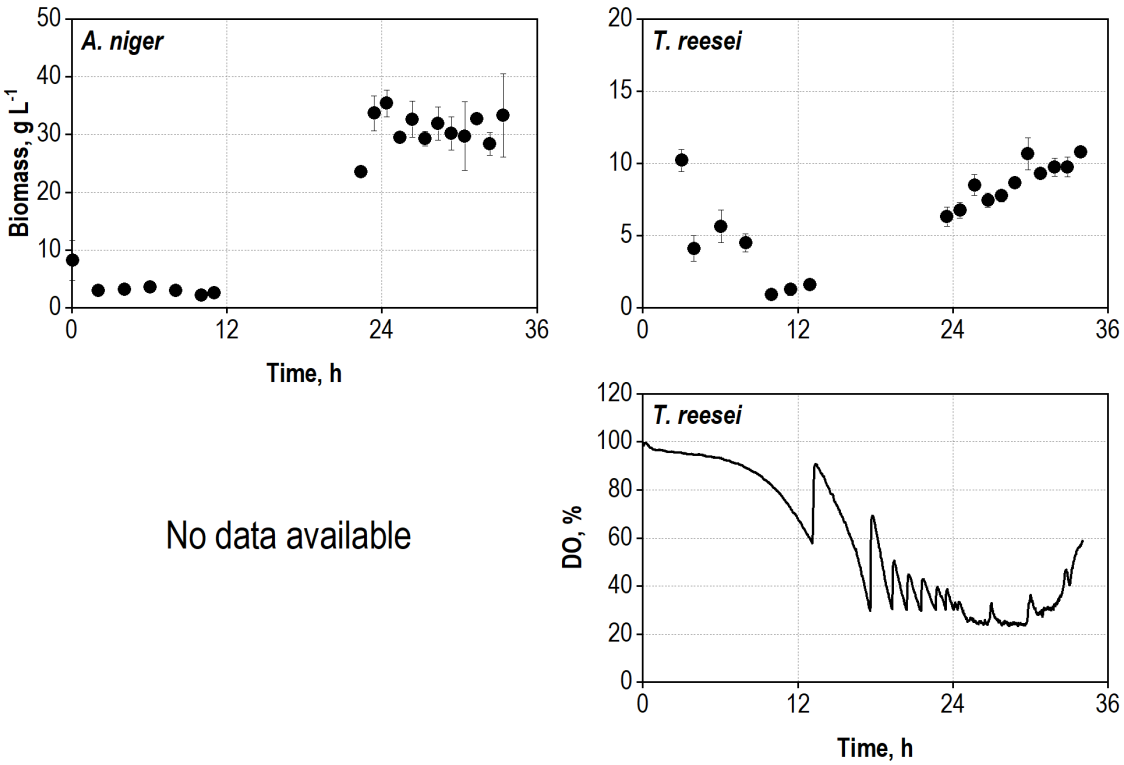

Figure 7.4: Biomass concentrations during batch cultivation of *A. niger* NRRL 2270 in a bioreactor on a 50 L scale (left), and *T. reesei* RUT-C30 in a bioreactor on a 25 L scale (right) using preculture medium (temperature 30 °C, pH 4.5).

A. niger displayed a distinct lag phase at the beginning of the batch process and had its main growth phase between 11-22 h after inoculation, reaching a biomass concentration of ~25 g L^{-1}. As the cells should be transferred to the main process in a stationary, yet active state, a preculture duration of 22 h was selected as suitable for *A. niger*.

The second strain, *T. reesei*, showed rather linear growth during cultivation in the 25 L reactor, and reached a biomass concentration of 11 g L^{-1} after 34 h process time. At this point in the process, the dissolved oxygen concentration in the fermentation broth increased rapidly. As this increase meant a drastically lowered oxygen consumption, it was interpreted as the end of the growth phase, and a suitable time point for the transfer to the main process.

7.2.2. Integrated enzyme production and hydrolysis

The integrated process on a 1000 L scale was conducted as established on a 25 L scale. 30 g L^{-1} wheat bran were used as substrate for fungal growth and enzyme production. The process was inoculated with precultures from the two separate bioreactors, as described before. The *A. niger* preculture was directly transferred into the 1000 L reactor via a transfer line and overpressure in the preculture reactor, whereas *T. reesei* was transported in sterile containers and pumped into the reactor by a peristaltic pump.

The 1000 L stirred-tank reactor was geometrically similar to the 25 L reactor used so far. The respective details are listed in Table 4.7 (25 L reactor) and Table 4.8 (1000 L reactor). In contrast to the inclined blade stirrers in the 25 L reactor, three Rushton impellers were installed in the 1000 L reactor. Thus, the initial stirrer tip speed was decreased from 1.9 m s^{-1} (25 L reactor) to 1.3 m s^{-1} (1000 L reactor) to reduce potential excess shear forces by the Rushton impeller. An initial aeration rate of 400 L min^{-1} (0.4 vvm, technical minimum) was applied. DO control was realized by a dynamic cascade controlling the agitation rate (80-200 min^{-1}) and aeration rate (400-2000 L min^{-1}).

The gassing rate and stirring rate as well as the DO are shown in Figure 7.5.

Fungal growth started without delay directly after inoculation. Consequently, the aeration rate and agitation rate were increased 6 h after inoculation to maintain a DO above 30% air saturation. The growth and enzyme production phase was finished after 35 h (rapid DO increase).

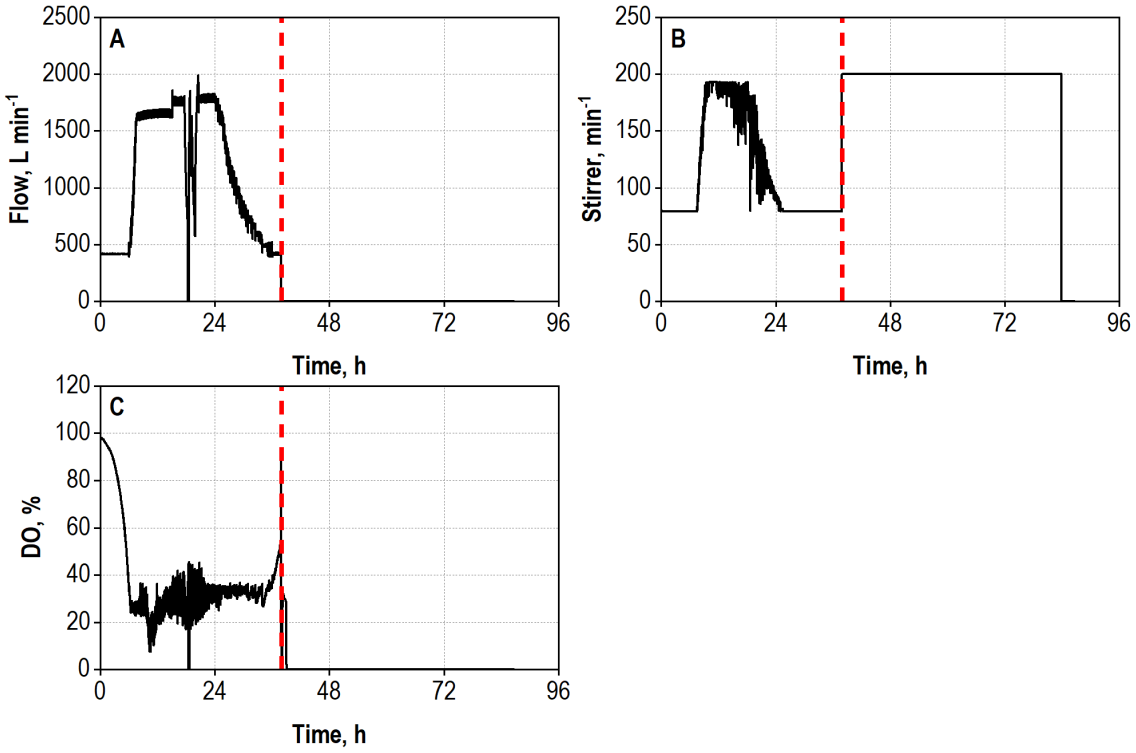

Figure 7.5: A: Air flow rate, B: Agitation rate, C: Dissolved oxygen concentration (DO) of a co-culture of *A. niger* NRRL 2270 and *T. reesei* RUT-C30 in a bioreactor on a 1000 L scale using 30 g L^{-1} wheat bran, followed by integrated hydrolysis at 50 °C. The process was started by simultaneous inoculation from the preculture reactor (*A. niger*) and from the transport containers (*T. reesei*) with an initial biomass concentration of 1.2 g L^{-1} (1.0 g L^{-1} *A. niger* and 0.2 g L^{-1} *T. reesei*; temperature 30 °C, pH 4.5). The dashed red line marks the increase of temperature to 50 °C and the addition of 100 g L^{-1} wheat bran for the integrated hydrolysis.

Figure 7.6 shows the resulting enzyme activities and the sugar concentrations in the supernatant samples in comparison to the 25 L scale.

Maximum enzyme activities were already reached before the end of the enzyme production phase. The activities determined at the start of the hydrolysis were significantly enhanced compared to the 25 L scale, with increases of 79% and 55% for xylanase and cellulase, respectively. Amylolytic activity was even multiplicated fourfold.

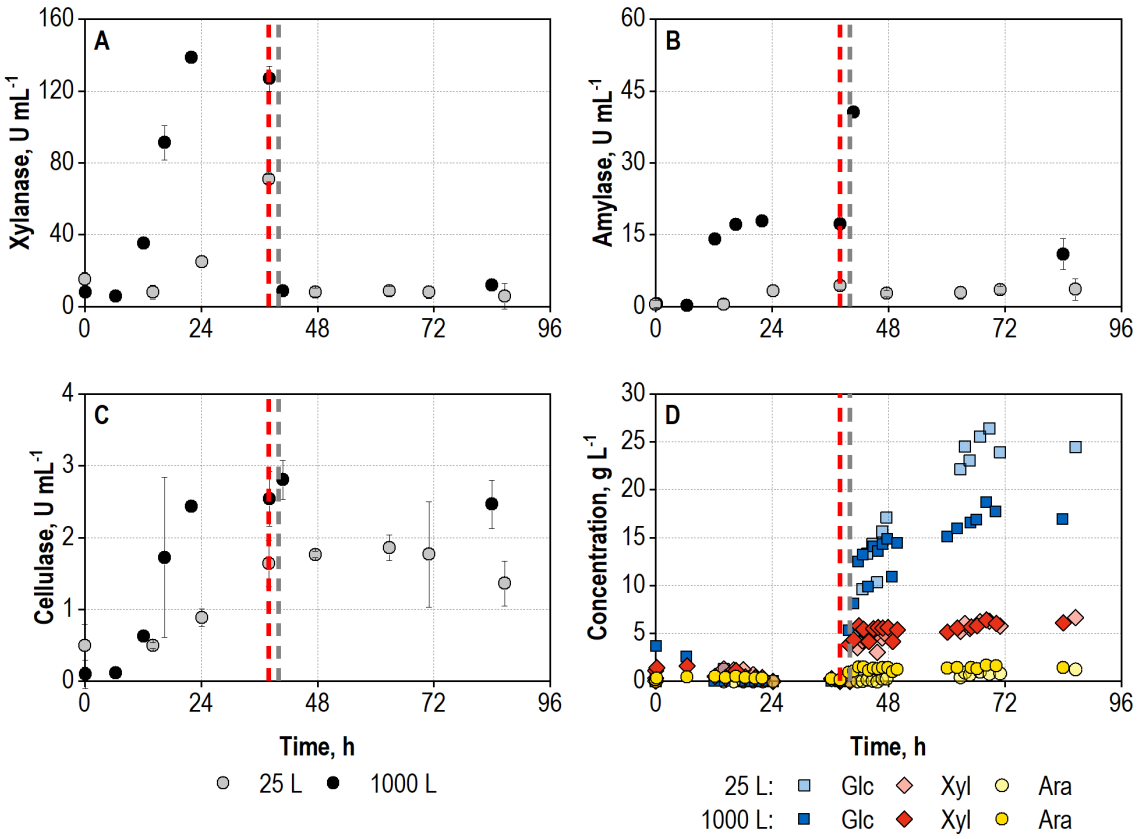

Figure 7.6: A: Xylanase activity, B: Amylase activity, C: Cellulase activity, D: Concentrations of glucose (Glc), xylose (Xyl) and arabinose (Ara), in the supernatant of a co-culture of *A. niger* NRRL 2270 and *T. reesei* RUT-C30 in a bioreactor on a 25 L scale (pale symbols) and a bioreactor on a 1000 L scale (dark symbols) using 30 g L^{-1} wheat bran, followed by integrated hydrolysis at 50 °C. The process was started by simultaneous inoculation with precultures from the preculture reactor (*A. niger*) and from the transport containers (*T. reesei*) with an initial biomass concentration of 1.2 g L^{-1} (1.0 g L^{-1} *A. niger* and 0.2 g L^{-1} *T. reesei*; temperature 30 °C, pH 4.5). The dashed lines mark the increase of temperature to 50 °C and the addition of 100 g L^{-1} wheat bran for the integrated hydrolysis (gray: 25 L, red: 1000 L). One unit (U) was defined as the amount of enzymatic activity releasing 1 µmol of xylose (A) or glucose (B, C) equivalents per minute under assay conditions (50 °C, pH 4.5).

Nevertheless, these increased enzyme activities did not lead to an improved hydrolysis of 100 g L^{-1} wheat bran added after a process time of 39.8 h. The initial space-time yield of total sugars of 5.0 g L^{-1} h^{-1} was slightly higher than on the 25 L scale (4.8 g L^{-1} h^{-1}), and an overall sugar concentration of 20.4 g L^{-1} was released after 6 h hydrolysis time

(25 L scale: 22.2 g L^{-1}). Afterwards, the hydrolysis appeared to slow down on the 1000 L scale and a total sugar concentration in the hydrolysate of 24.4 g L^{-1}, corresponding to a hydrolysis yield of 44%, was reached after 46 h hydrolysis time (25 L scale: 32.3 g L^{-1}, yield 58.2%). The total yield of the integrated process accounted for 33.8% when the 30 g L^{-1} wheat bran used for enzyme production were considered as well. The produced hydrolysate contained 16.9 g L^{-1} (69%) glucose, 6.1 g L^{-1} (25%) xylose and 1.4 g L^{-1} (6%) arabinose.

Discussion

The technical realization of the integrated enzyme production and hydrolysis was demonstrated on the 1000 L scale. However, the overall sugar yield of 44% was lower than on the 25 L scale (58.2%). This decrease was probably due to differences between the scales and the respective bioreactor systems, e.g. the stirrer configurations or variations in process control. Another potential explanation is posed by the usage of different batches of wheat bran, which varied in carbohydrate composition and particle size distribution. Consequently, the total integrated process yield before separation was also reduced to 33.8% (25 L scale: 37.3%).

The described integrated process also appears scalable to further, larger scales. The process is rather simple and does not require any special features of the stirred-tank bioreactors applied. Furthermore, wheat bran is a low-price feedstock that is globally available in vast amounts to be used in such processes.

7.2.3. Separation of biomass and hydrolysate

The wheat bran hydrolysate produced in the integrated process is intended to be applied as a sugar-rich medium for microbial production processes. Additionally, the residual solid material was found to be promising for animal nutrition. Therefore, an efficient separation method for the liquid hydrolysate and the solid biomass fraction is needed.

On a technical scale, a plate separator may be used. Unfortunately, the high solids content after hydrolysis instantly blocked the discharge container of the plate separator when applied directly after the end of hydrolysis. In consequence, the hydrolysis process was terminated by stopping the stirrers, and the hydrolysate was harvested via sedimentation, decanting and centrifugation. The reactor lid was lifted off the vessel after 1 h sedimentation time, the supernatant was pumped out of the reactor through a hose equipped with a mesh cap and was collected in a medium collection tank. Subsequently, the hydrolysate was conveyed through the plate separator and back to the collection tank until no more solid discharge was observed. Further details of the procedure are

described in Chapter 4.4.5. These proceedings resulted in 580 L wheat bran hydrolysate, which was thermally stabilized in the collection tank.

Discussion

The combination of sedimentation, decanting/filtration and centrifugation for downstream processing enabled the separation of hydrolysate and residual solids. However, this procedure resulted in only 14.2 kg sugars from 130 kg wheat bran, corresponding to a total sugar yield of the complete process of 20%. After the centrifugation step, noteworthy amounts remained in the residual biomass fraction, which still had a high water content.

The low total sugar concentrations in the hydrolysate could make additional evaporation of water necessary to achieve sufficient product concentrations for following batch production processes. However, the hydrolysate contains a broad variety of soluble nutrients like amino acids and peptides, phosphate or ammonia. Hence, it could be applied as a fermentation medium without supplementation of large amounts of salts or other media components, allowing lower costs for subsequent production processes. Exemplarily, lab scale experiments on the lipid production with the oleaginous yeast *Cutaneotrichosporon oleaginosus* using wheat bran hydrolysate are described in Chapter 10.4 in the Supplementary Material.

The residual solid fraction, consisting of plant and fungal biomass, was already described as a promising animal feed material in Chapter 7.1. One integrated process on the 1000 L scale results in ~100-120 kg dry biomass, which could be applied as feed material with improved properties compared to the original wheat bran.

8. Summary and outlook

Lignocellulosic plant biomass, for instance in agricultural residues, poses a largely untapped reservoir for useful compounds. In particular, the carbohydrates stored in polysaccharides are highly interesting for biotechnological approaches, as they can be converted into a large variety of products in microbial conversion processes (Amoah et al., 2019). A prominent representative of these residues is wheat bran, the main byproduct of flour production. Approximately 200 million tons of wheat bran are produced annually (Prueckler et al., 2014), and its carbohydrate content of 50-60% makes it a vastly abundant source of sugars like glucose and xylose, which can be turned into valuable products by microbial conversion processes.

Carbohydrates in wheat bran are mainly found in the form of the polysaccharides cellulose, hemicellulose and starch. These polymers are entangled with each other and form a stable and recalcitrant matrix. Therefore, the enzymatic degradation of wheat bran for the release of monomeric sugars is rather complex and requires a specialized set of hydrolytic enzymes. Xylanases can degrade the complex and heterogenous polymer hemicellulose with specific enzymes cleaving off the various side chains before the xylan backbone is depolymerized. Enzymes with amylolytic activity are able to hydrolyze glycosidic bonds in starch and release glucose monomers. Cellulolytic enzyme mixtures consist of different specific enzymes that gradually break down cellulose microfibrils. This process results in shorter oligosaccharides like cellobiose, and eventually in monomeric glucose. However, there is no microorganism described so far to produce all necessary enzymes in sufficient amounts to efficiently hydrolyze wheat bran. This obstacle can be overcome by genetic modification of one organism, the conduction of several enzyme production processes and enzyme mixing, or the co-cultivation of suitable enzyme-producing strains (Kolasa et al., 2014). In this work, a co-culture of two filamentous fungi was used to produce the hydrolytic enzyme cocktail. The well-researched cellulase producer *Trichoderma reesei* RUT-C30 was partnered with *Aspergillus niger*, which is known to secrete xylanases and amylases (Mandels and Reese, 1957, Cairns et al., 2018). However, co-cultivating two fungal strains comes with challenges. Microorganisms can react negatively to the presence of another species, and fungi are particularly known for actively antagonizing potential competitors (Boddy and Hiscox, 2016). These complex and possibly detrimental interactions must therefore be kept in mind. Additionally, the product formation of filamentous fungi strongly depends on their morphology, which is influenced by process conditions, among them mechanical power input by stirring (Pollard et al., 2007).

The first objective of this work was the investigation of suitable process conditions for the co-cultivation of *A. niger* and *T. reesei* to produce an enzyme solution for the hydrolysis of wheat bran. Different strategies for the inoculation of the co-cultivation processes were studies to establish a stable consortium, where both species can actively grow and produce their respective enzymes. Afterwards, suitable operation parameters were identified for the enzyme production, considering the relations between process conditions, fungal morphology and product formation. The resulting enzyme solution was separated from the biomass and directly applied for the hydrolysis of wheat bran. The hydrolytic performance was compared with the respective enzymes from monocultures to examine whether the co-culture enzymes are beneficial for the saccharification of wheat bran. The subsequent separation and purification procedures of the enzymes can be complex and cause a major part of the total process costs. Therefore, the possibility of a process integration of the separate enzyme production and hydrolysis processes into a one-pot process was examined to omit those additional laborious and costly steps.

In a first step a suitable strain of *Aspergillus niger* had to be identified. Six different *A. niger* strains (N400, N402, NRRL 3122, CBS 513.88 NRRL 328 and NRRL 2270) were compared in shaking flasks for their capabilities to produce xylanase or amylase activity with xylan or starch as substrate. Three strains were selected for a subsequent cultivation experiment in 0.7 L stirred-tank bioreactors under controlled conditions: *A. niger* N402 produced the maximum amylase activity, *A. niger* NRRL 3122 showed the highest xylanolytic activity, and *A. niger* NRRL 2270 was chosen for its overall performance with second-highest xylanase and amylase activities. *A. niger* NRRL 2270 confirmed these promising results with fast growth and high enzyme activities during cultivation in a stirred-tank bioreactor and was thus selected for the co-cultivation to produce enzymes for the hydrolysis of wheat bran.

The second microorganism intended for this co-culture, *T. reesei* RUT-C30, was initially characterized regarding its cellulase formation with different carbon sources including wheat bran. While the highest activities were secreted with the soluble substrates lactose and glucose, the fungus was also able to utilize the polymeric compounds carboxymethyl cellulose and Avicel (microcrystalline cellulose) as well as wheat bran for the production of cellulases.

Subsequently, the co-cultivation of *A. niger* and *T. reesei* was investigated in detail. A synthetic wheat bran medium with a defined carbon composition imitating wheat bran was used for those experiments to ensure reproducibility. Two different inoculation methods were applied for starting co-cultivation processes: inoculation with spore suspensions or with vegetative cells from shaking flasks. Spore inoculation allows the

application of highly defined initial spore concentrations and, in the case of a co-culture, spore concentration ratios. Vegetative precultures have the advantages of easier practical handling and better scalability. In the case of spore inoculation both strains were characterized in monocultures before conducting co-cultivations inoculated with an initial spore concentration ratio of 5:1 in favor of *A. niger*. It became clear that *A. niger* was able to grow faster than *T. reesei* and, in the case of simultaneous inoculation, could dominate and suppress the second strain. A delay in inoculation of *A. niger* spores resulted in inhibited growth and enzyme production of *A. niger*. Both strains were metabolically active when *A. niger* spores were added 16.5 h after the inoculation with *T. reesei*. Furthermore, in contrast to the monocultures, all three enzyme activities were produced in relevant quantities in the co-culture supernatant, showing its large potential for enzyme production for the hydrolysis of wheat bran.

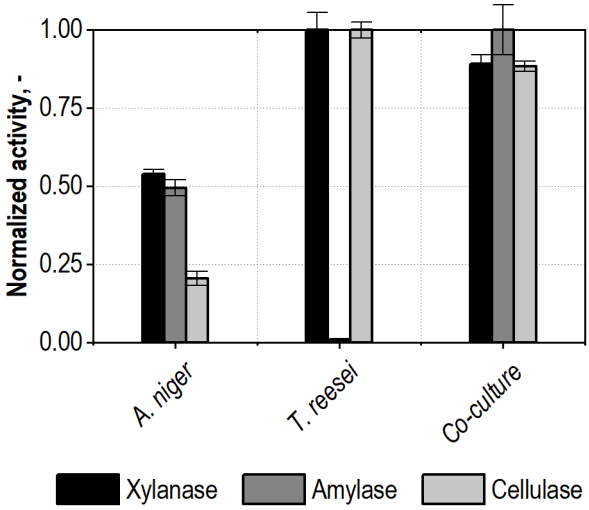

Figure 8.1: Normalized enzyme activities in the supernatant of *A. niger* NRRL 2270 and *T. reesei* RUT-C30 monocultures or a co-culture of *A. niger* NRRL 2270 and *T. reesei* RUT-C30 after 86 h in a stirred-tank bioreactor on a 0.7 L scale using synthetic wheat bran medium. The *A. niger* NRRL 2270 monoculture was inoculated with an initial spore concentration of 10^9 spores L^{-1}, the *T. reesei* RUT-C30 monoculture was inoculated with an initial spore concentration of 0.2×10^9 spores L^{-1}. The co-culture was started by inoculation with *T. reesei* RUT-C30 with an initial spore concentration of 0.2×10^9 spores L^{-1}, and *A. niger* NRRL 2270 was added after 16.5 h with an initial spore concentration of 10^9 spores L^{-1} (agitation rate 600 min^{-1}, aeration rate 0.2-2 vvm, temperature 30 °C, pH 4.5). One unit (U) was defined as the amount of enzymatic activity releasing 1 µmol of xylose (A) or glucose (B, C) equivalents per minute under assay conditions (50 °C, pH 4.5). Activities were normalized based on the respective maximum.

The initial biomass ratios of *A. niger* and *T. reesei* were varied for inoculation with vegetative shaking flask precultures. Again, assumably competitive or antagonistic interactions were observed. An initial biomass ratio of 5:1 in favor of *T. reesei* led to strongly decreased xylanase and amylase activity, whereas a predominance of *A. niger* did not have a similar effect of cellulase formation. Consequently, an initial biomass

concentration ratio of 5:1 in favor of *A. niger* resulted in the best enzyme formation. Furthermore, inoculation with vegetative precultures allowed shorter lag phases and thus shorter process times.

Fungal enzyme production is reported to be influenced by the mechanical power input of the agitation in stirred-tank bioreactors (Lejeune and Baron, 1995, Kelly et al., 2004, Lin et al., 2010). A limited oxygen supply can also impair growth and enzyme formation in fungi like *T. reesei* (Bonaccorsi et al., 2006). Hence, the identification of an optimal point of operation for the co-cultivation process was intended on the 0.7 L scale. Low agitation or aeration rates resulted in oxygen limitation of the cells. Either high agitation rates or low gassing rates were disadvantageous for xylanase and cellulase formation, whereas amylase formation benefitted from these conditions. Overall, an agitation rate of 800 min^{-1} and an initial aeration rate of 0.14 L min^{-1} (0.2 vvm, can be increased to 2 vvm) was selected as a suitable point of operation.

A process transfer to a geometrically not similar bioreactor on the 3.0 L scale was conducted using constant stirrer tip speed and constant volumetric aeration rate as criteria. The resulting point of operation at a stirring rate of 660 min^{-1} and an initial gassing rate of 0.6 L min^{-1} (0.2 vvm, increasable tenfold) had a nearly identical volumetric oxygen transfer coefficient k_La compared to the 0.7 L scale. Co-cultivation processes with spore inoculation as well as with inoculation with vegetative cells were conducted and resulted in highly similar enzyme activities compared to the smaller reactors. The inoculation with vegetative cells from shaking flask precultures led to increased enzyme activities (xylanase +24%, amylase +15%, cellulase +12%) in shorter process times (65 h instead of 86 h) in comparison to spore inoculation. A change in medium composition from birch wood xylan to corn xylan had a significant effect on xylanase and cellulase formation in the co-culture.

A transfer of the co-cultivation process to a geometrically not similar 25 L stirred-tank reactor based on constant stirrer tip speed (330 min^{-1}) and constant volumetric aeration rate (5-50 L min^{-1}) led to a reduced oxygen transfer coefficient k_La and extended periods of oxygen limitation for the cells. This resulted in drastically lowered enzyme formation (total protein -61%, amylase -23%, cellulase -71%). Successively, the implementation of a stirrer control cascade together with the installation of inclined blade stirrers helped to evade oxygen limitation, and the resulting protein secretion and enzyme activities were comparable to those from the 3.0 L scale, except for cellulase (-65% reduced).

The hydrolytic activities of the enzyme mixture produced by the co-culture of *A. niger* NRRL 2270 and *T. reesei* RUT-C30 were measured at temperatures between 20-70 °C

and pH 3.0-7.0 to find optimal reaction conditions. Those conditions were identified at 50 °C (cellulase) or 60 °C (xylanase, amylase) at pH 4.0-pH 4.5. Subsequent mL scale hydrolysis experiments yielded in overall sugar concentrations of 34.0 g L^{-1} (50 °C) and 26.4 g L^{-1} (60 °C) after 168 h. The hydrolysis conditions were therefore set to 50 °C and pH 4.5.

A comparative hydrolysis study was conducted in stirred-tank reactors on the 0.5 L scale to evaluate the potential of the co-culture of *A. niger* NRRL 2270 and *T. reesei* RUT-C30 for enzyme production. Enzymes from monocultures of *A. niger* NRRL 2270 and *T. reesei* RUT-C30, a 1:1 mixture of these monoculture enzymes and a co-culture enzyme solution were applied for the hydrolysis of 100 g L^{-1} wheat bran. Final sugar concentrations of 30.2 g L^{-1} (54.4% yield), 33.9 g L^{-1} (61.1% yield) and 32.3 g L^{-1} (58.4% yield) were measured after 45 h with *A. niger* monoculture enzymes, the enzyme mix and the co-culture enzymes, respectively. The corresponding hydrolysates had similar compositions with ~57% glucose, ~34% xylose and ~5% arabinose. *T. reesei* enzymes released significantly lower amounts of sugar, with a total concentration of 21.9 g L^{-1} (39.5% yield) and a remarkable accumulation of cellobiose (3.6 g L^{-1}) in the final hydrolysate. The co-culture enzymes additionally had the highest space-time yield, demonstrating its high potential for the hydrolysis of wheat bran. A comparable process on the 3.0 L scale resulted in a sugar concentration in the hydrolysate of 30.2 g L^{-1} (54% yield) within 51 h.

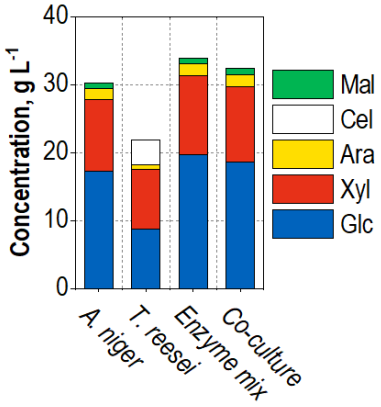

Figure 8.2: Hydrolysate composition after 45 h hydrolysis of 100 g L^{-1} wheat bran using enzymes from *A. niger* NRRL 2270 and *T. reesei* RUT-C30 monocultures, a 1:1 mixture of these enzymes and enzymes produced in a co-culture of *A. niger* NRRL 2270 and *T. reesei* RUT-C30. Hydrolysis was performed in 0.5 L reactors at 50 °C and pH 4.5, buffered with 50 mM sodium acetate. Wheat bran was sterilized at 121 °C for 20 min before 10% (v/v) enzyme solution were added into each reactor. Sugars released after sterilization and after enzymatic hydrolysis are summed up. Glc: glucose, Xyl: xylose, Ara: arabinose, Cel: cellobiose, Mal: Maltose.

The labor- and time-intensive separation and purification of the enzymes cause a large position within the total process cost as well as product loss. Therefore, the integration of enzyme production with *A. niger* and *T. reesei* and enzymatic hydrolysis of wheat bran into a one-pot process was examined as a possible solution. The enzyme production process was conducted on a 25 L scale as before, except the substrate was changed from a defined polysaccharide mixture to 30 g L^{-1} wheat bran. This change of substrate resulted in a significant shift in enzyme secretion, with strongly increased xylanase (+270%) and cellulase (+167%) activities, while the amylase activity was reduced by 80%. After the end of enzyme production, it was necessary to inactivate the fungal cells as well as potential contaminants to enable the accumulation of sugars in the hydrolysate. Moreover, the ideal reaction conditions for the hydrolysis of wheat bran differ from the cultivation conditions. Both issues could be tackled by increasing the temperature from 30 °C to 50 °C before 100 g L^{-1} unsterile wheat bran was added into the reactor for hydrolysis. The aeration was simultaneously minimized. This integrated hydrolysis reached the same space-time yield within the first 4 h than separate processes and resulted in an overall sugar concentration of 32.3 g L^{-1} (yield 58.2%), consisting of 76% glucose, 20% xylose and 4% arabinose. A mass balance of the complete one-pot process accounted for 673 g sugars produced from 3250 g wheat bran for enzyme production and hydrolysis, which equals to an overall process yield of 37.3%. The residual solid fraction from the process, composed of plant and fungal biomass, demonstrated improved nutritional properties compared to wheat bran, with higher contents of protein, sugars and fat as well as a decrease in phosphate concentration. This potential application as animal feed further enhances the valorization of wheat bran by the integrated enzyme production and hydrolysis process.

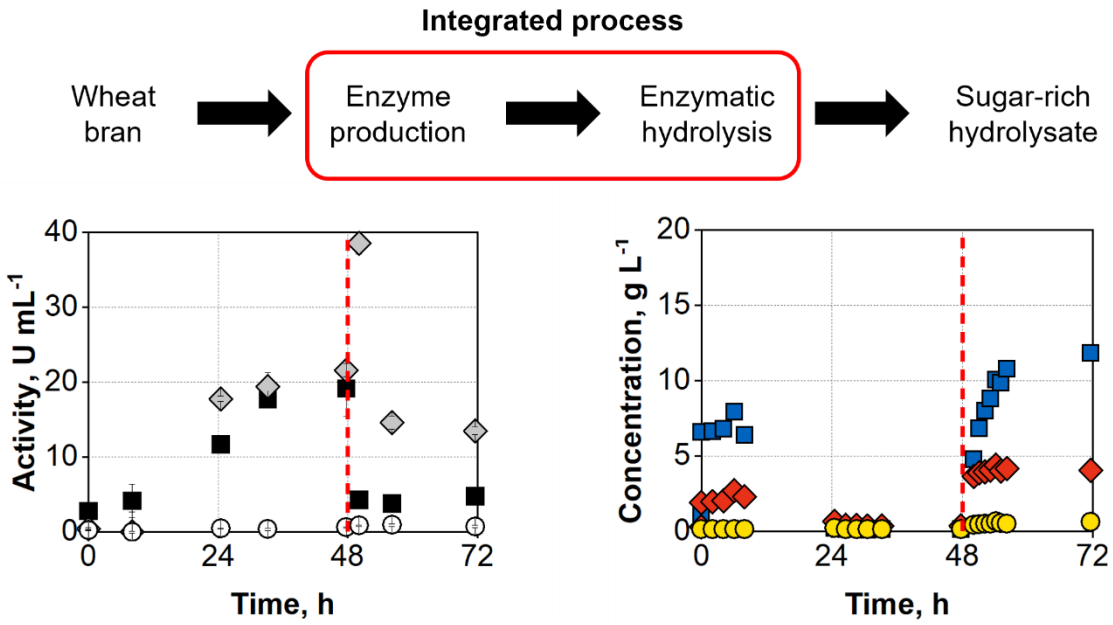

Figure 8.3: Schematic flow diagram of the integrated enzyme production and hydrolysis process. The graphs on the bottom display the enzymatic activities (xylanase: black squares, amylase: gray diamonds, cellulase: white circles) and the released sugar concentrations (glucose: blue squares, xylose: red diamonds, arabinose: yellow circles) in an exemplary process.

Eventually, the integrated process was transferred to the 1000 L scale. Precultures of *A. niger* and *T. reesei* were prepared in separate bioreactors prior to the inoculation of a 1000 L stirred-tank reactor. Enzyme production was conducted with 30 g L^{-1} wheat bran and resulted in substantially enhanced enzyme activities compared to the 25 L scale. The integrated hydrolysis was introduced by increasing the temperature to 50 °C and termination of gassing before 100 g L^{-1} wheat bran were added. Enzymatic hydrolysis yielded in 24.4 g L^{-1} total sugar (yield 44%). 580 L of the hydrolysate were subsequently separated from the solid biomass by a combination of sedimentation, decanting and centrifugation.

Outlook

After the first experiments on the 1000 L scale described in Chapter 7.2.2, it would be important to further improve the process on that scale. The integrated hydrolysis resulted in a lower yield than on the 25 L scale, although the enzymatic activities measured in supernatant samples were higher. Potential causes for this deterioration should be investigated and evaded to improve the overall sugar release.

Low sugar yields are a typical problem of the hydrolysis of agricultural residues like wheat bran. Further enhancement of sugar release could e.g. be achieved by smaller particle sizes and thus higher particle surface of the substrate, or a higher input of wheat bran. Additionally, a suitable downstream processing must be established. The equipment at

hand, consisting of a hose with filter cap and the plate separator, could not achieve sufficient separation, leaving an excessive amount of hydrolysate in the solid biomass. A chamber filter press, for instance, could support the improvement of the hydrolysate recovery.

As described within this work, the resulting wheat bran hydrolysate was intended as a medium component for microbial conversion processes. A broad variety of processes is imaginable, as the main sugar fractions glucose and xylose are easily convertible by many microorganisms. The utilization of the hydrolysate for microbial lipid production by the oleaginous yeast *Cutaneotrichosporon oleaginosus* is exemplified in the Supplementary Chapter 10.4.

The molecular interactions between *A. niger* and *T. reesei* in the co-culture are of great interest for the enzyme production in the co-culture and should therefore be investigated in detail. Initial steps were taken in this project, like secretome analysis via SDS-PAGE or Native-PAGE. However, these methods only provide qualitative data about protein secretion, and conclusions on population dynamics could only be drawn based on the comparison of band patterns. Advanced techniques for proteomics, transcriptomics and metabolomics could provide a deeper understanding of the relationship between the strains within the co-culture. Another potential approach is posed by strain-specific biomass quantification, for example by quantitative polymerase chain reaction (qPCR) for the determination of DNA concentrations.

A rather specific aspect regards the usage of the residual biomass after the integrated process as animal feed (see Chapter 7.1). So far, the applicability for livestock nutrition has only been evaluated by lab analytics regarding nutritional value. Consequently, feeding tests have to confirm the suitability as either sole animal feed or feed supplement. Additional attention should be given to the identification of potential mycotoxins in the feedstock, which can be produced by the applied fungal strains under stress conditions, e.g. competition by other organisms in a co-culture (Frisvad et al., 2018).

9. References

Abarca, M. L., M. R. Bragulat, G. Castellá and F. J. Cabañes (1994). "Ochratoxin A production by strains of Aspergillus niger var. niger." Applied and Environmental Microbiology **60**(7): 2650-2652.

Ahamed, A. and P. Vermette (2008). "Enhanced enzyme production from mixed cultures of Trichoderma reesei RUT-C30 and Aspergillus niger LMA grown as fed batch in a stirred tank bioreactor." Biochemical Engineering Journal **42**(1): 41-46.

Ahrens, S. (2023, 09.2024). "Erntemenge von Weizen weltweit in den Jahren 2000/2001 bis 2023/2024." Retrieved 03.07., 2024, from https://de.statista.com/statistik/daten/studie/153032/umfrage/erzeugungsmenge-von-weizen-weltweit-seit-1990/.

Aktas-Akyildiz, E., M. T. Masatcioglu and H. Köksel (2020). "Effect of extrusion treatment on enzymatic hydrolysis of wheat bran." Journal of Cereal Science **93**: 102941.

Amoah, J., P. Kahar, C. Ogino and A. Kondo (2019). "Bioenergy and biorefinery: feedstock, biotechnological conversion, and products." Biotechnology journal **14**(6): 1800494.

Amorim, C. C., C. S. Farinas and E. A. Miranda (2019). "Liquefied wheat bran as carbon source and inducer in high-solids submerged cultivation of Aspergillus niger for xylanase production." Biocatalysis and agricultural biotechnology **21**: 101346.

Andersen, M. R., M. P. Salazar, P. J. Schaap, P. J. van de Vondervoort, D. Culley, J. Thykaer, J. C. Frisvad, K. F. Nielsen, R. Albang and K. Albermann (2011). "Comparative genomics of citric-acid-producing Aspergillus niger ATCC 1015 versus enzyme-producing CBS 513.88." Genome research **21**(6): 885-897.

Andrews, J. F. (1968). "A mathematical model for the continuous culture of microorganisms utilizing inhibitory substrates." Biotechnology and bioengineering **10**(6): 707-723.

Apprich, S., Ö. Tirpanalan, J. Hell, M. Reisinger, S. Böhmdorfer, S. Siebenhandl-Ehn, S. Novalin and W. Kneifel (2014). "Wheat bran-based biorefinery 2: Valorization of products." LWT-Food Science and Technology **56**(2): 222-231.

Baker, S. E. (2006). "Aspergillus niger genomics: past, present and into the future." Medical mycology **44**(Supplement_1): S17-S21.

Baltussen, T. J., J. Zoll, P. E. Verweij and W. J. Melchers (2020). "Molecular mechanisms of conidial germination in Aspergillus spp." Microbiology and Molecular Biology Reviews **84**(1): 10.1128/mmbr. 00049-00019.

Bandyopadhyay, B., A. Humphrey and H. Taguchi (1967). "Dynamic measurement of the volumetric oxygen transfer coefficient in fermentation systems." Biotechnology and bioengineering **9**(4): 533-544.

Bartnicki-Garcia, S., F. Hergert and G. Gierz (1989). "Computer simulation of fungal morphogenesis and the mathematical basis for hyphal (tip) growth." Protoplasma **153**(1): 46-57.

Bäumler, M., V. Burgmaier, F. Herrmann, J. Mentges, M. Schneider, A. Ehrenreich, W. Liebl and D. Weuster-Botz (2023). "Continuous production of ethanol, 1-butanol and 1-hexanol from CO with a synthetic co-culture of Clostridia applying a cascade of stirred-tank bioreactors." Microorganisms **11**(4): 1003.

Bäumler, M., M. Schneider, A. Ehrenreich, W. Liebl and D. Weuster-Botz (2021). "Synthetic co-culture of autotrophic Clostridium carboxidivorans and chain elongating Clostridium kluyveri monitored by flow cytometry." Microb Biotechnol.

Bayer, E. A., E. Morag and R. Lamed (1994). "The cellulosome—a treasure-trove for biotechnology." Trends in biotechnology **12**(9): 379-386.

Bekiaris, P. S. and S. Klamt (2021). "Designing microbial communities to maximize the thermodynamic driving force for the production of chemicals." PLoS computational biology **17**(6): e1009093.

Bélaich, J.-p., C. Tardif, A. Bélaich and C. Gaudin (1997). "The cellulolytic system of Clostridium cellulolyticum." Journal of biotechnology **57**(1-3): 3-14.

Bendig, C. and D. Weuster-Botz (2013). "Reaction engineering analysis of cellulase production with Trichoderma reesei RUT-C30 with intermittent substrate supply." Bioprocess and biosystems engineering **36**(7): 893-900.

Berntsson, T., B. A. Sandén, L. Olsson and A. Åsblad (2012). "What is a biorefinery?".

Bhat, M. and S. Bhat (1997). "Cellulose degrading enzymes and their potential industrial applications." Biotechnology advances **15**(3-4): 583-620.

Biely, P., J. Puls and H. Schneider (1985). "Acetyl xylan esterases in fungal cellulolytic systems." FEBS letters **186**(1): 80-84.

Bischof, R. H., J. Ramoni and B. Seiboth (2016). "Cellulases and beyond: the first 70 years of the enzyme producer Trichoderma reesei." Microbial cell factories **15**: 1-13.

Blom, R., V. Pfeifer, A. Moyer, D. TraufRer, H. Conway, C. Crocker, R. Farison and D. Hannibal (1952). "Sodium gluconate production. Fermentation with Aspergillus niger." Industrial & Engineering Chemistry **44**(2): 435-440.

Boddy, L. and J. Hiscox (2016). "Fungal ecology: principles and mechanisms of colonization and competition by saprotrophic fungi." Microbiology spectrum **4**(6): 10.1128/microbiolspec. funk-0019-2016.

Boer, H. and A. Koivula (2003). "The relationship between thermal stability and pH optimum studied with wild-type and mutant Trichoderma reesei cellobiohydrolase Cel7A." European Journal of Biochemistry **270**(5): 841-848.

Bonaccorsi, E. D., A. J. Ferreira, F. S. Chambergo, A. S. Ramos, M. C. Mantovani, J. P. S. Farah, C. S. Sorio, A. K. Gombert, A. Tonso and H. El-Dorry (2006). "Transcriptional response of the obligatory aerobe Trichoderma reesei to hypoxia and transient anoxia: implications for energy production and survival in the absence of oxygen." Biochemistry **45**(12): 3912-3924.

Bonner, J. T. (1948). "A study of the temperature and humidity requirements of Aspergillus niger." Mycologia **40**(6): 728-738.

Boruta, T., A. Ścigaczewska and M. Bizukojć (2021). ""“Microbial wars” in a stirred tank bioreactor: Investigating the co-cultures of Streptomyces rimosus and Aspergillus terreus, filamentous microorganisms equipped with a rich arsenal of secondary metabolites." Frontiers in Bioengineering and Biotechnology **9**: 713639.

Bos, C., A. Debets, K. Swart, A. Huybers, G. Kobus and S. Slakhorst (1988). "Genetic analysis and the construction of master strains for assignment of genes to six linkage groups in Aspergillus niger." Current genetics **14**: 437-443.

Brandolini, A. and A. Hidalgo (2012). "Wheat germ: not only a by-product." International journal of food sciences and nutrition **63**(sup1): 71-74.

Brou, P., P. Taillandier, S. Beaufort and C. Brandam (2018). "Mixed culture fermentation using Torulaspora delbrueckii and Saccharomyces cerevisiae with direct and indirect contact: impact of anaerobic growth factors." European Food Research and Technology **244**(10): 1699-1710.

Buranov, A. U. and G. Mazza (2009). "Extraction and purification of ferulic acid from flax shives, wheat and corn bran by alkaline hydrolysis and pressurised solvents." Food Chemistry **115**(4): 1542-1548.

Cairns, T. C., L. Barthel and V. Meyer (2021). "Something old, something new: challenges and developments in Aspergillus niger biotechnology." Essays in Biochemistry **65**(2): 213-224.

Cairns, T. C., C. Nai and V. Meyer (2018). "How a fungus shapes biotechnology: 100 years of Aspergillus niger research." Fungal biology and biotechnology **5**(1): 1-14.

Carpita, N. C. (1996). "Structure and biogenesis of the cell walls of grasses." Annual review of plant biology **47**(1): 445-476.

Carpita, N. C. and M. C. McCann (2002). "The functions of cell wall polysaccharides in composition and architecture revealed through mutations." Plant and soil **247**: 71-80.

Chang, P.-K., J. W. Cary and M. D. Lebar (2020). "Biosynthesis of conidial and sclerotial pigments in Aspergillus species." Applied microbiology and biotechnology **104**: 2277-2286.

Chaudhary, K. and P. Tauro (1982). "Sequential release of cellulose enzymes during germination of Trichoderma reesei spores." Journal of biosciences **4**: 281-286.

Che, S. and Y. Men (2019). "Synthetic microbial consortia for biosynthesis and biodegradation: promises and challenges." Journal of Industrial Microbiology and Biotechnology **46**(9-10): 1343-1358.

Chiba, S. (1997). "Molecular mechanism in α-glucosidase and glucoamylase." Bioscience, biotechnology, and biochemistry **61**(8): 1233-1239.

Chmiel, H. and E. Walitza (2018). Transportvorgänge in Biosuspensionen, in: Bioprozesstechnik, Springer**:** 131-156.

Chmiel, H., D. Weuster-Botz, W. Himmelsbach, W. Himmelsbach, W. Himmelsbach, W. Himmelsbach, W. Himmelsbach, R. Takors, C. Posten and T. Ladner (2018). Bioreaktoren, in: Bioprozesstechnik, Springer**:** 157-229.

Chuang, W. Y., Y. C. Hsieh and T.-T. Lee (2020). "The effects of fungal feed additives in animals: A review." Animals **10**(5): 805.

Conacher, C. G., R. K. Naidoo-Blassoples, D. Rossouw and F. F. Bauer (2020). "Real-time monitoring of population dynamics and physical interactions in a synthetic yeast ecosystem by use of multicolour flow cytometry." Applied Microbiology and Biotechnology **104**(12): 5547-5562.

Cripwell, R., L. Favaro, S. H. Rose, M. Basaglia, L. Cagnin, S. Casella and W. van Zyl (2015). "Utilisation of wheat bran as a substrate for bioethanol production using recombinant cellulases and amylolytic yeast." Applied Energy **160**: 610-617.

Culleton, H., V. McKie and R. P. de Vries (2013). "Physiological and molecular aspects of degradation of plant polysaccharides by fungi: what have we learned from Aspergillus?" Biotechnology journal **8**(8): 884-894.

Currie, J. N. (1917). "The citric acid fermentation of Aspergillus niger." J Biol Chem **31**(1): 15-37.

Dai, Z., X. Mao, J. K. Magnuson and L. L. Lasure (2004). "Identification of genes associated with morphology in Aspergillus niger by using suppression subtractive hybridization." Applied and Environmental Microbiology **70**(4): 2474-2485.

Daly, P., J. M. van Munster, M. Kokolski, F. Sang, M. J. Blythe, S. Malla, J. V. de Castro Oliveira, G. H. Goldman and D. B. Archer (2017). "Transcriptomic responses of mixed cultures of ascomycete fungi to lignocellulose using dual RNA-seq reveal inter-species antagonism and limited beneficial effects on CAZyme expression." Fungal Genetics and Biology **102**: 4-21.

Danckwerts, P. (1951). "Significance of liquid-film coefficients in gas absorption." Industrial & Engineering Chemistry **43**(6): 1460-1467.

de Vries, R. P., J. Visser and L. H. de Graaff (1999). "CreA modulates the XlnR-induced expression on xylose of Aspergillus niger genes involved in xylan degradation." Research in Microbiology **150**(4): 281-285.

Debets, F., K. Swart, R. F. Hoekstra and C. J. Bos (1993). "Genetic maps of eight linkage groups of Aspergillus niger based on mitotic mapping." Current genetics **23**: 47-53.

Destatis (2023). Anbauflächen, Hektarerträge und Erntemengen ausgewählter Anbaukulturen im Zeitvergleich, Statistisches Bundesamt.

Dhanasekharan, K. M., J. Sanyal, A. Jain and A. Haidari (2005). "A generalized approach to model oxygen transfer in bioreactors using population balances and computational fluid dynamics." Chemical Engineering Science **60**(1): 213-218.

Diano, A., S. Bekker-Jensen, J. Dynesen and J. Nielsen (2006). "Polyol synthesis in Aspergillus niger: influence of oxygen availability, carbon and nitrogen sources on the metabolism." Biotechnology and bioengineering **94**(5): 899-908.

Domingues, F., J. Queiroz, J. Cabral and L. Fonseca (2000). "The influence of culture conditions on mycelial structure and cellulase production by Trichoderma reesei Rut C-30." Enzyme and Microbial Technology **26**(5-6): 394-401.

Dornez, E., K. Gebruers, S. Wiame, J. A. Delcour and C. M. Courtin (2006). "Insight into the distribution of arabinoxylans, endoxylanases, and endoxylanase inhibitors in industrial wheat roller mill streams." Journal of agricultural and food chemistry **54**(22): 8521-8529.

Driouch, H., R. Hänsch, T. Wucherpfennig, R. Krull and C. Wittmann (2012). "Improved enzyme production by bio-pellets of Aspergillus niger: Targeted morphology engineering using titanate microparticles." Biotechnology and Bioengineering **109**(2): 462-471.

Driouch, H., A. Roth, P. Dersch and C. Wittmann (2011). "Filamentous fungi in good shape: microparticles for tailor-made fungal morphology and enhanced enzyme production." Bioengineered bugs **2**(2): 100-104.

Driouch, H., B. Sommer and C. Wittmann (2010). "Morphology engineering of Aspergillus niger for improved enzyme production." Biotechnology and bioengineering **105**(6): 1058-1068.

Druzhinina, I. S. and C. P. Kubicek (2017). "Genetic engineering of Trichoderma reesei cellulases and their production." Microbial biotechnology **10**(6): 1485-1499.

Ebringerová, A. and T. Heinze (2000). "Xylan and xylan derivatives–biopolymers with valuable properties, 1. Naturally occurring xylans structures, isolation procedures and properties." Macromolecular rapid communications **21**(9): 542-556.

Eibinger, M., T. Ganner, P. Bubner, S. Rošker, D. Kracher, D. Haltrich, R. Ludwig, H. Plank and B. Nidetzky (2014). "Cellulose surface degradation by a lytic polysaccharide monooxygenase and its effect on cellulase hydrolytic efficiency." Journal of Biological Chemistry **289**(52): 35929-35938.

Ellena, V., S. J. Seekles, G. A. Vignolle, A. F. Ram and M. G. Steiger (2021). "Genome sequencing of the neotype strain CBS 554.65 reveals the MAT1–2 locus of Aspergillus niger." BMC genomics **22**: 1-16.

Fairbanks, G., T. L. Steck and D. Wallach (1971). "Electrophoretic analysis of the major polypeptides of the human erythrocyte membrane." Biochemistry **10**(13): 2606-2617.

Farkas, C., J. M. Rezessy-Szabó, V. K. Gupta, D. H. Truong, L. Friedrich, J. Felföldi and Q. D. Nguyen (2019). "Microbial saccharification of wheat bran for bioethanol fermentation." Journal of Cleaner Production **240**: 118269.

Favaro, L., M. Basaglia, W. H. van Zyl and S. Casella (2013). "Using an efficient fermenting yeast enhances ethanol production from unfiltered wheat bran hydrolysates." Applied Energy **102**: 170-178.

Ferreira, N. L., A. Margeot, S. Blanquet and J.-G. Berrin (2014). Chapter 17 - Use of Cellulases from Trichoderma reesei in the Twenty-First Century—Part I: Current Industrial Uses and Future Applications in the Production of Second Ethanol Generation, in: Biotechnology and Biology of Trichoderma. V. K. Gupta, M. Schmoll, A. Herrera-Estrella et al. Amsterdam, Elsevier**:** 245-261.

Ferreira, R. G., A. R. Azzoni and S. Freitas (2021). "On the production cost of lignocellulose-degrading enzymes." Biofuels, Bioproducts and Biorefining **15**(1): 85-99.

Fischer, A. J., S. Maiyuran and D. S. Yaver (2021). "Industrial relevance of Trichoderma reesei as an enzyme producer." Trichoderma reesei: Methods and Protocols: 23-43.

Freire, L., T. M. Guerreiro, A. K. R. Pia, E. O. Lima, D. N. Oliveira, C. F. O. R. Melo, R. R. Catharino and A. S. Sant'Ana (2018). "A quantitative study on growth variability and production of ochratoxin A and its derivatives by A. carbonarius and A. niger in grape-based medium." Scientific Reports **8**(1): 14573.

Frisvad, J. C., L. L. H. Møller, T. O. Larsen, R. Kumar and J. Arnau (2018). "Safety of the fungal workhorses of industrial biotechnology: update on the mycotoxin and secondary metabolite potential of Aspergillus niger, Aspergillus oryzae, and Trichoderma reesei." Applied Microbiology and Biotechnology **102**(22): 9481-9515.

Gabriela Roca, M., N. D. Read and A. E. Wheals (2005). "Conidial anastomosis tubes in filamentous fungi." FEMS Microbiology Letters **249**(2): 191-198.

García-Jiménez, B., J. Torres-Bacete and J. Nogales (2021). "Metabolic modelling approaches for describing and engineering microbial communities." Computational and Structural Biotechnology Journal **19**: 226.

Garcia-Ochoa, F. and E. Gomez (2009). "Bioreactor scale-up and oxygen transfer rate in microbial processes: an overview." Biotechnology advances **27**(2): 153-176.

Garcia-Ochoa, F., E. Gomez, V. E. Santos and J. C. Merchuk (2010). "Oxygen uptake rate in microbial processes: an overview." Biochemical engineering journal **49**(3): 289-307.

Ghorai, S., S. P. Banik, D. Verma, S. Chowdhury, S. Mukherjee and S. Khowala (2009). "Fungal biotechnology in food and feed processing." Food research international **42**(5-6): 577-587.

Gibbs, P., R. Seviour and F. Schmid (2000). "Growth of filamentous fungi in submerged culture: problems and possible solutions." Critical reviews in biotechnology **20**(1): 17-48.

Gooday, G. W. (1995). "The dynamics of hyphal growth." Mycological Research **99**(4): 385-394.

Grimm, L., S. Kelly, J. Hengstler, A. Göbel, R. Krull and D. Hempel (2004). "Kinetic studies on the aggregation of Aspergillus niger conidia." Biotechnology and bioengineering **87**(2): 213-218.

Grimm, L., S. Kelly, I. Völkerding, R. Krull and D. Hempel (2005). "Influence of mechanical stress and surface interaction on the aggregation of Aspergillus niger conidia." Biotechnology and bioengineering **92**(7): 879-888.

Haefner, S., A. Knietsch, E. Scholten, J. Braun, M. Lohscheidt and O. Zelder (2005). "Biotechnological production and applications of phytases." Applied Microbiology and Biotechnology **68**(5): 588-597.

Harris, P. V., D. Welner, K. McFarland, E. Re, J.-C. Navarro Poulsen, K. Brown, R. Salbo, H. Ding, E. Vlasenko and S. Merino (2010). "Stimulation of lignocellulosic biomass hydrolysis by proteins of glycoside hydrolase family 61: structure and function of a large, enigmatic family." Biochemistry **49**(15): 3305-3316.

Harris, S. D. (2008). "Branching of fungal hyphae: regulation, mechanisms and comparison with other branching systems." Mycologia **100**(6): 823-832.

Hayer, K., M. Stratford and D. B. Archer (2013). "Structural Features of Sugars That Trigger or Support Conidial Germination in the Filamentous Fungus Aspergillus niger." Applied and Environmental Microbiology **79**(22): 6924-6931.

Hayer, K., M. Stratford and D. B. Archer (2014). "Germination of Aspergillus niger conidia is triggered by nitrogen compounds related to L-amino acids." Applied and environmental microbiology **80**(19): 6046-6053.

Hemery, Y., X. Rouau, V. Lullien-Pellerin, C. Barron and J. Abecassis (2007). "Dry processes to develop wheat fractions and products with enhanced nutritional quality." Journal of Cereal Science **46**(3): 327-347.

Herpoël-Gimbert, I., A. Margeot, A. Dolla, G. Jan, D. Mollé, S. Lignon, H. Mathis, J.-C. Sigoillot, F. Monot and M. Asther (2008). "Comparative secretome analyses of two Trichoderma reesei RUT-C30 and CL847 hypersecretory strains." Biotechnology for biofuels **1**(1): 1-12.

Higbie, R. (1935). "The rate of absorption of pure gas into a still liquid during short periods of exposure." Trans. Am. Inst. Chem. Engrs. **31**: 365-389.

Hinrichs, J., H. Buck and G. Hauser (2018). "Sterilisation und Sterildesign." Bioprozesstechnik: 231-259.

Iiyama, K., T. B.-T. Lam and B. A. Stone (1994). "Covalent cross-links in the cell wall." Plant physiology **104**(2): 315.

Ilmén, M., M.-L. Onnela, S. Klemsdal, S. Keränen and M. Penttilä (1996). "Functional analysis of the cellobiohydrolase I promoter of the filamentous fungus Trichoderma reesei." Molecular and General Genetics MGG **253**: 303-314.

Izydorczyk, M. and J. Dexter (2008). "Barley β-glucans and arabinoxylans: Molecular structure, physicochemical properties, and uses in food products–a Review." Food Research International **41**(9): 850-868.

Jiang, S.-T. and N. Guo (2016). "The steam explosion pretreatment and enzymatic hydrolysis of wheat bran." Energy Sources, Part A: Recovery, Utilization, and Environmental Effects **38**(2): 295-299.

Jo, C., D. B. Bernstein, N. Vaisman, H. M. Frydman and D. Segrè (2021). "A co-culture microplate for real-time measurement of microbial interactions." bioRxiv.

Johnson, E. (2016). "Integrated enzyme production lowers the cost of cellulosic ethanol." Biofuels, Bioproducts and Biorefining **10**(2): 164-174.

Kaji, A. (1984). l-Arabinosidases, in: Advances in carbohydrate chemistry and biochemistry, Elsevier. **42:** 383-394.

Kamm, B. and M. Kamm (2007). "International biorefinery systems." Pure and Applied Chemistry **79**(11): 1983-1997.

Kelly, S., L. H. Grimm, J. Hengstler, E. Schultheis, R. Krull and D. C. Hempel (2004). "Agitation effects on submerged growth and product formation of Aspergillus niger." Bioprocess and Biosystems Engineering **26**(5): 315-323.

Kirchherr, J., D. Reike and M. Hekkert (2017). "Conceptualizing the circular economy: An analysis of 114 definitions." Resources, conservation and recycling **127**: 221-232.

Kisser, M., C. Kubicek and M. Röhr (1980). "Influence of manganese on morphology and cell wall composition of Aspergillus niger during citric acid fermentation." Archives of Microbiology **128**: 26-33.

Knesebeck, M., D. Schäfer, K. Schmitz, M. Rüllke, J. P. Benz and D. Weuster-Botz (2023). "Enzymatic One-Pot Hydrolysis of Extracted Sugar Beet Press Pulp after Solid-State Fermentation with an Engineered Aspergillus niger Strain." Fermentation **9**(7): 582.

Kolasa, M., B. K. Ahring, P. S. Lübeck and M. Lübeck (2014). "Co-cultivation of Trichoderma reesei RutC30 with three black Aspergillus strains facilitates efficient hydrolysis of pretreated wheat straw and shows promises for on-site enzyme production." Bioresource technology **169**: 143-148.

Koutinas, A. A., R. Wang, G. M. Campbell and C. Webb (2005). "A whole crop biorefinery system: a closed system for the manufacture of non-food products from cereals." Biorefineries-Industrial Processes and Products: Status Quo and Future Directions: 165-191.

Krijgsheld, P., R. v. Bleichrodt, G. Van Veluw, F. Wang, W. Müller, J. Dijksterhuis and H. Wösten (2013). "Development in aspergillus." Studies in mycology **74**(1): 1-29.

Krull, R., T. Wucherpfennig, M. E. Esfandabadi, R. Walisko, G. Melzer, D. C. Hempel, I. Kampen, A. Kwade and C. Wittmann (2013). "Characterization and control of fungal morphology for improved production performance in biotechnology." Journal of Biotechnology **163**(2): 112-123.

Kubicek, C. P., A. Herrera-Estrella, V. Seidl-Seiboth, D. A. Martinez, I. S. Druzhinina, M. Thon, S. Zeilinger, S. Casas-Flores, B. A. Horwitz and P. K. Mukherjee (2011). "Comparative genome sequence analysis underscores mycoparasitism as the ancestral life style of Trichoderma." Genome biology **12**: 1-15.

Kupski, L., F. A. Pagnussatt, J. G. Buffon and E. B. Furlong (2014). "Endoglucanase and total cellulase from newly isolated Rhizopus oryzae and Trichoderma reesei: production, characterization, and thermal stability." Applied biochemistry and biotechnology **172**: 458-468.

Laca, A., Z. Mousia, M. Díaz, C. Webb and S. S. Pandiella (2006). "Distribution of microbial contamination within cereal grains." Journal of Food engineering **72**(4): 332-338.

Laemmli, U. K. (1970). "Cleavage of structural proteins during the assembly of the head of bacteriophage T4." nature **227**(5259): 680-685.

Lejeune, R. and G. V. Baron (1995). "Effect of agitation on growth and enzyme production of Trichoderma reesei in batch fermentation." Applied Microbiology and Biotechnology **43**(2): 249-258.

Lejeune, R., J. Nielsen and G. Baron (1995). "Influence of pH on the morphology of Trichoderma reeseiqm 9414 in submerged culture." Biotechnology letters **17**: 341-344.

Levasseur, A., E. Drula, V. Lombard, P. M. Coutinho and B. Henrissat (2013). "Expansion of the enzymatic repertoire of the CAZy database to integrate auxiliary redox enzymes." Biotechnology for biofuels **6**: 1-14.

Levenspiel, O. (1980). "The Monod equation: a revisit and a generalization to product inhibition situations." Biotechnology and bioengineering **22**(8): 1671-1687.

Lever, M. (1972). "A new reaction for colorimetric determination of carbohydrates." Analytical biochemistry **47**(1): 273-279.

Lewis, W. K. and W. G. Whitman (1924). "Principles of gas absorption." Industrial & Engineering Chemistry **16**(12): 1215-1220.

Li, W., S. W. Cui and Y. Kakuda (2006). "Extraction, fractionation, structural and physical characterization of wheat β-D-glucans." Carbohydrate Polymers **63**(3): 408-416.

Li, Z., L. Han, Y. Ji, X. Wang and T. Tan (2010). "Fermentative production of L-lactic acid from hydrolysate of wheat bran by Lactobacillus rhamnosus." Biochemical Engineering Journal **49**(1): 138-142.

Lin, P.-J., A. Scholz and R. Krull (2010). "Effect of volumetric power input by aeration and agitation on pellet morphology and product formation of Aspergillus niger." Biochemical engineering journal **49**(2): 213-220.

Liu, Y., X. Tu, Q. Xu, C. Bai, C. Kong, Q. Liu, J. Yu, Q. Peng, X. Zhou and Y. Zhang (2018). "Engineered monoculture and co-culture of methylotrophic yeast for de novo production of monacolin J and lovastatin from methanol." Metabolic engineering **45**: 189-199.

Lo, C.-M., Q. Zhang, N. V. Callow and L.-K. Ju (2010). "Roles of extracellular lactose hydrolysis in cellulase production by Trichoderma reesei Rut C30 using lactose as inducing substrate." Process Biochemistry **45**(9): 1494-1503.

Lu, H., W. Cao, X. Liu, Y. Sui, L. Ouyang, J. Xia, M. Huang, Y. Zhuang, S. Zhang and H. Noorman (2018). "Multi-omics integrative analysis with genome-scale metabolic model simulation reveals global cellular adaptation of Aspergillus niger under industrial enzyme production condition." Scientific reports **8**(1): 14404.

Lubertozzi, D. and J. D. Keasling (2009). "Developing Aspergillus as a host for heterologous expression." Biotechnology advances **27**(1): 53-75.

Lynd, L. R., P. J. Weimer, W. H. Van Zyl and I. S. Pretorius (2002). "Microbial cellulose utilization: fundamentals and biotechnology." Microbiology and molecular biology reviews **66**(3): 506-577.

Mach-Aigner, A. R., J. Omony, B. Jovanovic, A. J. van Boxtel and L. H. de Graaff (2012). "D-Xylose concentration-dependent hydrolase expression profiles and the function of CreA and XlnR in Aspergillus niger." Applied and environmental microbiology **78**(9): 3145-3155.

Maehara, L., S. C. Pereira, A. J. Silva and C. S. Farinas (2018). "One-pot strategy for on-site enzyme production, biomass hydrolysis, and ethanol production using the whole solid-state fermentation medium of mixed filamentous fungi." Biotechnology progress **34**(3): 671-680.

Mandels, M. and E. T. Reese (1957). "Induction of cellulase in Trichoderma viride as influenced by carbon sources and metals." Journal of bacteriology **73**(2): 269-278.

Mandels, M., J. Weber and R. Parizek (1971). "Enhanced cellulase production by a mutant of Trichoderma viride." Applied microbiology **21**(1): 152-154.

Margaritis, A. and J. E. Zajic (1978). "Mixing, mass transfer, and scale-up of polysaccharide fermentations." Biotechnology and bioengineering **20**(7): 939-1001.

Marjamaa, K., J. Rahikainen, M. Karjalainen, N. Maiorova, U. Holopainen-Mantila, M. Molinier, N. Aro, H. Nygren, A. Mikkelson and A. Koivula (2022). "Oxidative modification of cellulosic fibres by lytic polysaccharide monooxygenase AA9A from Trichoderma reesei." Cellulose **29**(11): 6021-6038.

Martin, J. (2007). "The 17 great challenges of the twenty-first century." Futurist **41**(1): 20.

Martinez, D., R. M. Berka, B. Henrissat, M. Saloheimo, M. Arvas, S. E. Baker, J. Chapman, O. Chertkov, P. M. Coutinho and D. Cullen (2008). "Genome sequencing and analysis of the biomass-degrading fungus Trichoderma reesei (syn. Hypocrea jecorina)." Nature biotechnology **26**(5): 553-560.

Masri, M. A., D. Garbe, N. Mehlmer and T. B. Brück (2019). "A sustainable, high-performance process for the economic production of waste-free microbial oils that can replace plant-based equivalents." Energy & Environmental Science **12**(9): 2717-2732.

McCartney, A. and J. West (2007). Dispersal of fungal spores through the air, in: Food Mycology, CRC press**:** 79-96.

McDaniel, A., E. Fuchs, Y. Liu and C. Ford (2008). "Directed evolution of Aspergillus niger glucoamylase to increase thermostability." Microbial biotechnology **1**(6): 523-531.

Membrillo Venegas, I., J. Fuentes-Hernández, M. García-Rivero and A. Martínez-Trujillo (2013). "Characteristics of Aspergillus niger xylanases produced on rice husk and wheat bran in submerged culture and solid-state fermentation for an applicability proposal." International journal of food science & technology **48**(9): 1798-1807.

Meo, A., X. L. Priebe and D. Weuster-Botz (2017). "Lipid production with Trichosporon oleaginosus in a membrane bioreactor using microalgae hydrolysate." Journal of Biotechnology **241**: 1-10.

Merino, S. T. and J. Cherry (2007). "Progress and challenges in enzyme development for biomass utilization." Biofuels: 95-120.

Metz, B. and N. Kossen (1977). "The growth of molds in the form of pellets–a literature review." Biotechnology and bioengineering **19**(6): 781-799.

Meyer, V., E. Y. Basenko, J. P. Benz, G. H. Braus, M. X. Caddick, M. Csukai, R. P. De Vries, D. Endy, J. C. Frisvad and N. Gunde-Cimerman (2020). "Growing a circular economy with fungal biotechnology: a white paper." Fungal biology and biotechnology **7**(1): 1-23.

Meyer, V., B. Wu and A. F. Ram (2011). "Aspergillus as a multi-purpose cell factory: current status and perspectives." Biotechnology letters **33**: 469-476.

Monod, J. (1949). "The growth of bacterial cultures." Annual review of microbiology **3**(1): 371-394.

Montenecourt, B. S. and D. Eveleigh (1977). "Preparation of mutants of Trichoderma reesei with enhanced cellulase production." Applied and environmental microbiology **34**(6): 777-782.

Montenecourt, B. S. and D. E. Eveleigh (1979). Selective screening methods for the isolation of high yielding cellulase mutants of Trichoderma reesei, in, ACS Publications.

Moyer, A., E. Umberger and J. Stubbs (1940). "Fermentation of concentrated solutions of glucose to gluconic acid improved process." Industrial & Engineering Chemistry **32**(10): 1379-1383.

Musaalbakri, A. M. and C. Webb (2018). "Estimation of growth in solid state fermentation: a review." Malaysian Journal of Microbiology **14**(1): 61-69.

Muscat, A., E. De Olde, I. J. de Boer and R. Ripoll-Bosch (2020). "The battle for biomass: a systematic review of food-feed-fuel competition." Global Food Security **25**: 100330.

Nandini, C. D. and P. V. Salimath (2001). "Carbohydrate composition of wheat, wheat bran, sorghum and bajra with good chapati/roti (Indian flat bread) making quality." Food Chemistry **73**(2): 197-203.

Nevalainen, H., P. Suominen and K. Taimisto (1994). "On the safety of Trichoderma reesei." Journal of Biotechnology **37**(3): 193-200.

Neves, M. A. d., T. Kimura, N. Shimizu and K. Shiiba (2006). "Production of alcohol by simultaneous saccharification and fermentation of low-grade wheat flour." Brazilian archives of biology and technology **49**: 481-490.

Nielsen, J. (1993). "A simple morphologically structured model describing the growth of filamentous microorganisms." Biotechnology and bioengineering **41**(7): 715-727.

Nielsen, J. (1996). "Modelling the morphology of filamentous microorganisms." Trends in Biotechnology **14**(11): 438-443.

Nienow, A. (1990). "Agitators for mycelial fermentations." Trends in biotechnology **8**: 224-233.

Osama, A. S., M. A. Khaled and M. H. Abir (2013). "Bioconversion of some agricultural wastes into animal feed by Trichoderma spp." Journal of American Science **9**(6): 203-212.

Osherov, N. and G. S. May (2001). "The molecular mechanisms of conidial germination." FEMS microbiology letters **199**(2): 153-160.

Palmarola-Adrados, B., P. Chotěborská, M. Galbe and G. Zacchi (2005). "Ethanol production from non-starch carbohydrates of wheat bran." Bioresource technology **96**(7): 843-850.

Papagianni, M. (2004). "Fungal morphology and metabolite production in submerged mycelial processes." Biotechnology advances **22**(3): 189-259.

Papagianni, M. and M. Mattey (2004). "Physiological aspects of free and immobilized Aspergillus niger cultures producing citric acid under various glucose concentrations." Process Biochemistry **39**(12): 1963-1970.

Papagianni, M., M. Mattey and B. Kristiansen (1994). "Morphology and citric acid production of Aspergillus niger PM 1." Biotechnology letters **16**: 929-934.

Papagianni, M., M. Mattey and B. Kristiansen (1998). "Citric acid production and morphology of Aspergillus niger as functions of the mixing intensity in a stirred tank and a tubular loop bioreactor." Biochemical engineering journal **2**(3): 197-205.

Papagianni, M., M. Mattey and B. Kristiansen (1999). "The influence of glucose concentration on citric acid production and morphology of Aspergillus niger in batch and culture." Enzyme and Microbial Technology **25**(8-9): 710-717.

Paul, G., M. Priede and C. Thomas (1999). "Relationship between morphology and citric acid production in submerged Aspergillus niger fermentations." Biochemical Engineering Journal **3**(2): 121-129.

Pazouki, M. and T. Panda (2000). "Understanding the morphology of fungi." Bioprocess Engineering **22**(2): 127-143.

Pel, H. J., J. H. de Winde, D. B. Archer, P. S. Dyer, G. Hofmann, P. J. Schaap, G. Turner, R. P. de Vries, R. Albang and K. Albermann (2007). "Genome sequencing and analysis of the versatile cell factory Aspergillus niger CBS 513.88." Nature biotechnology **25**(2): 221-231.

Perlman, D., D. Kita and W. Peterson (1946). "Production of citric acid from cane molasses." Archives of biochemistry **11**: 123-129.

Person, A. K., S. M. Chudgar, B. L. Norton, B. C. Tong and J. E. Stout (2010). "Aspergillus niger: an unusual cause of invasive pulmonary aspergillosis." Journal of Medical Microbiology **59**(7): 834-838.

Peterson, R. and H. Nevalainen (2012). "Trichoderma reesei RUT-C30–thirty years of strain improvement." Microbiology **158**(1): 58-68.

Pirota, R. D., F. C. Baleeiro and C. S. Farinas (2013). "Saccharification of biomass using whole solid-state fermentation medium to avoid additional separation steps." Biotechnology Progress **29**(6): 1430-1440.

Polizeli, M. d. L. T. d. M., A. Rizzatti, R. Monti, H. F. Terenzi, J. A. Jorge and D. d. S. Amorim (2005). "Xylanases from fungi: properties and industrial applications." Applied microbiology and biotechnology **67**(5): 577-591.

Pollard, D., T. Kirschner, G. Hunt, I. T. Tong, R. Stieber and P. Salmon (2007). "Scale up of a viscous fungal fermentation: Application of scale-up criteria with regime analysis and operating boundary conditions." Biotechnology and bioengineering **96**(2): 307-317.

Pontecorvo, G., J. Roper and E. Forbes (1953). "Genetic recombination without sexual reproduction in Aspergillus niger." Microbiology **8**(1): 198-210.

Pribowo, A., V. Arantes and J. N. Saddler (2012). "The adsorption and enzyme activity profiles of specific Trichoderma reesei cellulase/xylanase components when hydrolyzing steam pretreated corn stover." Enzyme and Microbial Technology **50**(3): 195-203.

Prueckler, M., S. Siebenhandl-Ehn, S. Apprich, S. Hoeltinger, C. Haas, E. Schmid and W. Kneifel (2014). "Wheat bran-based biorefinery 1: Composition of wheat bran and strategies of functionalization." LWT-Food Science and Technology **56**(2): 211-221.

Puls, J., O. Schmidt and C. Granzow (1987). "α-Glucuronidase in two microbial xylanolytic systems." Enzyme and Microbial Technology **9**(2): 83-88.

Radenkovs, V., D. Klava and K. Juhnevica (2013). "Microbiology and safety of bran from Latvia." International Proceedings of Chemical, Biological and Environmental

Engineering. Nutrition and Food Science II, IACSIT Press, Jurong West, Street **71**: 87-92.

Rautio, J. J., B. A. Smit, M. Wiebe, M. Penttilä and M. Saloheimo (2006). "Transcriptional monitoring of steady state and effects of anaerobic phases in chemostat cultures of the filamentous fungus Trichoderma reesei." BMC genomics **7**: 1-15.

Ray, A. C. and R. Eakin (1975). "Studies on the biosynthesis of aspergillin by Aspergillus niger." Applied microbiology **30**(6): 909-915.

Reese, E. T. and M. Mandels (1980). "Stability of the cellulase of Trichoderma reesei under use conditions." Biotechnology and Bioengineering **22**(2): 323-335.

Reisinger, M., Ö. Tirpanalan, M. Prückler, F. Huber, W. Kneifel and S. Novalin (2013). "Wheat bran biorefinery–a detailed investigation on hydrothermal and enzymatic treatment." Bioresource technology **144**: 179-185.

Riley, G., K. Tucker, G. Paul and C. Thomas (2000). "Effect of biomass concentration and mycelial morphology on fermentation broth rheology." Biotechnology and bioengineering **68**(2): 160-172.

Roberts, P. J., D. H. Simmonds, M. Wootton and C. W. Wrigley (1985). "Extraction of protein and solids from wheat bran." Journal of the Science of Food and Agriculture **36**(1): 5-10.

Ryu, D. D. and M. Mandels (1980). "Cellulases: biosynthesis and applications." Enzyme and Microbial Technology **2**(2): 91-102.

Saini, J. K., A. Kaur and A. Mathur (2022). "Strategies to enhance enzymatic hydrolysis of lignocellulosic biomass for biorefinery applications: a review." Bioresource technology **360**: 127517.

Saini, M., L.-J. Lin, C.-J. Chiang and Y.-P. Chao (2017). "Synthetic consortium of Escherichia coli for n-butanol production by fermentation of the glucose–xylose mixture." Journal of agricultural and food chemistry **65**(46): 10040-10047.

Saini, P., M. Islam, R. Das, S. Shekhar, A. S. K. Sinha and K. Prasad (2023). "Wheat bran as potential source of dietary fiber: Prospects and challenges." Journal of Food Composition and Analysis **116**: 105030.

Saloheimo, M., M. Paloheimo, S. Hakola, J. Pere, B. Swanson, E. Nyyssönen, A. Bhatia, M. Ward and M. Penttilä (2002). "Swollenin, a Trichoderma reesei protein with sequence similarity to the plant expansins, exhibits disruption activity on cellulosic materials." European journal of biochemistry **269**(17): 4202-4211.

Saranraj, P. and D. Stella (2013). "Fungal amylase—a review." Int. J. Microbiol. Res **4**(2): 203-211.

Scazzocchio, C. (2009). "Aspergillus: a multifaceted genus." Encyclopedia of microbiology: 401-421.

Schäfer, D., K. Schmitz, D. Weuster-Botz and J. P. Benz (2020). "Comparative evaluation of Aspergillus niger strains for endogenous pectin-depolymerization capacity and suitability for d-galacturonic acid production." Bioprocess and biosystems engineering **43**(9): 1549-1560.

Schlembach, I., A. Grünberger, M. A. Rosenbaum and L. Regestein (2021). "Measurement techniques to resolve and control population dynamics of mixed-culture processes." Trends in Biotechnology.

Schlembach, I., H. Hosseinpour Tehrani, L. M. Blank, J. Büchs, N. Wierckx, L. Regestein and M. A. Rosenbaum (2020). "Consolidated bioprocessing of cellulose to itaconic acid by a co-culture of Trichoderma reesei and Ustilago maydis." Biotechnology for biofuels **13**(1): 1-18.

Schroeder, P., K. Anggraeni and U. Weber (2019). "The relevance of circular economy practices to the sustainable development goals." Journal of Industrial Ecology **23**(1): 77-95.

Schuster, E., N. Dunn-Coleman, J. Frisvad and P. Van Dijck (2002). "On the safety of Aspergillus niger–a review." Applied microbiology and biotechnology **59**: 426-435.

Seiboth, B., L. Hartl, N. Salovuori, K. Lanthaler, G. D. Robson, J. Vehmaanperä, M. E. Penttilä and C. P. Kubicek (2005). "Role of the bga1-encoded extracellular β-galactosidase of Hypocrea jecorina in cellulase induction by lactose." Applied and environmental microbiology **71**(2): 851-857.

Seiboth, B., C. Ivanova and V. Seidl-Seiboth (2011). "Trichoderma reesei: a fungal enzyme producer for cellulosic biofuels." Biofuel production-recent developments and prospects: 309-340.

Shahab, R. L., J. S. Luterbacher, S. Brethauer and M. H. Studer (2018). "Consolidated bioprocessing of lignocellulosic biomass to lactic acid by a synthetic fungal-bacterial consortium." Biotechnology and bioengineering **115**(5): 1207-1215.

Shin, W.-S., D. Lee, S. Kim, Y.-S. Jeong and G.-T. Chun (2013). "Application of Scale-Up Criterion of Constant Oxygen Mass Transfer Coefficient ($ k_La $) for Production of Itaconic Acid in a 50 L Pilot-Scale Fermentor by Fungal Cells of Aspergillus terreus." Journal of microbiology and biotechnology **23**(10): 1445-1453.

Sideman, S. (1966). "The equivalence of the penetration and potential flow theories." Industrial & Engineering Chemistry **58**(2): 54-58.

Šimonovičová, A., H. Vojtkova, S. Nosalj, E. Piecková, H. Švehláková, L. Kraková, H. Drahovska, B. Stalmachova, K. Kučová and D. Pangallo (2021). "Aspergillus

niger environmental isolates and their specific diversity through metabolite profiling." Frontiers in Microbiology **12**: 658010.

Singhania, R., A. Patel and A. Pandey (2017). Biotechnology for Agricultural Waste Recycling, in: Current Developments in Biotechnology and Bioengineering, Elsevier**:** 223-240.

Soetaert, W. and E. Vandamme (2006). "The impact of industrial biotechnology." Biotechnology Journal: Healthcare Nutrition Technology **1**(7-8): 756-769.

Souza, P. M. d., M. L. d. A. Bittencourt, C. C. Caprara, M. d. Freitas, R. P. C. d. Almeida, D. Silveira, Y. M. Fonseca, E. X. Ferreira Filho, A. Pessoa and P. O. Magalhães (2015). "A biotechnology perspective of fungal proteases." Brazilian Journal of Microbiology **46**(2): 337-346.

Sovová, K., J. Čepl, A. Markoš and P. Španěl (2013). "Real time monitoring of population dynamics in concurrent bacterial growth using SIFT-MS quantification of volatile metabolites." Analyst **138**(17): 4795-4801.

Steinberg, G. (2007). "Hyphal Growth: a Tale of Motors, Lipids, and the Spitzenkörper." Eukaryotic Cell **6**(3): 351-360.

Steinberg, G., M. A. Peñalva, M. Riquelme, H. A. Wösten and S. D. Harris (2017). "Cell biology of hyphal growth." Microbiology spectrum **5**(2): 10.1128/microbiolspec. funk-0034-2016.

Sun, Y., S. W. Cui, X. Gu and J. Zhang (2011). "Isolation and structural characterization of water unextractable arabinoxylans from Chinese black-grained wheat bran." Carbohydrate Polymers **85**(3): 615-621.

Tagawa, K. and A. Kaji (1988). α-L-Arabinofuranosidase from Aspergillus niger, in: Methods in Enzymology, Elsevier. **160:** 707-712.

Takors, R. (2014). Kommentierte Formelsammlung Bioverfahrenstechnik, Springer.

Takors, R. and D. Weuster-Botz (2018). Prozessmodelle, in: Bioprozesstechnik. H. Chmiel, R. Takors and D. Weuster-Botz. Berlin, Springer. **4:** 73-106.

Tenkanen, M., J. Schuseil, J. Puls and K. Poutanen (1991). "Production, purification and characterization of an esterase liberating phenolic acids from lignocellulosics." Journal of Biotechnology **18**(1-2): 69-83.

Tirpanalan, Ö., M. Reisinger, M. Smerilli, F. Huber, M. Neureiter, W. Kneifel and S. Novalin (2015). "Wheat bran biorefinery–an insight into the process chain for the production of lactic acid." Bioresource technology **180**: 242-249.

UN (2015). Resolution 70/1. Transforming our world: the 2030 Agenda for Sustainable Development, United Nations.

Van Der Maarel, M. J., B. Van der Veen, J. C. Uitdehaag, H. Leemhuis and L. Dijkhuizen (2002). "Properties and applications of starch-converting enzymes of the α-amylase family." Journal of biotechnology **94**(2): 137-155.

van Dijck, P. W., G. C. Selten and R. A. Hempenius (2003). "On the safety of a new generation of DSM Aspergillus niger enzyme production strains." Regulatory Toxicology and Pharmacology **38**(1): 27-35.

Van Lanen, J. M. and M. B. Smith (1968). Process of producing glucamylase and an alcohol product, Google Patents.

Velasco-Muñoz, J. F., J. A. Aznar-Sánchez, B. López-Felices and I. M. Román-Sánchez (2022). "Circular economy in agriculture. An analysis of the state of research based on the life cycle." Sustainable Production and Consumption.

Vesth, T. C., J. L. Nybo, S. Theobald, J. C. Frisvad, T. O. Larsen, K. F. Nielsen, J. B. Hoof, J. Brandl, A. Salamov and R. Riley (2018). "Investigation of inter-and intraspecies variation through genome sequencing of Aspergillus section Nigri." Nature Genetics **50**(12): 1688-1695.

Vishniac, W. and M. Santer (1957). "The thiobacilli." Bacteriological reviews **21**(3): 195-213.

Wang, X., Z. Li, L. Policarpio, M. A. Koffas and H. Zhang (2020). "De novo biosynthesis of complex natural product sakuranetin using modular co-culture engineering." Applied microbiology and biotechnology **104**(11): 4849-4861.

Wang, Y., E. Fuchs, R. da Silva, A. McDaniel, J. Seibel and C. Ford (2006). "Improvement of Aspergillus niger glucoamylase thermostability by directed evolution." Starch-Stärke **58**(10): 501-508.

Watanabe, K. (2001). "Microorganisms relevant to bioremediation." Current Opinion in Biotechnology **12**(3): 237-241.

Weuster-Botz, D. and R. Takors (2018). Wachstumskinetik, in: Bioprozesstechnik, Springer**:** 45-70.

Wong, K., L. Tan and J. N. Saddler (1988). "Multiplicity of beta-1, 4-xylanase in microorganisms: functions and applications." Microbiological reviews **52**(3): 305-317.

Wood, T. M. and K. M. Bhat (1988). Methods for measuring cellulase activities, in: Methods in enzymology, Elsevier. **160:** 87-112.

Woodley, J. M. (2020). "Towards the sustainable production of bulk-chemicals using biotechnology." New biotechnology **59**: 59-64.

Woodward, J. and S. L. Arnold (1981). "The inhibition of β-glucosidase activity in Trichoderma reesei C30 cellulase by derivatives and isomers of glucose." Biotechnology and bioengineering **23**(7): 1553-1562.

Wu, P., G. Wang, G. Wang, B. T. Børresen, H. Liu and J. Zhang (2016). "Butanol production under microaerobic conditions with a symbiotic system of Clostridium acetobutylicum and Bacillus cereus." Microbial cell factories **15**(1): 1-11.

Wucherpfennig, T., T. Hestler and R. Krull (2011). "Morphology engineering-osmolality and its effect on Aspergillus niger morphology and productivity." Microbial cell factories **10**(1): 1-15.

Xie, X. S., S. W. Cui, W. Li and R. Tsao (2008). "Isolation and characterization of wheat bran starch." Food Research International **41**(9): 882-887.

Xu, Y., L. Shan, Y. Zhou, Z. Xie, A. S. Ball, W. Cao and H. Liu (2019). "Development of a Cre-lox P-based genetic system in Aspergillus niger ATCC1015 and its application to construction of efficient organic acid-producing cell factories." Applied microbiology and biotechnology **103**: 8105-8114.

Yaashikaa, P., P. S. Kumar and S. Varjani (2022). "Valorization of agro-industrial wastes for biorefinery process and circular bioeconomy: A critical review." Bioresource Technology **343**: 126126.

Yanagita, T. (1957). "Biochemical aspects on the germination of conidiospores of Aspergillus niger." Archiv für Mikrobiologie **26**: 329-344.

Zhang, B., X. Xu and L. Zhu (2017). "Structure and function of the microbial consortia of activated sludge in typical municipal wastewater treatment plants in winter." Scientific Reports **7**(1): 17930.

Zhang, L., L. Chen, J. Diao, X. Song, M. Shi and W. Zhang (2020). "Construction and analysis of an artificial consortium based on the fast-growing cyanobacterium Synechococcus elongatus UTEX 2973 to produce the platform chemical 3-hydroxypropionic acid from CO 2." Biotechnology for biofuels **13**(1): 1-14.

Zhao, C., L. Deng and H. Fang (2018). "Mixed culture of recombinant Trichoderma reesei and Aspergillus niger for cellulase production to increase the cellulose degrading capability." Biomass and Bioenergy **112**: 93-98.

Zhou, K., K. Qiao, S. Edgar and G. Stephanopoulos (2015). "Distributing a metabolic pathway among a microbial consortium enhances production of natural products." Nature biotechnology **33**(4): 377-383.

Zhou, Z., D. Liu and X. Zhao (2021). "Conversion of lignocellulose to biofuels and chemicals via sugar platform: An updated review on chemistry and mechanisms of acid hydrolysis of lignocellulose." Renewable and Sustainable Energy Reviews **146**: 111169.

Zoglowek, M., G. H. Hansen, P. S. Lübeck and M. Lübeck (2016). "Fungal consortia for conversion of lignocellulose into bioproducts." Fungal Biotechnology for Biofuel Production: 329-365.

Zuroff, T. R., S. B. Xiques and W. R. Curtis (2013). "Consortia-mediated bioprocessing of cellulose to ethanol with a symbiotic Clostridium phytofermentans/yeast co-culture." Biotechnology for biofuels **6**(1): 1-12.

10. Supplemental material

10.1. Hydrolysis of wheat bran with enzymes from different *A. niger* strains

The enzyme supernatants from the six strains of *A. niger* cultivated in shaking flasks with either xylan or starch (Chapter 5.1) were used in initial hydrolysis experiments. These experiments were conducted on the 40 mL scale as described in Chapter 4.4.1. It must be noted that commercially purchased wheat bran (Spielberger GmbH, Brackenheim, Germany) was used instead of the bran provided by the project partner. Sugar concentrations were determined from samples after 163 h process time and are displayed in Figure 10.1.

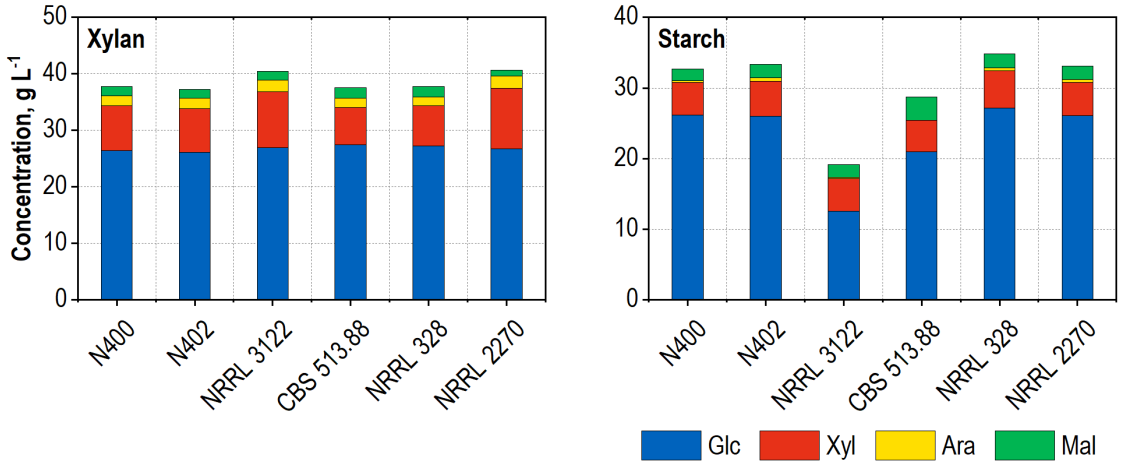

Figure 10.1: Sugar concentrations released from 100 g L^{-1} commercial wheat bran (Spielberger GmbH, Brackenheim, Germany) using enzymes from different *A. niger* strains cultivated with xylan (left) or starch (right) as carbon source in shaking flasks. Hydrolysis was performed on a 40 mL scale in glass bottles (30 °C, pH 4.5). The wheat bran was sterilized in a dry state at 121 °C for 20 min before a mixture of 10% (v/v) enzyme solution and 90% (v/v) 100 mM sodium acetate buffer (pH 4.5) were added. Glc: glucose, Xyl: xylose, Ara: arabinose, Mal: maltose.

The hydrolysates from enzymes produced with xylan as carbon source showed only little differences in their composition. Released sugar concentrations ranging from 37.2-40.6 g L^{-1} were quantified (highest with *A. niger* NRRL 3122 and *A. niger* NRRL 2270), with shares of 66-73% glucose, 18-26% xylose and 4.2-5.9% arabinose.

More significant differences in the hydrolysates were detected when using enzymes produced with starch. More than 32 g L^{-1} sugars were measured in all batches except with the strains originally described as good enzyme producers, *A. niger* NRRL 3122 (19.1 g L^{-1}) and CBS 513.88 (28.6 g L^{-1}). Enzymes produced with starch released noticeably smaller shares of the hemicellulosic sugars xylose and arabinose, but higher concentrations of the glucose dimer maltose.

Discussion

The results from enzymes produced with xylan had only marginal differences regarding hydrolytic performance and hydrolysate composition (relative difference of 8% between highest and lowest total sugar concentration). The major sugar share in the hydrolysate was glucose, followed by xylose. Surprisingly, only a small amount of arabinose was released despite the high content in the bran's hemicellulosic fraction (see Chapter 3.3.2). Potential causes could lie in a lack of induction of arabinofuranosidase secretion or in a competitive product inhibition of the respective enzyme (Tagawa and Kaji, 1988). The accumulation of glucose and maltose during hydrolysis with xylan-based enzymes indicates the formation of amylases by *A. niger* in the absence of starch.

The enzymes of two strains, *A. niger* NRRL 3122 and *A. niger* CBS 513.88, released significantly lower sugar concentrations than the others, despite being described as good enzyme producers in literature (Van Lanen and Smith, 1968, Pel et al., 2007). In case of *A. niger* NRRL 3122, the low yield was probably caused by the low protein concentration secreted by this strain using starch as carbon source. *A. niger* CBS 513.88 only showed little growth with starch and consequently secreted less amylolytic enzymes compared to other strains. Significantly lower xylose and arabinose concentrations were released with the starch-based enzymes, pointing at lower xylanase activities. On the one hand, this indicates that xylanase formation must be induced by xylan, xylo-oligomers or xylose (Mach-Aigner et al., 2012, Amorim et al., 2019), on the other hand, the expression of genes linked with xylan degradation are reported to be carbon catabolite-repressed in the presence of glucose (de Vries et al., 1999).

10.2. Secretome analysis of mono- and co-culture samples via SDS-PAGE

Conclusions regarding strain dominance in co-cultures (see Chapter 5.2.1) were based on the results of SDS-PAGE secretome analysis. Relevant samples from experiments described in Chapter 5.2.1 are displayed in Figure 10.2.

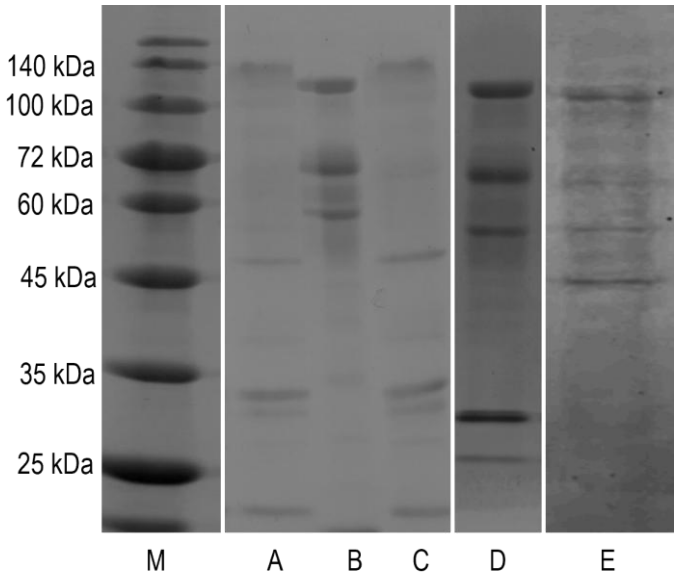

Figure 10.2: Protein band patterns after SDS-PAGE analysis (12.5% polyacrylamide gel, 35 mA, 60 min) of mono- and co-cultures of *A. niger* NRRL 2270 and *T. reesei* RUT-C30 cultivated in 0.7 L bioreactors using synthetic wheat bran medium. M: marker (JustBlue protein ladder, NIPPON Genetics Europe); A: *A. niger* NRRL 2270 monoculture; B: *T. reesei* RUT-C30 monoculture; C-E: Co-cultures of *A. niger* NRRL 2270 and *T. reesei* RUT-C30 (initial spore concentrations *A. niger* 10^9 spores L^{-1}, *T. reesei* 0.2×10^9 spores L^{-1}). Spores of *A. niger* were added simultaneously (C), 24 h after *T. reesei* spores (D) or 16.5 h after *T. reesei* spores (E). Samples were taken at the end of the cultivation processes.

The lines A and B show the specific band pattern of *A. niger* NRRL 2270 and *T. reesei* RUT-C30, respectively, in a monoculture. Strong dominance of *A. niger* was assumed in a simultaneously inoculated co-culture (line C), confirmed by an identical protein band pattern as the *A. niger* monoculture. Line D, from a co-culture with 24 h delay of *A. niger* spore addition, demonstrates high similarity with the *T. reesei* monoculture pattern, indicating dominance of *T. reesei*. The pattern in line E also resembles line B (*T. reesei* monoculture), however an *A. niger*-specific band at ~45 kDa is clearly visible. It was therefore concluded that both strains were able to secrete their respective enzymes, which stands in accordance with other results of this experiment (CER profile, enzyme activities).

10.3. HPLC results during variation of inoculation times

Figure 10.3 shows the concentrations of relevant sugars in supernatant samples of a co-culture of *A. niger* NRRL 2270 and *T. reesei* RUT-C30 during the investigations of suitable initial spore concentrations and delayed inoculation. In this case, *A. niger* spores were added 24 h after inoculation with *T. reesei*. It is visible that small amounts of glucose are present in the medium until 67 h process time, indicating that a glucose limitation was probably not the cause of the reduced growth and enzyme production of *A. niger*

(see Chapter 5.2.1). The increase of glucose concentration between 40-48 h process time additionally points to the availability of polysaccharidic substrates at the time.

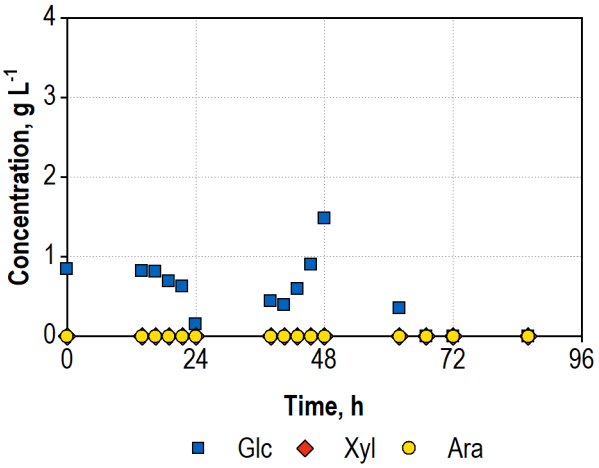

Figure 10.3: Sugar concentrations in a co-culture of *A. niger* NRRL 2270 and *T. reesei* RUT-C30 in a bioreactor on a 0.7 L scale using synthetic wheat bran medium. *T. reesei* RUT-C30 was inoculated with an initial spore concentration of 0.2 × 10^9 spores L^{-1}. *A. niger* NRRL 2270 was added after 24 h with an initial spore concentration of 10^9 spores L^{-1} (agitation rate 600 min^{-1}, aeration rate 0.2-2 vvm, temperature 30 °C, pH 4.5).

10.4. Utilization of wheat bran hydrolysate for lipid production

The utilization of wheat bran hydrolysate should be demonstrated exemplarily with the cultivation of the oleaginous yeast *Cutaneotrichosporon oleaginosus* for the production of microbial lipids.

10.4.1. Initial growth experiments with *C. oleaginosus*

Initial cultivation experiments were conducted in the 3 L reactor to prove the ability of *C. oleaginosus* to grow with wheat bran hydrolysate as carbon source. Lipid formation in this microorganism can be induced by a limitation of nitrogen, phosphorus or sulfur with simultaneous carbon excess (Meo et al., 2017). As a nitrogen elimination appears not feasible in a biomass hydrolysate, it was attempted to remove the phosphorus by precipitation with iron(III) chloride in a stoichiometric ratio of 1:1. The composition of the minimal medium was adapted from literature (Masri et al., 2019). Either sterile-filtration (0.2 µm) or autoclaving (121 °C for 20 min) was applied for sterilization of the hydrolysate. The courses of CER and biomass concentration for the cultivation with sterile-filtered hydrolysate are shown in Figure 10.4.

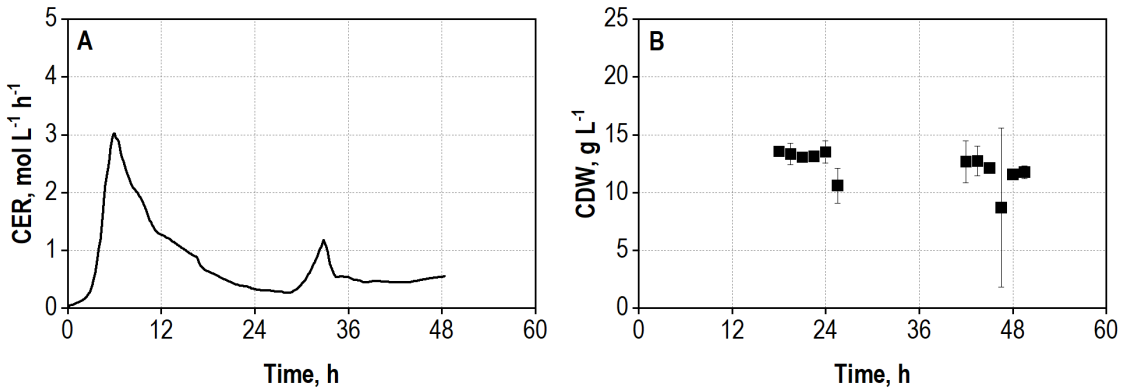

Figure 10.4: A: Carbon dioxide evolution rate (CER), and B: cell dry weight concentration (CDW) during batch cultivation of *C. oleaginosus* in a 3.0 L bioreactor using $FeCl_3$-pretreated and sterile-filtered wheat bran hydrolysate as carbon source in minimal medium.

The growth of *C. oleaginosus* commenced almost instantly after inoculation and reached the maximum metabolic activity already after approx. 6 h. As this rapid growth came unexpectedly at night, no samples for biomass quantification were taken. The cell dry weight concentration was first measured after 18 h and remained nearly constant at approx. 12-14 g L^{-1} throughout the process.

The effect of thermal sterilization of the hydrolysate instead of sterile filtration was investigated in an otherwise identical cultivation. The hydrolysate composition was analyzed via HPLC after autoclaving and did not show any significant changes regarding the carbohydrates, while some unidentified peaks became visible. The cultivation data for CER and biomass are displayed in Figure 10.5.

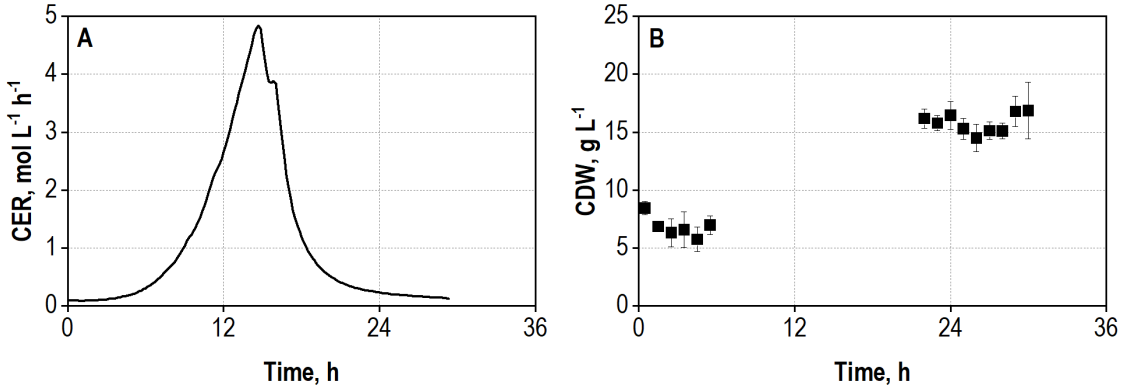

Figure 10.5: A: Carbon dioxide evolution rate (CER), and B: cell dry weight concentration (CDW) during batch cultivation of *C. oleaginosus* in a 3.0 L bioreactor using $FeCl_3$-pretreated and thermally sterilized wheat bran hydrolysate as carbon source in minimal medium.

Cell growth appeared to be time-delayed compared to the process above, with a shift of the CER maximum to 15 h process time. However, the maximum respiration was higher than with filtrated hydrolysate, and an increased biomass concentration was measured

(16.9 ± 2.4 g L^{-1} after 30 h). This result showed that the thermal treatment of the hydrolysate did at least not have any detrimental effects for the growth of *C. oleaginosus*.

Overall, it was demonstrated that wheat bran hydrolysate is a suitable growth medium for the oleaginous yeast *C. oleaginosus*. Nevertheless, no lipid formation could be observed, indicating that the phosphate limitation was not sufficient.

10.4.2. Elimination of free phosphate

As mentioned above, lipid formation was not feasible so far due to high remaining phosphate concentrations in the wheat bran hydrolysate. The pretreatment with $FeCl_3$ with a stoichiometric ratio of Fe:P of 1:1 only removed a minor part of the phosphate ions (reduction of 5-7% (w/v), measured by a colorimetric assay). Consequently, different approaches to improve the precipitation were tested, including higher stoichiometric Fe:P ratios, direct addition of $FeCl_3$ salt for even higher iron concentration, or repeated cycles of precipitation and separation by filtration. In case of repeated cycles, the remaining phosphate concentration was determined after each step, and the added volume of 0.5 M $FeCl_3$ was adapted accordingly. The results of these experiments are summed up in Table 10.1.

Table 10.1: Approaches for phosphate removal from wheat bran hydrolysate and respective results. A 0.5 M $FeCl_3$ solution was prepared, and the according volume was added, 200 mM $FeCl_3$ was added as salt. The batches were titrated to pH 5.5 and incubated for 30 min before precipitated phosphate was separated via centrifugation and filtration. The phosphate concentration before and after treatment was determined colorimetrically.

Method	Fe:P	Removal, %	Remaining P, mM
10% (v/v) 0.5 M $FeCl_3$	1:1	7.7	43.7
20% (v/v) 0.5 M $FeCl_3$	2:1	11.8	41.7
30% (v/v) 0.5 M $FeCl_3$	3:1	59.7	19.1
3 cycles w/ 0.5 M $FeCl_3$	2:1 each	69.8	14.3
3 cycles w/ 0.5 M $FeCl_3$	3:1 each	77.7	10.6
200 mM $FeCl_3$ (salt)	4:1	14.9	40.3

The highest elimination of phosphate was achieved by three repeated cycles of precipitation with a Fe:P ratio of 3:1, incubation and separation, which reduced the contained phosphate by ~78%, corresponding to a remaining concentration of ca. 10 mM. Experimental data from previous projects suggested a C:P ratio of 3000-4000 in the medium as sufficient for lipid accumulation. The results presented here only account for a C:P ratio of 100-120, meaning the mark was missed by far. The original substrate

wheat bran was identified as the main source of the phosphate, resulting in 4 g L^{-1} in the hydrolysate. An additional 1 g L^{-1} was added by the enzyme solution.

10.4.3. Lipid production using acetic acid as titration agent

The induction of lipid formation by nutrient limitation was not successful due to the high nitrogen and phosphate concentrations in the hydrolysate. An alternative approach to achieve lipid accumulation in *C. oleaginosus* described in literature is the usage of acetate as co-substrate (Masri et al., 2019). In this study, acetic acid was applied as a titration agent to ensure a continuous and balanced presence of excess acetate in the medium.

As a first step, a batch process with wheat bran hydrolysate, supplemented with 4.1 g L^{-1} sodium acetate, as carbon source should provide data regarding the uptake rates of the sugars and the potential for lipid production. Figure 10.6 displays the results for substrate consumption as well as biomass and product formation.

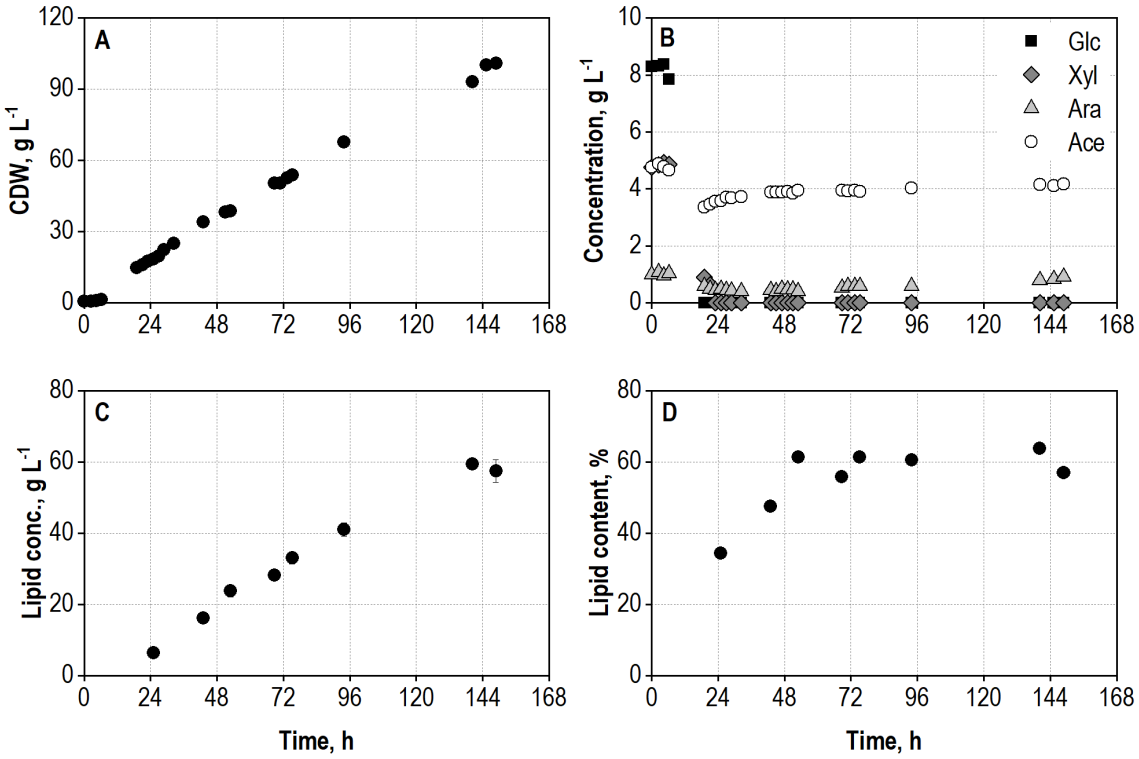

Figure 10.6: A: Biomass concentration, B: Concentrations of glucose (Glc), xylose (Xyl), arabinose (Ara) and acetate (Ace), C: Lipid concentration and D: Lipid content during batch cultivation of *C. oleaginosus* in a 3 L bioreactor using minimal medium with wheat bran hydrolysate + 4.1 g L^{-1} sodium acetate. Acetic acid (100%) was used as a titration agent.

All sugars in the hydrolysate (mainly glucose and xylose) were depleted after max. 24 h process time, glucose already after 10 h. At this point in the process, a biomass concentration of 18 g L^{-1} with a lipid content of 34% was achieved. Subsequently growth

continued using acetate as substrate, and reached a total biomass concentration of 100.8 g L^{-1} after 148 h. The lipid content increased to 60% during the first 48 h and remained nearly constant afterwards. As the hydrolysate's carbohydrates were depleted at an earlier point, biomass and lipid formation was mainly based on acetate. The automated addition of acetic acid for pH control commenced after the depletion of the sugars and kept an almost constant acetate concentration of 4 g L^{-1} in the medium throughout the process.

One of the goals of the batch process was to investigate the uptake rates of the main sugars glucose and xylose. The glucose uptake rate could only be estimated roughly at 2 g L^{-1} h^{-1}, as the exact moment of total depletion is unknown. The maximum xylose uptake rate was calculated at 0.32 g L^{-1} h^{-1}. The feed rate for the fed-batch process was set based on these data.

The fed-batch process was conceived with the longest run time possible, which could be achieved by the application of a constant feed rate. The process was started with an initial volume of 1 L, containing 0.75 L hydrolysate with 4.1 g L^{-1} sodium acetate and 0.25 L of nitrogen source and salts. The feed rate was set to 60 g h^{-1} hydrolysate, corresponding to 0.3 g L^{-1} h^{-1} xylose to avoid its accumulation. The fermentation was terminated after 50 h when the complete 3 L hydrolysate were fed into the reactor. The data for biomass, sugar and lipid concentration as well as the intracellular lipid content are shown in Figure 10.7.

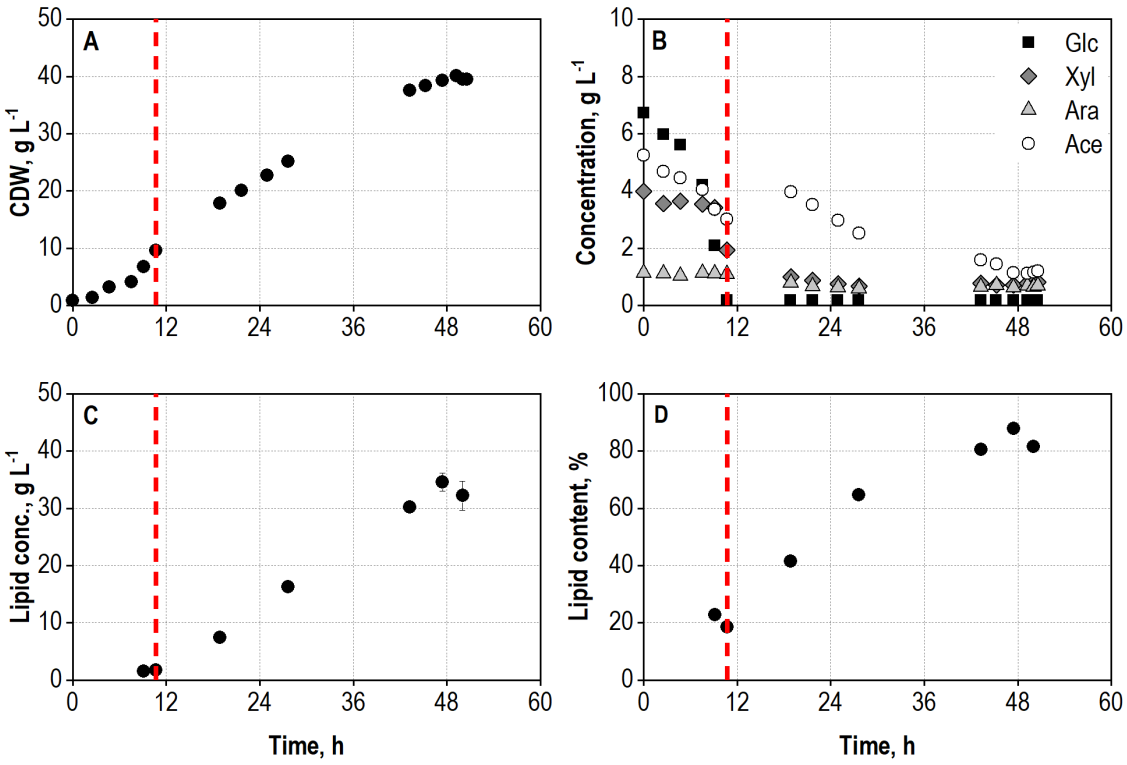

Figure 10.7: A: Biomass concentration, B: Concentrations of glucose (Glc), xylose (Xyl), arabinose (Ara) and acetate (Ace), C: Lipid concentration, and D: Lipid content during fed-batch cultivation of *C. oleaginosus* in a 3 L bioreactor using minimal medium with wheat bran hydrolysate + 4.1 g L^{-1} sodium acetate. Wheat bran hydrolysate was fed at a constant rate, and acetic acid (100%) was used as titration agent. The dashed line marks the start of the feed phase.

Cell growth commenced immediately after inoculation and showed an exponential course within the first 10.7 h until the end of the batch phase. The feed was started manually after 11 h, as HPLC analysis confirmed the complete depletion of glucose at this point. The addition of acetic acid for pH control started at the same time. Both hydrolysate and acid addition were traced gravimetrically and had a similar linear profile over the process (see Figure 10.8). Growth appeared to be limited during the feed phase and reached a maximum biomass concentration of 40 g L^{-1}. Lipid accumulation started with the beginning of the feed phase and acid addition. At the end of the process, a maximum lipid concentration of 34.6 g L^{-1}, corresponding to a lipid content of > 80% could be detected. Until the end of the process an overall mass of 33 g sugars and 338 g acetate were added. A preliminary carbon balance showed that 1.6 mol carbon came from sugars, and 11.2 mol from acetate, hence 87.5% of the carbon stemmed from acetic acid.

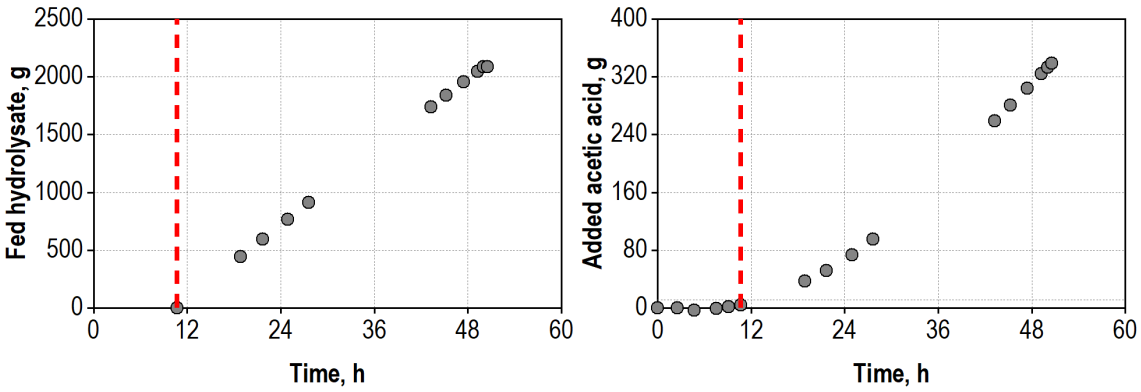

Figure 10.8: Left: Mass of hydrolysate fed into the reactor, and Right: Mass of acetic acid added for titration during fed-batch cultivation of *C. oleaginosus* in a 3 L bioreactor using minimal medium with wheat bran hydrolysate + 4.1 g L^{-1} sodium acetate. Wheat bran hydrolysate was fed at a constant rate, and acetic acid (100%) was used as titration agent. The dashed line marks the start of the feed phase.

10.5. Data tables

10.5.1. Influence of agitation and aeration rate (Figure 5.13)

Table 10.2: Total protein concentrations, mg L^{-1}, in the supernatant of co-cultures of *A. niger* NRRL 2270 and *T. reesei* RUT-C30 after 86 h process time in a 0.7 L bioreactor with synthetic wheat bran medium and varying agitation and aeration rates. *T. reesei* RUT-C30 was inoculated with an initial spore concentration of 0.2 × 10^9 spores L^{-1}, *A. niger* NRRL 2270 was added after 16.5 h process time with an initial spore concentration of 10^9 spores L^{-1} (temperature 30 °C, pH 4.5). Data are graphically displayed in Figure 5.12.

Agitation/aeration	0.1-1 vvm	0.2-2 vvm	0.3-3 vvm
400 min^{-1}		399.9	469.7
600 min^{-1}	201.3	393.0	412.9
800 min^{-1}	331.0	546.1	520.7
1000 min^{-1}	251.4	350.5	

Table 10.3: Xylanase activity, U mL^{-1}, in the supernatant of co-cultures of *A. niger* NRRL 2270 and *T. reesei* RUT-C30 after 86 h process time in a 0.7 L bioreactor with synthetic wheat bran medium and varying agitation and aeration rates. *T. reesei* RUT-C30 was inoculated with an initial spore concentration of 0.2 × 10^9 spores L^{-1}, *A. niger* NRRL 2270 was added after 16.5 h process time with an initial spore concentration of 10^9 spores L^{-1} (temperature 30 °C, pH 4.5). One unit (U) was defined as the amount of enzymatic activity releasing 1 µmol of xylose equivalents per minute under assay conditions (50 °C, pH 4.5). Data are graphically displayed in Figure 5.12.

Agitation\aeration	0.1-1 vvm	0.2-2 vvm	0.3-3 vvm
400 min^{-1}		42.1	35.2
600 min^{-1}	15.9	23.1	21.2
800 min^{-1}	21.6	42.5	36.8
1000 min^{-1}	17.1	20.2	

Table 10.4: Amylase activity, U mL^{-1}, in the supernatant of co-cultures of *A. niger* NRRL 2270 and *T. reesei* RUT-C30 after 86 h process time in a 0.7 L bioreactor with synthetic wheat bran medium and varying agitation and aeration rates. *T. reesei* RUT-C30 was inoculated with an initial spore concentration of 0.2 × 10^9 spores L^{-1}, *A. niger* NRRL 2270 was added after 16.5 h process time with an initial spore concentration of 10^9 spores L^{-1} (temperature 30 °C, pH 4.5). One unit (U) was defined as the amount of enzymatic activity releasing 1 µmol of glucose equivalents per minute under assay conditions (50 °C, pH 4.5). Data are graphically displayed in Figure 5.12.

Agitation\aeration	0.1-1 vvm	0.2-2 vvm	0.3-3 vvm
400 min^{-1}		1.68	3.38
600 min^{-1}	8.10	9.05	6.85
800 min^{-1}	11.75	10.43	5.48
1000 min^{-1}	11.15	9.79	

Table 10.5: Cellulase activity, U mL^{-1}, in the supernatant of co-cultures of *A. niger* NRRL 2270 and *T. reesei* RUT-C30 after 86 h process time in a 0.7 L bioreactor with synthetic wheat bran medium and varying agitation and aeration rates. *T. reesei* RUT-C30 was inoculated with an initial spore concentration of 0.2 × 10^9 spores L^{-1}, *A. niger* NRRL 2270 was added after 16.5 h process time with an initial spore concentration of 10^9 spores L^{-1} (temperature 30 °C, pH 4.5). One unit (U) was defined as the amount of enzymatic activity releasing 1 µmol of glucose equivalents per minute under assay conditions (50 °C, pH 4.5). Data are graphically displayed in Figure 5.12.

Agitation\aeration	0.1-1 vvm	0.2-2 vvm	0.3-3 vvm
400 min^{-1}		1.85	2.30
600 min^{-1}	1.09	1.12	1.22
800 min^{-1}	1.63	2.70	1.58
1000 min^{-1}	1.03	1.23	

10.5.2. Characterization of co-culture enzyme solution (Figure 6.1)

Table 10.6: Xylanase activities at varying temperatures and pH of the enzyme solution at varying temperatures and pH produced by a co-culture of *A. niger* NRRL 2270 and *T. reesei* RUT-C30. One unit (U) was defined as the amount of enzymatic activity releasing 1 µmol of xylose equivalents per minute under assay conditions (50 °C, pH 4.5, reaction time 50 min). Data are graphically displayed in Figure 6.1.

T \ pH	pH 3.0	pH 3.5	pH 4.0	pH 4.5	pH 5.0	pH 5.5	pH 6.0	pH 7.0
20 °C	4.52	1.79	1.43	2.24	1.99	1.54	1.80	1.63
30 °C	7.28	9.79	13.47	13.93	12.13	11.20	9.09	5.91
40 °C	5.30	5.93	7.76	8.55	8.16	8.03	5.10	5.39
50 °C	10.86	14.02	18.46	17.04	16.09	15.95	14.96	10.48
60 °C	9.53	15.99	19.91	24.65	20.77	18.36	13.54	1.52
70 °C	1.06	1.06	2.38	3.24	1.97	2.57	1.14	2.71

Table 10.7: Amylase activities at varying temperatures and pH of the enzyme solution at varying temperatures and pH produced by a co-culture of *A. niger* NRRL 2270 and *T. reesei* RUT-C30. One unit (U) was defined as the amount of enzymatic activity releasing 1 µmol of glucose equivalents per minute under assay conditions (50 °C, pH 4.5, reaction time 30 min). Data are graphically displayed in Figure 6.1.

T \ pH	pH 3.0	pH 3.5	pH 4.0	pH 4.5	pH 5.0	pH 5.5	pH 6.0	pH 7.0
20 °C	0.28	0.14	0.14	0.16	0.16	0.27	0.22	0.08
30 °C	0.59	0.64	0.64	0.64	0.62	0.54	0.71	0.25
40 °C	1.04	1.04	1.05	1.05	0.99	0.65	0.69	0.26
50 °C	2.20	2.30	2.28	2.16	2.09	1.70	1.19	0.52
60 °C	2.75	2.80	2.80	2.78	2.86	2.39	1.65	0.60
70 °C	1.27	2.07	2.59	2.57	1.59	0.32	0.03	0.01

Table 10.8: Cellulase activities at varying temperatures and pH of the enzyme solution at varying temperatures and pH produced by a co-culture of *A. niger* NRRL 2270 and *T. reesei* RUT-C30. One unit (U) was defined as the amount of enzymatic activity releasing 1 µmol of glucose equivalents per minute under assay conditions (50 °C, pH 4.5, reaction time 30 min). Data are graphically displayed in Figure 6.1.

T \ pH	pH 3.0	pH 3.5	pH 4.0	pH 4.5	pH 5.0	pH 5.5	pH 6.0	pH 7.0
20 °C	0.48	0.25	0.30	0.45	0.42	0.48	0.20	0.20
30 °C	0.72	0.84	1.11	1.21	1.36	1.19	1.06	0.54
40 °C	0.99	1.14	1.25	1.41	1.33	1.22	1.09	0.54
50 °C	1.59	2.08	2.22	1.92	1.83	1.29	0.84	0.02
60 °C	1.59	1.62	1.47	1.57	1.30	0.96	0.50	0.10
70 °C	1.26	1.28	1.32	1.15	1.00	0.43	0.13	0.00

10.6. List of abbreviations and symbols

Table 10.9: List of abbreviations

Abbreviation	Meaning
ABE	Acetone – butanol – ethanol fermentation
Ace	Acetate
Ara	Arabinose
A. niger	*Aspergillus niger*
BSA	Bovine serum albumin
CBH	Cellobiohydrolases
CDW	Cell dry weight concentration
Cel	Cellobiose
CER	Carbon dioxide evolution rate
CFD	Computational fluid dynamics
CMC	Carboxymethyl cellulose
CO_2	Carbon dioxide
C. carboxidivorans	*Clostridium carboxidivorans*
C. cellulolyticum	*Clostridium cellulolyticum*
C. kluyveri	*Clostridium kluyveri*
C. oleaginosus	*Cutaneotrichosporon oleaginosus*
C. phytofermentans	*Clostridium phytofermentans*
C. thermocellum	*Clostridium thermocellum*
ddH_2O	Double-deionized water
DNA	Desoxyribonucleic acid
DO	Dissolved oxygen concentration
E. coli	*Escherichia coli*
FDA	US Food and Drug Administration
FISH	Fluorescence in situ hybridization
Glc	Glucose
GRAS	Generally Regarded As Safe
HPLC	High-performance liquid chromatography
k_La	Volumetric oxygen transfer coefficient
LfL	Bayerische Landesanstalt für Landwirtschaft (Bavarian State Institution for Agriculture)
LPMO	Lytic polysaccharide monooxygenases
Mal	Maltose
NaAc	Sodium acetate
NADH	Nicotinamide adenine dinucleotide

Native-PAGE	Native polyacrylamide gel electrophoresis
O_2	Oxygen
OD_{600}	Optical density at 600 nm
OTR	Oxygen transfer rate
OUR	Oxygen uptake rate
PCR	Polymerase chain reaction
pHBAH	4-hydroxybenzhydrazide
PPG	Polypropylene glycol
qPCR	Quantitative polymerase chain reaction
RI	Refractive index (detector)
RNA	Ribonucleic acid
RQ	Respirational quotient
SDS-PAGE	Sodium dodecylsulfate polyacrylamide gel electrophoresis
S. cerevisiae	*Saccharomyces cerevisiae*
TUM	Technical University of Munich
T. reesei	*Trichoderma reesei*
UV	Ultraviolet (radiation)
vvm	Vessel volumes per minute
WSSB	Werner Siemens Chair for Synthetic Biotechnology
Xyl	Xylose

Table 10.10: List of symbols

Symbol	Meaning	Unit
A	Exchange surface	m^2
CER	Carbon dioxide evolution rate	mol L^{-1} h^{-1}
c_i	Concentration of component i	g L^{-1}
$c_{i,in}$	Concentration of component i flowing into the reaction	g L^{-1}
$c_{O_2,L}$	Oxygen concentration in the bulk phase	mol L^{-1}
$c^*_{O_2,L}$	Oxygen equilibrium concentration in the boundary layer	mol L^{-1}
c_S	Substrate concentration	g L^{-1}
c_X	Biomass concentration	g L^{-1}
d_i	Diameter of stirrer i	cm
$d_{Reactor}$	Inner diameter of the respective reactor	cm

$d_{Stirrer}$	Diameter of the Rushton turbines in the respective reactor	cm
g	Acceleration of gravity (9.81 m s^{-1})	m s^{-1}
H_{Liquid}	Liquid height in the reactor	m
k_i	Rate constants for morphogenesis reaction i	h^{-1}
k_L	Mass transfer coefficient	m h^{-1}
$k_L a$	Specific oxygen transfer coefficient	h^{-1}
K_S	Half-velocity constant, with $\mu = 0.5\ \mu_{max}$	g L^{-1}
m_i	Mass of component i	g
μ	Growth rate	h^{-1}
μ_A, μ_S	Growth rate of apical (A) and subapical (S) compartments	h^{-1}
μ_{max}	Maximum growth rate	h^{-1}
n_i	Agitation rate of stirrer i	min^{-1}
$\dot{n}_{O_2,L}$	Molar oxygen current across the interface	mol h^{-1}
OTR	Oxygen transfer rate	mol L^{-1} h^{-1}
OUR	Oxygen uptake rate	mol L^{-1} h^{-1}
p	Pressure	bar
q_P	Specific product formation rate	g g^{-1} h^{-1}
q_S	Specific substrate uptake rate	g g^{-1} h^{-1}
R	Ideal gas constant (8.314 J mol^{-1} K^{-1})	J mol^{-1} K^{-1}
r_i	Reaction rate of component i	g L^{-1} h^{-1}
RQ	Respirational quotient	-
T	Temperature	K
t	Time	h
V	Reaction volume	L
V_L	Liquid volume	L
V_m	Molar volume of an ideal gas (22.4 L mol^{-1})	L mol^{-1}
$\dot{V}_g$	Gas flow rate/aeration rate	L h^{-1}
$\dot{V}_{in}$	Flow rate into the reaction	L h^{-1}
$\dot{V}_{out}$	Flow rate out of the reaction	L h^{-1}
x_{CO_2}	Carbon dioxide concentration	%
x_{O_2}	Oxygen concentration	%
z_A, z_S, z_H	Mass fractions of apical (A), subapical (S) and hyphal (H) compartments	-

10.7. List of chemicals, consumables and devices

Table 10.11: List of chemicals

Compound	Chemical formula or abbreviation	Manufacturer
4-hydroxybenzhydrazide	pHBAH	Merck, Darmstadt, D
Acetic acid, 100%	-	neoFroxx, Einhausen, D
Acrylamide/bisacrylamide, 40%	-	Carl Roth, Karlsruhe, D
Ammonium heptamolybdate tetrahydrate	$(NH_4)_6Mo_7O_{24} \cdot 4\ H_2O$	Carl Roth, Karlsruhe, D
Ammonium persulfate	APS	Merck, Darmstadt, D
Ammonium sulfate	$(NH_4)_2SO_4$	Carl Roth, Karlsruhe, D Domo Chemicals, Leuna, D
Avicel (microcrystalline cellulose)	-	Merck, Darmstadt, D
β-mercaptoethanol	-	Carl Roth, Karlsruhe, D
Bovine serum albumin	BSA	Thermo Fisher, Waltham, USA
Bromophenol blue	-	Carl Roth, Karlsruhe, D
Calcium chloride dihydrate	$CaCl_2 \cdot 2\ H_2O$	Carl Roth, Karlsruhe, D
Carboxymethyl cellulose, sodium salt, low viscosity	CMC	Merck, Darmstadt, D
Cellobiose	-	Merck, Darmstadt, D
Cobalt chloride hexahydrate	$CoCl_2 \cdot 6\ H_2O$	Carl Roth, Karlsruhe, D
Coomassie Plus (Bradford) Assay Kit	-	Thermo Fisher, Waltham, USA
Copper sulfate pentahydrate	$CuSO_4 \cdot 5\ H_2O$	Carl Roth, Karlsruhe, D
Ethylenediaminetetraacetic acid dihydrate	$EDTA \cdot 2\ H_2O$	Carl Roth, Karlsruhe, D
Glucose monohydrate	-	Carl Roth, Karlsruhe, D
Glycerol, 100%	-	CLN, Langenbach, D
Hydrochloric acid, 37%	HCl	Carl Roth, Karlsruhe, D
Immersion oil for microscopy	-	Carl Roth, Karlsruhe, D
Iron(III) chloride hexahydrate	$FeCl_3 \cdot 6\ H_2O$	Carl Roth, Karlsruhe, D
Iron(II) sulfate heptahydrate	$FeSO_4 \cdot 7\ H_2O$	Carl Roth, Karlsruhe, D

Lactose monohydrate	-	Carl Roth, Karlsruhe, D
Magnesium sulfate heptahydrate	$MgSO_4 \cdot 7\ H_2O$	AppliChem, Darmstadt, D
Maltose monohydrate	-	Carl Roth, Karlsruhe, D
Manganese chloride tetrahydrate	$MnCl_2 \cdot 4\ H_2O$	Carl Roth, Karlsruhe, D
pH calibration buffer, pH 7.01	HI 7007	Hanna Instruments, USA
pH calibration buffer, pH 10.01	HI 7010	Hanna Instruments, USA
Polypropylene glycol P2000	PPG P2000	Merck, Darmstadt, D
Potassium acetate	KAc	Carl Roth, Karlsruhe, D
Potassium chloride	KCl	Carl Roth, Karlsruhe, D
Potassium citrate	KCit	Carl Roth, Karlsruhe, D
Potassium dihydrogen phosphate	$KH_2PO_4 \cdot 2\ H_2O$	Carl Roth, Karlsruhe, D
Potassium hydroxide	KOH	Carl Roth, Karlsruhe, D
Potato extract dextrose agar	PDA	Carl Roth, Karlsruhe, D
SDS-PAGE buffer, 10×	ROTIPHORESE®	Carl Roth, Karlsruhe, D
Sodium chloride	NaCl	Carl Roth, Karlsruhe, D
Sodium dodecylsulfate	SDS	Carl Roth, Karlsruhe, D
Sodium hydroxide	NaOH	Carl Roth, Karlsruhe, D
Starch, soluble	-	Merck, Darmstadt, D
Sulfuric acid, 96%	H_2SO_4	Merck, Darmstadt, D
Tetramethyl ethylenediamine	TEMED	Carl Roth, Karlsruhe, D
Tris (base)	-	Carl Roth, Karlsruhe, D
Tris-HCl	-	Carl Roth, Karlsruhe, D
tri-Sodium acetate dihydrate	NaAc	Carl Roth, Karlsruhe, D
tri-Sodium citrate dihydrate	NaCit	neoFroxx, Einhausen, D
Tween 80	-	Carl Roth, Karlsruhe, D
Wheat bran, commercial	-	Spielberger, Brackenheim, D
Wheat bran, project partners	-	Meyermühle, Landshut, D
Xanthan gum	-	Carl Roth, Karlsruhe, D
Xylan, birch wood	-	Carl Roth, Karlsruhe, D
Xylan, corn	-	Carl Roth, Karlsruhe, D
Xylose	-	Carl Roth, Karlsruhe, D
Yeast extract	-	Carl Roth, Karlsruhe, D
Zinc sulfate heptahydrate	$ZnSO_4 \cdot 7\ H_2O$	Merck, Darmstadt, D

Table 10.12: List of consumables

Type	Description	Manufacturer
Air filter	Acro® 50, Emflon® II membrane	PALL, Crailsheim, D
Air filter	Acro® 50, PTFE membrane	PALL, Crailsheim, D
Bottletop filter	Steritop® PES membrane, 45 mm	Merck, Darmstadt, D
Cover foil	for PCR plates, adhesive	neoLab, Heidelberg, D
Cover slip	18 × 18 mm	Carl Roth, Karlsruhe, D
Filter paper	Whatman™, grade 1, 55 mm	GE Healthcare, Solingen, D
Filter paper	Whatman™, grade 5, 55 mm	GE Healthcare, Solingen, D
HPLC vial	N11	Macherey-Nagel, Düren, D
HPLC vial cap	N11	Macherey-Nagel, Düren, D
Microtiter plate	96-well, PP, flat-bottom, clear	Sarstedt, Nümbrecht, D
Needle	STERICAN® 0.80 × 120 mm	Braun, Melsungen, D
Needle	STERICAN® 0.90 × 70 mm	Braun, Melsungen, D
Object slide	Menzel Gläser	Thermo Fisher Inc., Waltham, USA
PCR plate	ROTILABO® 96-well	Carl Roth, Karlsruhe, D
Petri dish	-	Greiner, Frickenhausen, D
Pipette tip	2-200 µL	Brand, Wertheim, D
Pipette tip	50-1000 µL	Brand, Wertheim, D
Pipette tip	1-10 mL	Brand, Wertheim, D
Pipette filter tip	TipOne® 20 µL UltraPoint	STARLAB, Hamburg, D
Pipette filter tip	TipOne® 200 µL UltraPoint	STARLAB, Hamburg, D
Pipette filter tip	TipOne® 1000 µL XL RPT	STARLAB, Hamburg, D
Reaction tube	Safe-Lock 1.5 mL	Eppendorf, Hamburg, D
Reaction tube	Safe-Lock 2.0 mL	Eppendorf, Hamburg, D
Reaction tube	Cellstar®, 15 mL, conical base	Greiner, Frickenhausen, D
Reaction tube	Cellstar®, 50 mL, conical base	Greiner, Frickenhausen, D
Storage bag	WhirlPak® 125 × 380 mm, PE	neoLab, Heidelberg, D
Syringe	Omnifix® F Solo 1 mL	Braun, Melsungen, D
Syringe	BD Discardit™ 10 mL	Becton Dickinson, Fraga, E
Syringe	BD Discardit™ 20 mL	Becton Dickinson, Fraga, E
Syringe	BD Discardit™ 50 mL	Becton Dickinson, Fraga, E
Syringe tip filter	Chromafil® RC-20/15 MS	Macherey-Nagel, Düren, D

Table 10.13: List of lab devices

Device	Description	Manufacturer
Analytical scale	Explorer E12145	Ohaus, Gießen, D
Analytical scale	Explorer E1M213	Ohaus, Gießen, D
Analytical scale	ADB 200-4	Kern, Balingen, D
Analytical scale	XA 204	Mettler-Toledo, Columbus, USA
Autoclave	Varioklav EC Zyklondampf	H+P, Oberschleißheim, D
Autoclave	VX150	Systec, Wettenberg, D
Centrifuge	5424 R	Eppendorf, Hamburg, D
Centrifuge	5810 R	Eppendorf, Hamburg, D
Centrifuge	Rotanta 460 R	Hettich, Tuttlingen, D
Centrifuge	Rotixa 50 RS	Hettich, Tuttlingen, D
Heating block	Standard Block Heater	VWR, Darmstadt, D
Incubator	Cultura M	Almedica, Galmitz, CH
Incubator	WIS-20R	Witeg, Wertheim, D
Magnetic stirrer	D-6010	neoLab, Heidelberg, D
Magnetic stirrer	MR Hei-Standard	Heidolph, Schwabach, D
Magnetic stirrer	Variomag Mobil Telemodul 80 M 200	H+P, Oberschleißheim, D
Magnetic stirrer	Variomag Monotherm	H+P, Oberschleißheim, D
Microplate reader	Multiskan FC	Thermo Fisher, Waltham, USA
Microscope	Axioplan	Zeiss, Oberkochen, D
Microscope camera	AxioCam ICc3	Zeiss, Oberkochen, D
Microscope objectives	EC Plan-NEOFLUAR 2.5×/10×/40×	Zeiss, Oberkochen, D
Microscope software	ZEN Blue Edition	Zeiss, Oberkochen, D
pH meter	Five Easy pH/mV	Mettler Toledo, Columbus, USA
pH meter	Lab 850 + BlueLine pH 14	Schott, Mainz, D
Pipettes	Transferpette S 200 µL, 1 mL, 5 mL	Brand, Wertheim, D
Plate separator	CSA 8-06-476	GEA Westfalia, Oelde, D
Peristaltic pump	Ismatec® BVP Standard + Master® II Easy-Load®	Cole Palmer, Wertheim, D
Rheometer	Rheolab QC	Anton Paar, Graz, A

Rheometer measuring system	Measuring system (general) + Measuring Cup C-DG42/SS/QC-LTD	Anton Paar, Graz, A
Rheometer thermostat	rheotherm115	Contraves, Zurich, CH
Sterile bench	Heraeus HeraSafe KS 12	Thermo Fisher, Waltham, USA
Sterile bench	SWB Klasse 1 FAZ 3	Waldner, Wangen, D
Thermo shaker	ThermoMixer® comfort	Eppendorf, Hamburg, D
Vortex mixer	Sunlab SU1900	neoLab, Heidelberg, D

Table 10.14: Setup of the parallel bioreactor system (0.7 L scale)

Component	Description	Manufacturer
DO probe	VisiFerm DO EXS 225 H0	Hamilton, Bonaduz, CH
Off-gas analyzer	BlueVary	BlueSens, Herten, D
Gassing module	DASGIP® MX4/4	Eppendorf, Hamburg, D
pH probe	EasyFerm Plus PHI K8 225	Hamilton, Bonaduz, CH
pH & DO control module	DASGIP® PHPO	Eppendorf, Hamburg, D
Pump module	DASGIP® MP8	Eppendorf, Hamburg, D
Reactor block + vessels	DASGIP® Parallel Bioreactor System	Eppendorf, Hamburg, D
Software	DASware® control	Eppendorf, Hamburg, D
Temperature & stirrer control module	DASGIP® TC4SC4	Eppendorf, Hamburg, D

Table 10.15: Setup of the 7.5 L stirred-tank bioreactor system (3.0 L scale)

Component	Description	Manufacturer
DO probe	VisiFerm DO Arc 425	Hamilton, Bonaduz, CH
Off-gas analyzer	BlueVary	BlueSens, Herten, D
pH probe	EasyFerm Plus Arc 425	Hamilton, Bonaduz, CH
Reactor system	Labfors 5	Infors, Bottmingen, CH
Software	eve®	Infors, Bottmingen, CH

Table 10.16: Setup of the 42 L stirred-tank bioreactor system (25 L scale)

Component	Description	Manufacturer
DO probe	322756800/2023295	Mettler Toledo, Columbus, USA
Gassing filter	Emflon II AB02V0022PVH4	PALL, Crailsheim, D
Off-gas analyzer	Easyline	ABB, Zurich, CH
Off-gas filter	AB05PFR2PVH4 (0.2 µm)	PALL, Crailsheim, D
pH probe	405-DPAS-SC-K8SH50	Mettler Toledo, Columbus, USA
Pressure sensor	PR-25HT8931A	Keller, Winterthur, CH
Reactor system	Techfors 42L K1577	Infors, Bottmingen, CH
Software	IRIS NT V4.0	Infors, Bottmingen, CH
Steam generator	PS 100	Stritzel, Mülheim, D

Table 10.17: Setup of the 50 L and 1000 L stirred-tank bioreactor systems

Component	Description	Manufacturer
Control units	Modular cabinets (IFM units)	Bioengineering, Wald, CH
DO probe	InPro6800	Mettler Toledo, Columbus, USA
Peristaltic pumps	Peripex W1 & W2	Bioengineering, Wald, CH
pH probe	405-DPAS-SC-K8S/425	Mettler Toledo, Columbus, USA
Reactor 50 L	LP75L	Bioengineering, Wald, CH
Reactor 1000 L	LP1500	Bioengineering, Wald, CH
Software	BioSCADALab	Bioengineering, Wald, CH

Table 10.18: Setup of the HPLC system for quantification of sugars and organic acids

Component	Description	Manufacturer
Autosampler	1100 Series G1313A	Agilent, Santa Clara, USA
Cation exchange column	Rezex ROA-Organic Acid H+ (8%) LC Column (300×7.8 mm)	Phenomenex, Aschaffenburg, D
Column oven	Mistral™	Spark Holland, Emmen, NL
Degasser	1100 Series G1322A	Agilent, Santa Clara, USA

Pre-column	SecurityGuard Cartridge Carbo-H (4×3.0 mm)	Phenomenex, Aschaffenburg, D
Pump module	1100 Series G1311A	Agilent, Santa Clara, USA
RI detector	1200 Series G1362A	Agilent, Santa Clara, USA
Software	ChemStation	Agilent, Santa Clara, USA